Evaluation of New Ultrasound Techniques for Clinical Imaging in selected Liver and Vascular Applications

Brandt, Andreas Hjelm; Nielsen, Michael Bachmann; Jensen, Jørgen Arendt; Hansen, Kristoffer Lindskov; Hemmsen, Martin Christian

Publication date:
2017

Document Version
Publisher's PDF, also known as Version of record

UNIVERSITY OF COPENHAGEN
FACULTY OF HEALTH AND MEDICAL SCIENCES

Ph.D. Thesis

Andreas Hjelm Brandt M.D.
Department of Radiology
Copenhagen University Hospital, Rigshospitalet
Denmark

Evaluation of New Ultrasound Techniques for Clinical Imaging in selected Liver and Vascular Applications

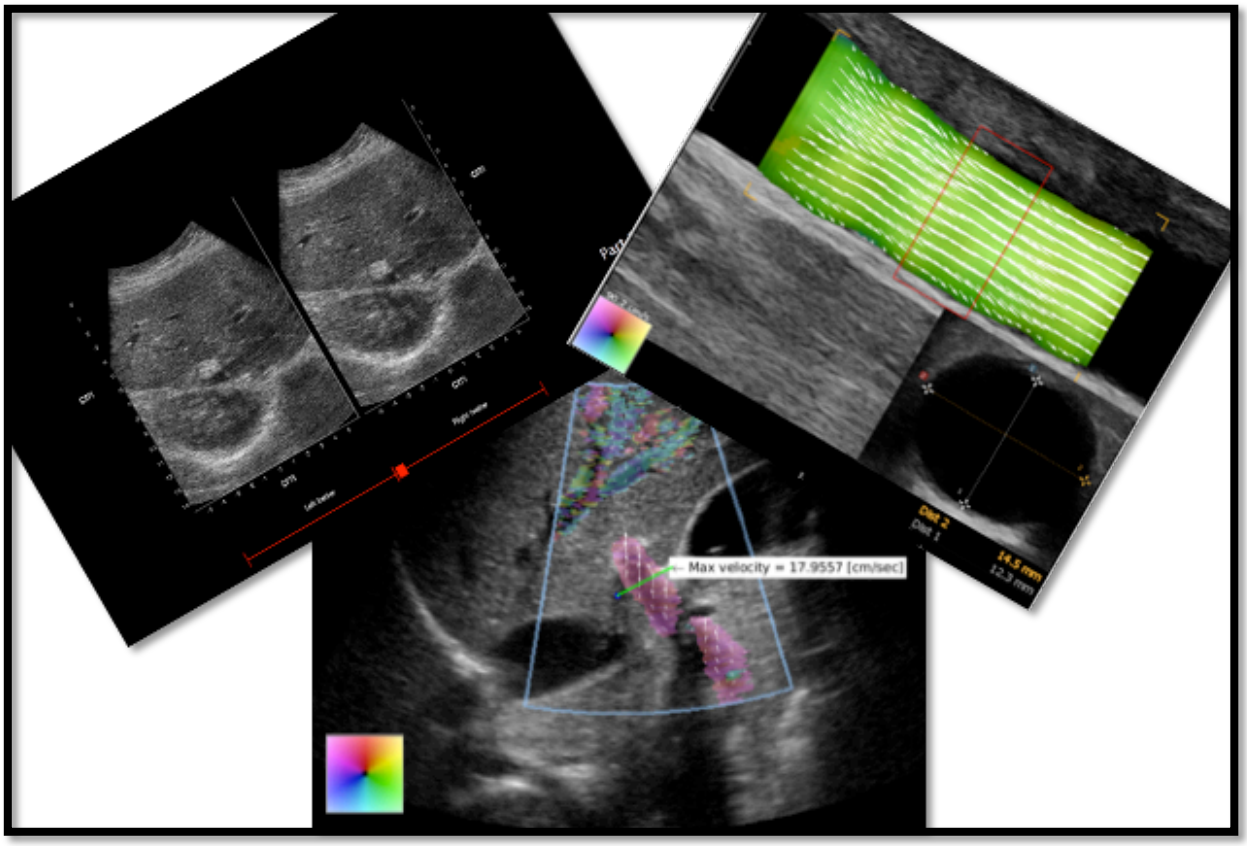

The thesis has been submitted to the Graduate School of Health and Medical Sciences at the University of Copenhagen, September 2016

Main Supervisor

Michael Bachmann Nielsen, M.D., Ph.D., Dr. Med., Professor

Department of Radiology

Copenhagen University Hospital, Rigshospitalet, Denmark

Project Supervisors

Jørgen Arendt Jensen, M.Sc., Ph.D., Dr. Techn., Professor

DTU elektro, Center for Fast Ultrasound Imaging

Technical University of Denmark, Denmark

Kristoffer Lindskov Hansen, M.D., Ph.D.

Department of Radiology

Copenhagen University Hospital, Rigshospitalet, Denmark

Martin Christian Hemmsen, M.Sc., Ph.D.

DTU elektro, Center for Fast Ultrasound Imaging

Technical University of Denmark, Denmark

Evaluating Committee

Andreas Kjær, M.D., Ph.D., Dr. Med., Professor

Department of Clinical Physiology, Nuclear Medicine and PET

Copenhagen University Hospital, Rigshospitalet, Denmark

David H. Evans, Ph.D., DSc., Professor

Department of Cardiovascular Sciences and Medical Physics

The University of Leicester, Leicester, United Kingdom

Jens Karstoft, M.D., Ph.D., Associate Professor

Department of Radiology

Odense University Hospital, Odense, Denmark

Contents

1 Preface and acknowledgments

The work of this thesis was carried out from November 1st, 2013, to November 2016 at the Department of Radiology at Copenhagen University Hospital, Rigshospital, and the Center for Fast Ultrasound Imaging at the Technical University of Denmark in Lyngby. The work culminated in three journal papers, three conference papers, five oral presentations, and three poster presentations.

A huge thanks goes to my supervisor Michael Bachmann Nielsen and Jørgen Arendt Jensen for their support. Without their commitment this work would never have been the same. Your guidance in study planning, data analysis, and paper writing was priceless. A special thank you goes to Kristoffer Lindskov Hansen for his enormous enthusiasm and willingness to teach and inspire me for research. Also a thanks goes to Martin Christian Hemmsen, Peter Møller Hansen, and Lars Lönn for guidance in the study completion. Besides learning to conduct scientific studies, the last years have given me the opportunity to add a new technical dimension to my existing medical experience. I am sure this will be of great use in my future career.

During the past three years, the projects have brought me to places around the world, including Taiwan, Athens, Chicago, Orlando, Helsingborg, and Vienna. I have enjoyed working with engineers and physicists, and I have had great help in their desire to teach me how to process data. I also got the opportunity to teach students in medicine and medical technology about the basic principles in clinical ultrasound and X-ray computed tomography.

Thanks must certainly also go to The Danish National Advanced Technology Foundation for financial support and a huge thank you also to the head of the Department of Radiology, Ilse Vejborg, for financial and academic support.

While working I really enjoyed the company of the entire Ph.D. group at Rigshospitalet and the Center of Fast Ultrasound Imaging. All of you provided a very educational and supportive environment. I consider you all good friends.

Finally, I would like to thank my wonderful girlfriend Kristine, my son Sigurd, and my family for their support and encouragement during the last three years.

2 Summaries

2.1 Dansk Resume

Dette PhD projekt baserer sig på et mangeårigt samarbejde mellem fysikere og ingeniører fra Center of Fast Ultrasound Imaging (CFU) på Danmark Tekniske Universitet og læger fra Radiologisk Klinik på Rigshospitalet. Ved dette samarbejde kan nye ultralydmetoder blive valideret til klinisk brug i fremtiden.

Studie I behandler et sammenligningsstudie af to B-mode ultralydmetoder, hvor den nye eksperimentelle teknik Synthetic Aperture Sequential Beamforming kombineret med Tissue Harmonic Imaging (SASB-THI) sammenlignes med en konventionel ultralyd teknik kombineret med THI. SASB's fordel er, at datamængden reduceres, således trådløs overførsel bliver muliggjort og en trådløs transducer kan baseret på denne teknik. THI har været brugt flere år i klinikken og kan forbedre billedets opløsning, kontrast og skaber færre artefakter. Enogtredive patienter med verificeret levertumor blev skannet og optagelser med og uden synlig patologi blev foretaget. Efterfølgende evaluerede otte radiologer, som var blindet for oplysninger omkring teknikken, hvilket B-mode de foretrak, samt tilstedeværelsen af patologi. Evalueringen viste, at teknikkerne blev præfereret ens og tumor kunne detekteres lige godt på begge teknikker.

Studie II berører vector flow imagings (VFI) evne at overvåge patienter med arteriovenøse fistler til hæmodialyse for kommende stenoser. VFI er en vinkeluafhængig metode til at bestemme den retning og hastighed, hvormed blodet strømmer. Volume flow kan bestemmes ved integrering over hastighedsprofilen ganget op med tværsnitsarealet. Nitten patienter blev monitoreret månedligt over en periode på 6 måneder og indsamlet data blev sammenlignet med referencemetoden ultrasound dilution technique (UDT) målinger. VFI volumen flow estimaterne var ikke signifikant forskellige fra UDT og havde en bedre præcision end UDT. Konkordansen mellem VFI og UDT var høj ved store forandringer (større end 25%) i volumen flow mellem dialyse sessionerne. Metoderne kunne dog ikke betragtes som at være udskiftelig én til én.

Studie III omhandler VFI's evne til at bestemme spidshastigheder i portalvenen. Den gængse anvendte ultralydmetode til at bestemme spidshastigheden i portalvenen er spectral Doppler. Ulempen ved spectral Doppler er, at den vides at overestimere hastigheder, når vinklen mellem blodkarret og ultralydbølgen bliver over 70 grader. Denne overestimering bliver større, jo større vinklen er. VFI kan derimod bruges til at bestemme spidshastigheden vinkeluafhængigt. Toogtredive raske frivillige blev skannet med spectral Doppler og VFI med to skan positioner af portalvenen (intercostal og subcostal). Studiet viste, at VFI kunne estimere samme spidshastigheder som spectral Doppler. Yderligere viste studiet, at VFI havde bedre præcision og kunne estimere de samme hastigheder med en skan position, hvor spectral Doppler ikke kunne. Inter- og intraobserver overensstemmelse var ydermere højere ved VFI.

Alle tre studier indikerer, at teknikkerne vil kunne bruges i klinikken og formentlig være en del af den kliniske hverdag indenfor den nærmeste fremtid.

2.2 English Summary

This Ph.D. project is based on a longstanding collaboration between physicists and engineers from the Center of Fast Ultrasound Imaging (CFU) at the Technical University of Denmark and medical doctors from the department of Radiology at Rigshospitalet. The intent of this cooperation is to validate new ultrasonic methods for future clinical use.

Study I compares two B-mode ultrasound methods: the new experimental technique Synthetic Aperture Sequential Beamforming combined with Tissue Harmonic Imaging (SASB-THI), and a conventional technique combined with THI. While SASB reduces the amount of data transformation, thus enabling wireless transmission, THI can improve resolution and image contrast, and creates fewer artifacts. Thirty-one patients with verified liver tumors were scanned and recordings with and without visible pathology were performed. Subsequently, eight radiologists evaluated blinded to information about the technique, which B-mode images they preferred, as well as detection of pathology. Evaluation showed that the techniques were preferred equally and tumor could be detected equally well.

Study II deals with the ability of vector flow imaging (VFI) to monitor patients with arteriovenous fistulas for hemodialysis for upcoming stenosis. VFI is an angle-independent method for determining blood flow direction and velocity. Volume can be determined by integrating the velocity profile multiplied by the cross-sectional area. Nineteen patients were monitored monthly over a period of six months, and VFI estimates were compared with the reference ultrasound dilution technique (UDT). VFI volume flow values were not significantly different from UDT and had a better precision. Concordance between VFI and UDT was high when large volume flow changes (greater than 25%) occurred between dialysis sessions. However, the methods could not be regarded as interchangeable.

Study III deals with VFI's ability to determine peak velocity in the portal vein. The commonly used ultrasound method for this is spectral Doppler, which is known to overestimate peak velocity when the angle between the blood vessel and the beam is more than 70 degrees; this overestimation becomes even larger when the angle becomes larger. VFI can determine the peak velocity angle independently. Thirty-two healthy volunteers were scanned with spectral Doppler and VFI with two portal vein scan positions (intercostal and subcostal). The study showed that VFI estimates the same peak velocity as spectral Doppler. Furthermore, VFI has better precision and can estimate the same peak velocity with a scan position, where spectral Doppler cannot. Finally, inter- and intra-observer agreement is higher for VFI.

All three studies indicate that the techniques can be used in the clinic and probably will be part of everyday practice in the near future.

3 List of Papers

Clinical Evaluation of Synthetic Aperture Harmonic Imaging for scanning Focal Malignant Liver Lesions

Andreas Hjelm Brandt, Martin Christian Hemmsen, Peter Møller Hansen, Signe Sloth Madsen, Paul Suno Krohn, Theis Lange, Kristoffer Lindskov Hansen, Jørgen Arendt Jensen, and Michael Bachmann Nielsen

Ultrasound Med Biol. 2015;41(9):2368-2375.

Included in appendix I

Surveillance for Hemodialysis Access Stenosis: Usefulness of Ultrasound Vector Volume Flow

Andreas Hjelm Brandt, Jonas Jensen, Kristoffer Lindskov Hansen, Peter Møller Hansen, Jonas Jensen, Theis Lange, Kristoffer Lindskov Hansen, Jørgen Arendt Jensen Michael Bachmann Nielsen

J Vasc Access, in press.

Included in appendix II

Ultrasound Vector Flow makes Insonation Angle irrelevant in Portal Vein Velocity Measurements

Andreas Hjelm Brandt, Ramin Moshavegh, Kristoffer Lindskov Hansen, Thor Bechsgaard, Jørgen Arendt Jensen, Lars Lönn, and Michael Bachmann Nielsen

Submitted.

Included in appendix III

4 Abbreviations

CFU: Center of Fast Ultrasound Imaging

RAD: Department of Radiology at Copenhagen University Hospital (Rigshospitalet)

B-mode: Brightness mode

TO: Transverse Oscillation

VFI: Vector Flow Imaging

SASB-THI: Synthetic Aperture Sequential Beamforming - Tissue Harmonic Imaging

SASB: Synthetic Aperture Sequential Beamforming

THI: Tissue Harmonic Imaging

SA: Synthetic Aperture

UDT: Ultrasound Dilution Technique

CT: Computed Tomography

MR: Magnetic Resonance

DRF-THI: Dynamic Receive Focusing - Tissue Harmonic Imaging

LOA: Limit of Agreement

STD: Standard deviation

IQap: Image Quality assessment program

VAS: Visual Analog Scale

LOA: Limit of Agreement

STD: Standard deviation

ICC: Intra-class Correlation Coefficients

MRA: Magnetic resonance angiography

5 Introduction and Background

Ultrasound has been a clinical imaging tool for almost 50 years. In the 1970s, the technology experienced an improvement with the introduction of real-time brightness mode (B-mode) and the superposition of Doppler data as a color overlay on the gray-scale B-mode (1). The combination of gray-scale B-mode and color Doppler imaging permitted visualization of anatomy, while at the same time information about blood flow was given (2). Ultrasound has, at the same time, developed from a cumbersome machine producing poor images to a portable instrument that can be moved freely around a hospital producing highly accurate anatomical images. This has required medical doctors, physicists, and engineers to work together (3) to bring ideas and development to medical ultrasound.

This thesis is part of a longstanding collaboration between medical doctors at the Department of Radiology (RAD) at Copenhagen University Hospital (Rigshospitalet), and physicists and engineers from the Center for Fast Ultrasound Imaging (CFU) at the Technical University of Denmark. CFU develop new ultrasound methods for B-mode imaging and blood flow imaging and medical doctors are validating the techniques for clinical imaging. The first study in this thesis concerns a clinical validation of the B-mode imaging technique Synthetic Aperture Sequential Beamforming combined with Tissue Harmonic Imaging (SASB-THI). SASB-THI is based on the ideas of Synthetic Aperture (SA) and Synthetic Aperture Sequential Beamforming (SASB), which were developed by CFU and validated by scanning healthy volunteers and patients with liver tumors in collaboration with RAD. Combining SASB with tissue harmonic imaging (THI) was developed by CFU as the next improvement, and its clinical validation was the natural follow-up. The second and third study addresses vector flow imaging (VFI), an angle-independent technique for blood flow imaging. VFI was developed by CFU and validated in collaboration with RAD on an experimental scanner. After this, VFI continued its expansion into a commercially available system and some early clinical studies have been performed. Continuation of the validation and deployment of VFI in everyday clinical practice is the next apparent step for the collaboration between CFU and RAD. The second study focuses on VFI's ability to gauge volume flow in arteriovenous fistulas for hemodialysis, while the third study focuses on its ability to estimate portal vein velocity.

The introduction continues with a description of the theory behind B-mode imaging followed by description of new methods for it (section 5.1). Later, the conventional flow technique is described vis-à-vis angle-independent blood flow imaging (section 5.2). The last part of the introduction addresses comparative statistics (section 5.3).

5.1 B-mode

5.1.1 Conventional B-mode imaging

The conventional B-mode image comprises a number of lines. A focused pulse is emitted into the tissue; as it does, echoes are generated by reflections and scattering from the tissue elements. Once the transducer detects all echoes, an image line can be produced. Normally, information from pulses and echoes from one or several elements in the array of the transducer are used to create each image line. For creation of the full B-mode image with several image lines, the active elements are moved stepwise to the side, and a new focused pulse is emitted and echoes received until all elements have been used. None of the previous generated image lines are reused for the next full B-mode image. These conditions sets limits to the temporal resolution as the frame rate of a full B-mode image is limited by the number of image lines, the speed of sound in tissue, and scans depth. The resolution of the B-mode images turns out to be additionally limited by these restrictions, as a high number of image lines are needed for a high resolution. To some extent, the resolution can be improved by applying multiple focused pulses; however, this reduces the frame rate (4). Given this, the conventional B-mode technique has indisputable drawbacks.

5.1.2 Synthetic Aperture B-mode imaging

SA imaging is an alternative B-mode technique. SA was initially developed for radar technology (5) and suggested for use in ultrasound in 1974 (6). SA's limitation has been its high computational requirements; however, the availability throughout the 1990s of fast computers enabled development of a fully integrated SA system (7, 8).

When using SA as a B-mode technique, one or a group of elements in the transducer emits a spherical wave. During receive mode, all elements in the transducer record echoes

at the same time, as opposed to the conventional B-mode technique, where only the elements that emit are receiving. As the received echo contains information from all directions a low-resolution B-mode can be composed. From multiple low resolution images obtained from several emitted and received pulses a final high resolution image can be summed (Fig.1) (9). Applying SA for B-mode construction can generate a higher frame rate than with conventional imaging. Furthermore, SA has proven to heighten resolution and improve penetration depth compared to a conventional B-mode technique (10).

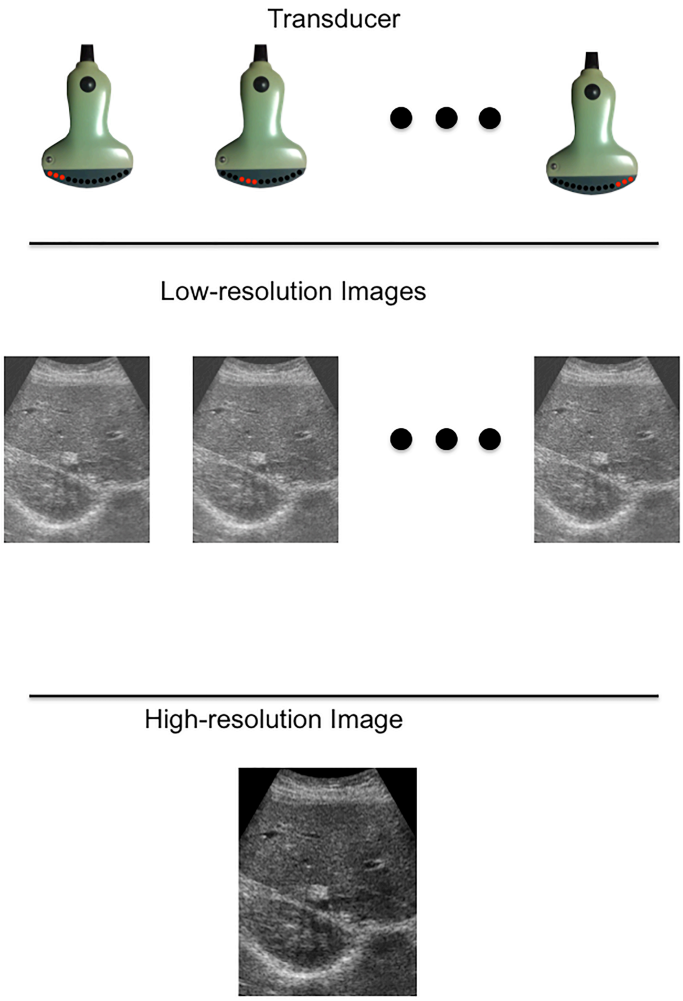

Figure 1: Illustration of Synthetic Aperture (SA). A high-resolution image is achieved by summing low-resolution images. One or a group of elements emit a spherical wave and all elements receive the signal to acquire a low-resolution image.

5.1.3 Synthetic Aperture Sequential Beamforming

In 2008, Kortbek et al. purposed a solution (11) that separates the beamforming process into two stages, thereby reducing SA system computational requirements. In the first stage, beamformer scan lines are generated with a single focus point in emit and receive; in the second stage, a set of high-resolution image points combine information from multiple focused scan lines acquired in the first stage (11). As an extra benefit of SASBs, the beamforming process reduces the data requirements to a single output signal, that is, a factor of 64 for a 64 channel system, enabling wireless RF data transfer. A wireless transducer system implemented on a commercial mobile device can be based on SASB with safe and reliable real-time data transmission (12). SASB's ability to produce B-mode images has been validated in a blinded preclinical and clinical study, where medical doctors evaluated B-mode images of abdominal organs, and noted that SASB image quality matched conventional techniques (13, 14).

5.1.4 Synthetic Aperture Sequential Beamforming combined with Tissue Harmonic Imaging

Besides reducing the SA system computational load, SASB can produce sufficient acoustic energy to create harmonic components for THI. Combining SASB and THI was, thus, a logic way to go, since SASB B-mode image quality could be improved with THI (Fig. 2) (15-17).

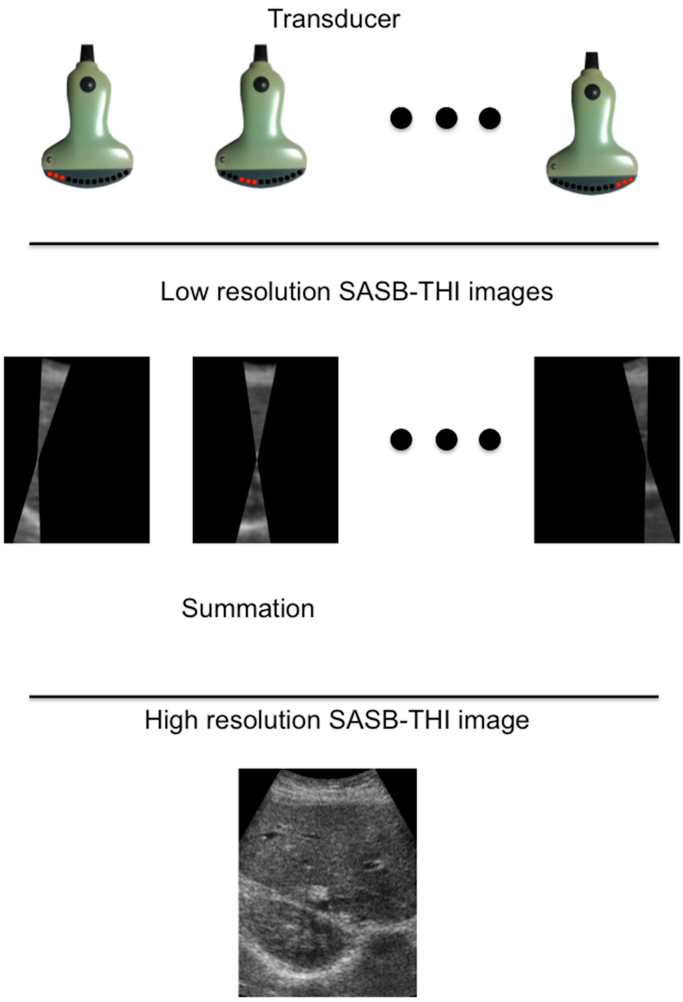

Figure 2: Even harmonics are separated by the pulse inversion technique (15, 16), and each beam is perceived as a virtual ultrasound source emitting from the beam focal point. The received beam echoes are summed to yield the high resolution. Transmit and receive elements are identical for each emission.

THI has been used for many years in clinical imaging to improve spatial and contrast resolution, and deliver fewer artifacts. The basic theory is to image the “harmonic” signal created by the tissue. The tissue reflects the ultrasound signal with a so-called *fundamental* frequency, but also with additional frequencies termed the *harmonics* (Fig. 3). Once the fundamental and the harmonic frequencies are received, the ultrasound system can process only the latter. The harmonic frequencies build to a maximum intensity, then decay because of attenuation. The second harmonic signal is normally used for imaging (18, 19). The combination of SASB and THI was clinically evaluated in the first study of this thesis (appendix I). Patients with biopsy- or computed tomography/ magnetic

resonance (CT/MR)-verified malignant focal liver lesions were scanned the day before surgery.

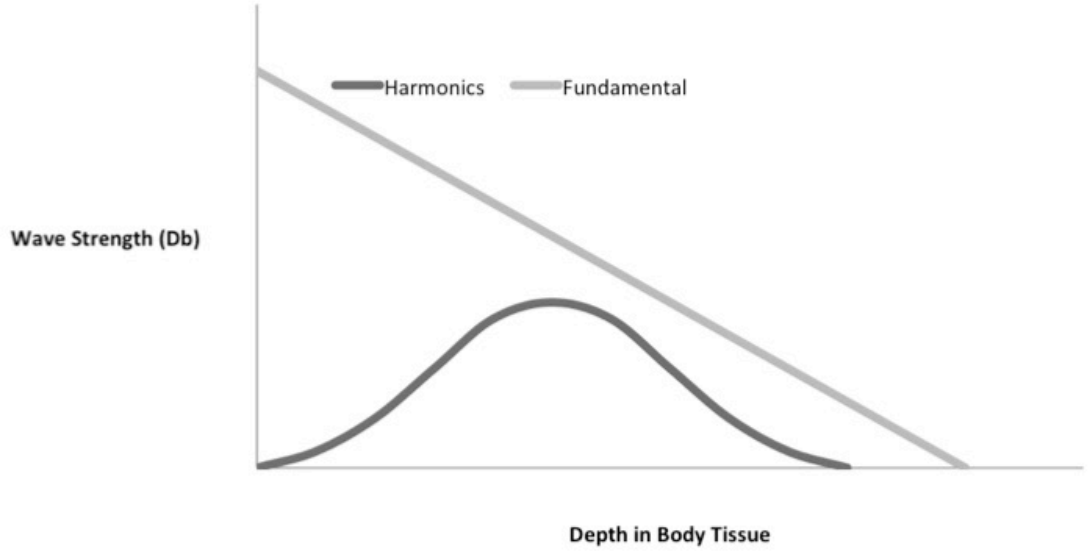

Figure 3: A schematic illustration of the strength changes of the received fundamental and harmonic waves with increasing tissue depth.

5.2 Flow Imaging

5.2.1 Conventional flow imaging

The standard method for evaluating flow direction is color Doppler ultrasound, while blood velocity is determined with spectral Doppler. These two techniques are widely used in flow imaging and have proven to be of great importance in evaluating, for example, hepatic vasculature (20, 21), hemodialysis vascular access (22, 23), carotid artery stenosis (24), and renal stenosis (25, 26). A major problem with color Doppler ultrasound is that only blood flow in the direction of the emitted beam and only velocities towards or away from the transducer can be estimated, that is, in the axial direction (4). However, frequently a vessel is located at a different beam-to-flow angle than the axial direction. The operator is obliged to adjust the transducer to an angle of less than 70 degrees to visualize flow direction. At 90 degrees no flow is seen (Fig. 4).

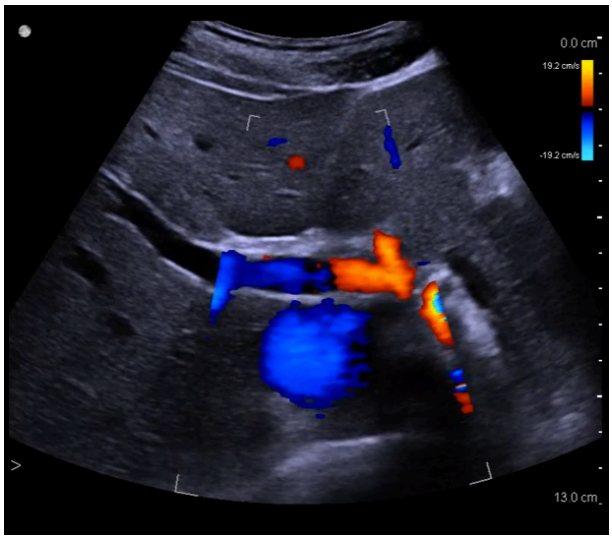

Figure 4: *Color Doppler*: The colors indicate the direction of the flow. Blue indicates flow going away from the transducer and red indicates flow going towards the transducer. No information about velocities is given; thus, the technique can only be used for flow direction assessment. The image shows the portal vein scanned in a subcostal position. Note that with an angle of 90 degrees no flow is seen.

In spectral Doppler, angle correction is applied when estimating velocities. Within an operator-selected range gate, angle correction is performed and a quantitative velocity value is displayed on the scanner (Fig. 5).

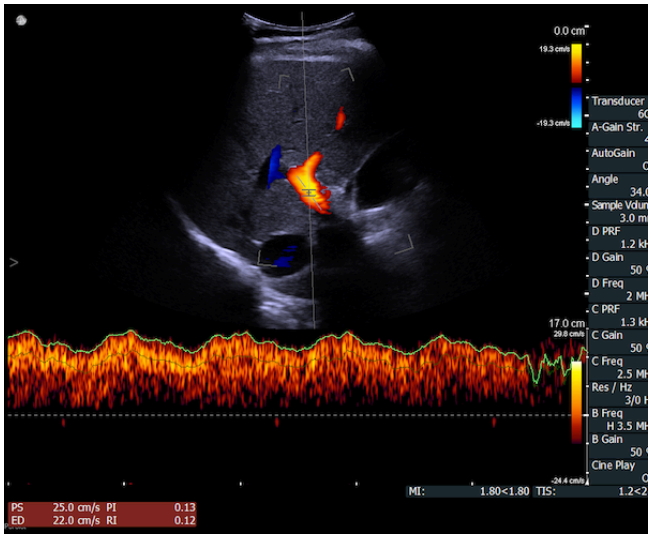

Figure 5: *Spectral Doppler* measurement of the flow in the main portal vein. The flow velocity is illustrated within a spectrogram. Angle of insonation is less than 70 degrees, indicating a reliable measurement. Flow is only measured within the range gate.

What is supposed to be the true velocity v can be determined by the equation stated below:

$$v = v_z / \cos \theta,$$

where v_z is the axial velocity and θ is the angle of insonation. The operator sets the angle, assuming that the flow is parallel to the vessel and laminar. This is certainly a simplification, since a vessel often is curved, contains branches, can be stenotic or

aneurysmatic, or can contract or dilate, giving a much more disturbed flow (27-29). The angle correction is one of the main reasons for overestimating the flow. When the angle approaches 90 degrees reliable velocity estimates cannot be achieved since *cos* (90) = 0. As with color Doppler, it is therefore necessary to achieve an angle of insonation of less than 70 degrees (30, 31). Even though the beam-to-flow angle is less than 70 degrees, spectral Doppler overestimates the true velocity (32). A small deviation between the beam-to-flow and the beam direction can result in a large error, when calculating the velocity *v* (31). The low inter-observer variability and high inter-equipment variation is another concern with spectral Doppler (33). Previous studies have shown poor inter-observer variability; however, a training program could improve agreement (34).

5.2.2 Angle-independent flow imaging

Problems with angle dependencies can be solved by vector velocity estimation, where the blood motion is found in more directions than just the axial (35). Hence, blood flow velocities are obtained independent of beam-to-flow, which results in an improved flow understanding. Combining multiple Doppler measurements was proposed as early as 1970, and Dunmire et al., provided a full overview of the different approaches (36). Although numerous methods combining multiple Doppler measurements have been developed and evaluated both in-vitro and in-vivo, none have become a mainstream clinical work instrument. Another approach is speckle tracking. Bohs et al. described its limitations (37), with the main one being its inability to track the axial component correctly; speckle tracking has likewise not managed to become a mainstream clinical instrument. The first technique to become a mainstream product is Transverse Oscillation (TO), which was developed by Jensen and Munk and estimates the transverse velocity and the axial velocity at the same time (38, 39). For transmission, a conventional ultrasound pulse is emitted. The axial velocity is found similar to a conventional ultrasound technique, while the transverse velocity is found by manipulating the apodization during receive beamforming. The combination of the axial and transverse velocity can be used to calculate the vector velocity. Even though TO is now available, commercial ultrasound scanner vector techniques share the problem. None of them have had any clinical impact and both color and spectral Doppler are still the industry standard for daily clinical vascular ultrasound (40).

5.2.3 Vector Flow Imaging

VFI is the commercial setup for TO and provides 2-D images of the blood flow. Each pixel contains quantitative information about direction and velocity. Arrows can be superimposed in real time on the color-coded pixels for flow-profile interpretation as displayed in Figure 6. Several clinical studies from the collaboration between the RAD, and CFU have validated its use in a clinical setting. Hansen et al. found VFI obtained volume flow values in the common carotid artery comparable to magnetic resonance angiography (27, 41). Pedersen et al. compared spectral Doppler estimated flow angle, peak systolic velocity, end diastolic velocity, and resistive index in the common carotid artery to VFI and found significant difference in flow angle and peak systolic velocity (42). Furthermore, Pedersen et al. found that VFI vector concentration could be used to distinguish between laminar and complex flow (43). Hansen et al. found VFI applicable to measure volume flow in arteriovenous fistula for hemodialysis with a better reproducibility than the reference method Ultrasound Dilution Technique (UDT) (44). For cardiac imaging, Hansen et al. showed that VFI can provide new insight into cardiac imaging regarding flow (45, 46). Overall, VFI shows some promising results; however, final implementation in daily clinical routine has not yet been managed. This is most likely caused by the lack of TO implementation on more than a linear probe. The first implementation of TO on a commercially available convex transducer is addressed in this thesis (appendix III).

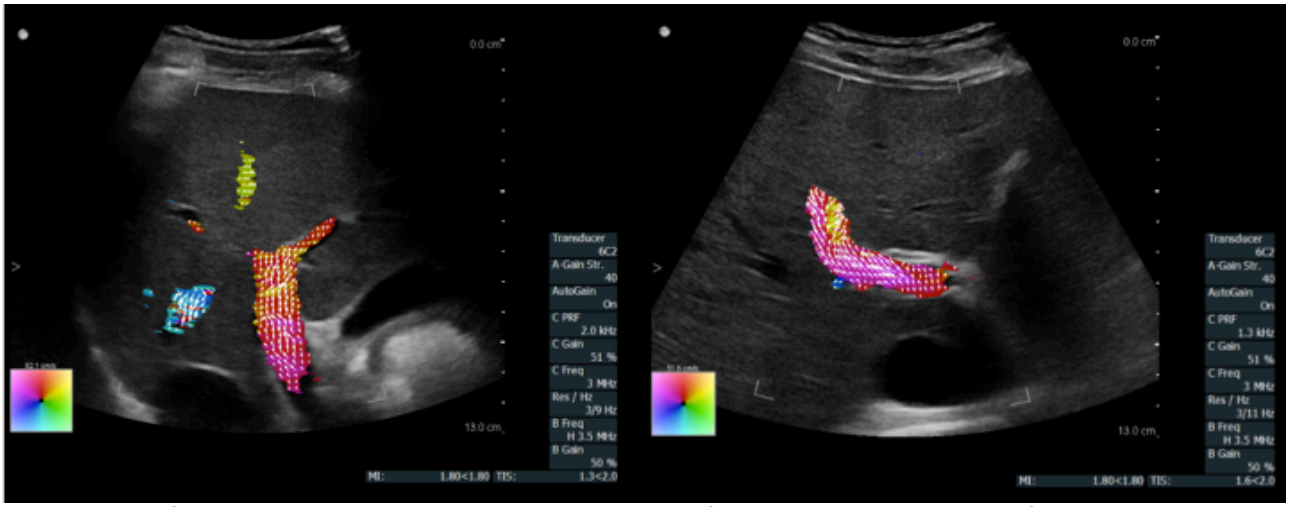

Figure 6: The figures displays the portal vein obtained with from an intercostal view (left) and subcostal view (right). The flow looks laminar and parabolic, with shorter arrows along the vessel walls than centrally in the vessel lumen.

5.2.4 Vector Volume Flow

VFI can be used for volume flow calculation in arteriovenous fistula for hemodialysis; however, VFI underestimates the flow (44). The volume flow can be found by integrating the vector-velocity profile over the cross-sectional vessel. A problem with superficial vessels such as an arteriovenous fistula is that they are easily compressed under the weight of the transducer, which will change the cross-sectional geometry. Furthermore, it is difficult for the user to place the transducer in the center intersection of the vessel and steer the ultrasound beam in the direction along one center of the epileptic geometry (Fig. 7). These errors were described by Jensen et al. and corrected for in the estimating scheme for volume flow in arteriovenous fistula in this thesis (appendix II) (47, 48).

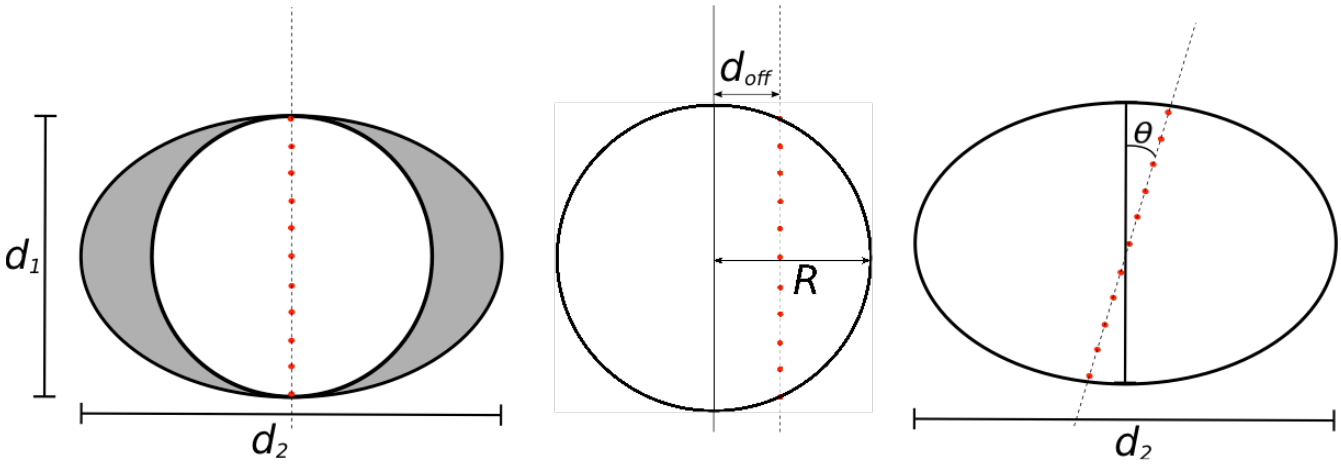

Figure 7: The figure illustrates sources of error in volume flow estimation of superficial vessels. Elliptic cross-section (left), beam-off axis (middle), and steering in an elliptic vessel (right). The image is used by permission (47).

Vector volume is evaluated against the reference method in arteriovenous fistula volume flow determination ultrasound dilution technique (UDT) (Fig. 8) (49, 50). UDT is an indicator dilution technique described by Krivitski and Depner (51, 52). A known quantity of saline is added to the blood stream during a dialysis session. Changes in the resulting blood concentration as a function of time can be used to estimate volume flow. The dialysis machine is set to reverse the blood stream, recirculating some of the blood in the arteriovenous fistula (51).

Figure 8: The figure illustrates volume flow estimation with UDT. Measurements can only be performed while the patient is in hemodialysis.

5.3 Comparison Statistics

The second and third studies compared two techniques using the generally accepted Bland-Altman analysis (53). The limit of agreement (LOA) must be within an acceptable limit. A 30 percent error has been proposed as the acceptable LOA in a Bland-Altman analysis. However, this criterion assumes a 20 percent error on the reference method and the method being validated (54). A precise determination of each individual method is therefore necessary before the LOA in a Bland-Altman comparison can be accepted. The comparison was based on two independent measurements with each technique. Calculation was performed as two standard deviations (STD) of the difference between two measurements of method *a* and *b* of method *x* over all included patients, divided by the mean of all measurements and multiplied by 100 to be expressed in percentage (54). The equation for the precision calculation is given as:

$$P = \frac{2 * STD\left(x_n^a - x_n^b\right)}{\bar{x}} * 100 \,,$$

where *n* is the number of patients, and $\bar{x}$ is the average value. After the precision of each method is determined, the excepted LOA can be calculated. The equation for the expected LOA is given as:

$$Exp\_LOA_{x,y} = \sqrt{P_x^2 + P_y^2}$$

where *P* is the precision for each method *x* and *y*. The LOA of a Bland-Altman should not be wider than expected and below 30 percent for the two methods to be interchangeable

(55, 56). For the second and third studies, analysis of interchangeability was conducted for VFI compared to the reference methods.

6 Study Aims

The first study of this thesis evaluates a new ultrasound technique's image quality and detection rate (sensitivity and specificity), while the second and third study address blood flow in, respectively, arteriovenous fistulas and the portal vein with the ultrasound technique VFI. An overview of the three studies is provided in Table 1.

Study I

Aim: To perform a clinical comparision of a conventional imaging technique and SASB-THI using liver scans from patients with confirmed malignant focal liver cancer. The generated image sequences, SASB-THI and conventional technique videos, were evaluated by radiologists for detection of malignant focal liver lesions and to assess the image quality of SASB-THI compared with that of a conventional technique in a clinical setting.

Study II

Aim: The agreement between volume-flow estimates by VFI and UDT, and VFI's ability to detect changes in volume flow for hemodialysis monitoring have not been studied previously. In this study, the primary aim was to analyze the agreement between UDT and VFI, and determine if VFI can detect changes in volume flow over time, compared to corresponding estimates obtained by UDT.

Study III

Aim: To investigate whether the angle-independent VFI technique is an alternative to spectral Doppler for portal vein peak velocity estimation. VFI was validated in-vitro using a flowrig and in-vivo compared to spectral Doppler in two scan positions of the portal vein. Furthermore, intra- and inter-observer agreement for VFI and spectral Doppler was assessed in-vivo.

Study Number	I	II	III
Subjects	Patients with liver tumors	Patients with arteriovenous fistulas for hemodialysis	Healthy volunteers
Ultrasound method	SASB-THI	VFI linear array	VFI convex array
Number of participants	31	19	32
Number of scans	127	57	84
Evaluation	Side-by-side comparison	Comparison to reference for arteriovenous fistulas volume flow surveillance	Flowrig validation and comparison to reference for portal vein peak velocity estimation
Reference method	Conventional B-mode combined with harmonics	Ultrasound dilution technique (UDT)	Flowrig and spectral Doppler
Parameters investigated	• Diagnostic accuracy • Preference of image quality • Inter-observer and intra-observer variability	• Agreement between UDT and VFI • Detection of volume flow change by VFI	• Agreement between VFI and flowrig • Agreement between VFI and spectral Doppler • Intra- and inter-observer agreement
Statistics	• Sensitivity and specificity • Wilcoxon Signed Rank Test • Fleiss' kappa statistic	• Precision analysis • ANOVA • Bland-Altman • Linear regression • Four-Quadrant Plot	• Precision analysis • Paired T-test • Bland-Altman • Linear regression • Intraclass Correlation Coefficients
Main findings	• Sensitivity and specificity for SASB-THI and the reference were equally good • There was no difference in image quality • Inter-observer variability showed poor agreement and intra-observer variability showed slight agreement	• VFI had a better precision then UDT • VFI estimates were not significantly different from UDT • For detection of large changes between hemodialysis sessions, VFI and UDT were in concordance.	• VFI had a better precision then spectral Doppler • VFI estimated same values regardless of scan view, unattainable for spectral Doppler • Intra- and inter-observer agreements were higher for VFI than for spectral Doppler

Table 1: Overview of studies I-III.

7 Materials, methods, and results

7.1 Study I

Clinical evaluation of synthetic aperture harmonic imaging for scanning focal malignant liver lesions – published in Ultrasound Med Biol. 2015;41(9):2368-2375 (appendix I).

7.1.1 Aim

The aim of the study was to perform a clinical comparison of SASB-THI and the conventional imaging technique combined with THI. Images were evaluated regarding image quality and detection rate (sensitivity and specificity). Patients with focal malignant liver tumors were scanned for the study.

7.1.2 Materials and methods

Scans from 31 patients with malignant focal liver tumors were included in the evaluation. Both scans with and without visible tumors were included in the study. Diagnoses were confirmed by biopsy or computed tomography/magnetic resonance (CT/MR). The scans were performed with a conventional ultrasound scanner (UltraView 800, BK Medical, Herlev, Denmark) equipped with a research interface and an abdominal 3.5 MHz convex array transducer (Sound Technology Inc., Pennsylvania, US). The conventional technique was dynamic receive focusing combined with tissue harmonic imaging (DRF-THI). Images from the same anatomical part were recorded by SASB-THI and DRF-THI interleaved. One frame generated with SASB-THI followed one frame generated DRF-THI, giving almost simultaneously recorded images. Eight radiologists subsequently evaluated them in an image quality assessment program (IQap) that presented the images randomly side by side in real time. The imaging techniques were blinded to the evaluator. A visual analog scale (VAS) was placed at the bottom of the IQap, where the evaluator could drag a bar to the image with the preferred quality (Fig. 9). All sequences were shown twice with a different right-left position. A total of 2,032 evaluations were performed. For predicting the detection rate (sensitivity and specificity), the image sequences were shown separately where the evaluator could drag a bar to the bottom if he or she considered a tumor been present. The evaluation here was also performed in the IQap.

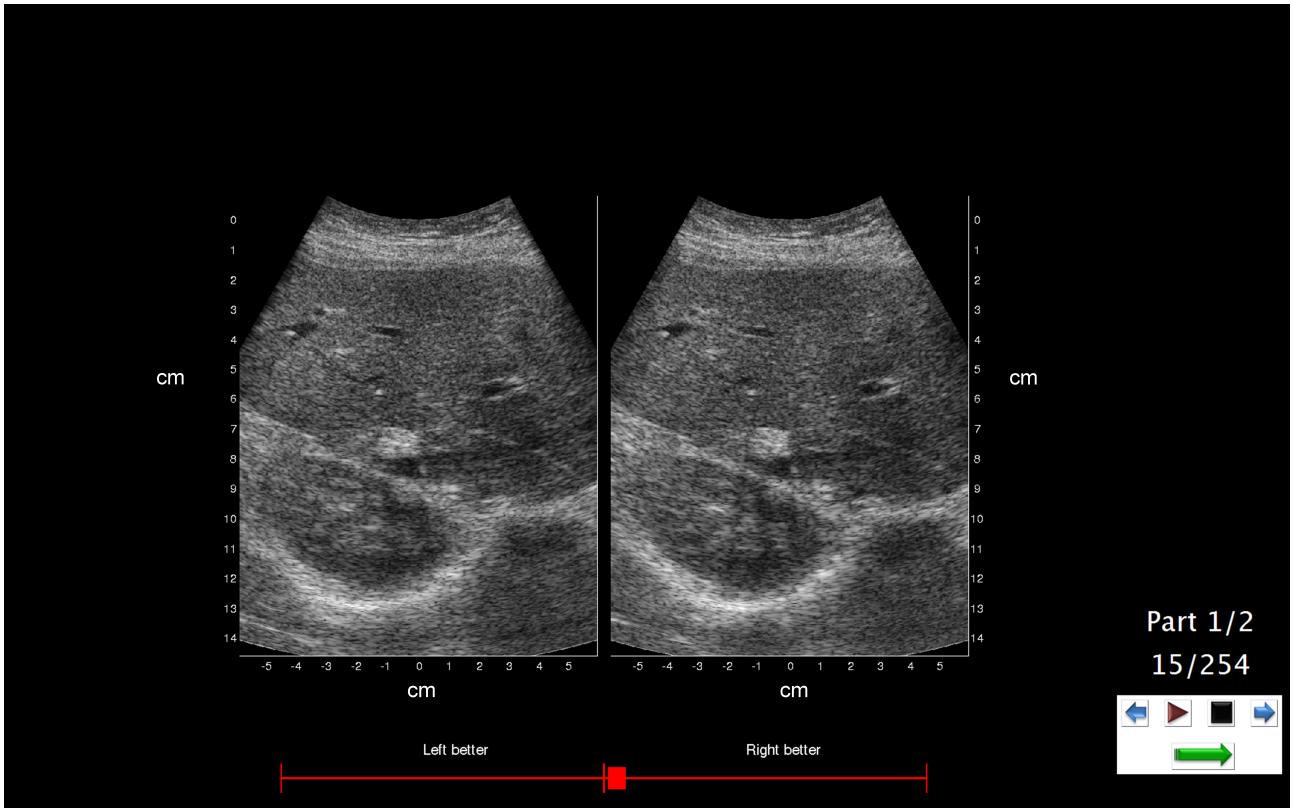

Figure 9: In the image the IQap is presented. At the bottom is the VAS, where a bar is dragged to the image the evaluator prefers. In the right corner is a control bar, where the evaluator could choose to see single image frames or a full video.

7.1.3 Results

The radiologist's evaluation showed no difference in preference between SASB-THI and DRF-THI in 63 percent of the evaluations. SASB-THI was favored in 16 percent of the ratings, while 21 percent favored DRF-THI. The average rating for all radiologists was -0.10 (95%CI: -0.47 to 0.26) and the statistical analysis gave a p-value of 0.63. The inter-observer variability was poor with a kappa value of 0.0045, and the intra-observer variability for each radiologist showed slight agreement with a kappa value of 0.11.

Sensitivity and specificity for all rating radiologists is shown in Fig. 10. SASB-THI and DRF-THI performed similarly with regard to detection of focal malignant liver lesions (sensitivity: p=0.54, specificity: p=0.67). Inter-observer variability showed moderate agreement with a kappa value of 0.48 when rating image sequences were generated by SASB-THI, and fair agreement with a kappa value of 0.37 for images generated with DRF-

THI.

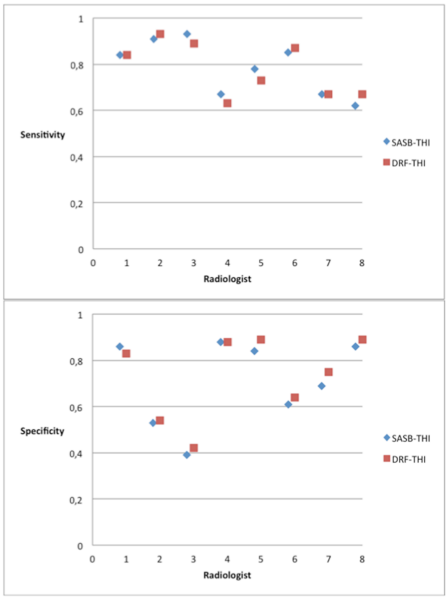

Figure 10: SASB-THI and DRF-THI sensitivity and specificity is illustrated for each radiologist.

7.1.4 Conclusion

In this study, eight radiologists preferred SASB-THI and DRF-THI image quality equally good and found them to be equally good at detecting malignant focal liver lesions. This shows that SASB-THI can perform in a daily clinical work situation. A wireless real-time ultrasound system implemented on a commercial mobile device is not far in the future.

7.2 Study II

Surveillance for Hemodialysis Access Stenosis: Usefulness of Ultrasound Vector Volume Flow – Published in J Vasc Access, in press (appendix II).

7.2.1 Aim

The aim of the study was to perform volume flow surveillance on arteriovenous fistulas with VFI. Volume flow measurements with VFI were compared to corresponding estimates of the reference method UDT with repeated measurements over a six-month period.

Agreement between UDT and VFI, and VFI's ability to detect changes in volume flow were analyzed.

7.2.2 Materials and methods

Nineteen patients with matured and functional arteriovenous fistulae were included in the study. Each patient was examined monthly over a six-month period with VFI and UDT. VFI measurements were performed on a commercial ultrasound scanner (UltraView 800, BK Medical, Herlev, Denmark) equipped with a linear transducer (8670, 9MHz, BK Medical, Herlev, Denmark). All VFI measurements were performed before the UDT measurement. Initial B-mode scans were performed for orientation. Three VFI recordings were performed with a longitudinal view at a position with laminar flow. For each recording, the color box was adjusted to cover the lumen of the arteriovenous fistula segment, and the pulse repetition frequency (PRF) was adjusted to the highest velocities without aliasing. To avoid blooming artifacts, wall filter and color gain were set to optimal filling of the vessel. Between each recording, the transducer was raised and repositioned to attain a new location. Along with the longitudinal VFI recording, an accompanying transverse B-mode recording was conducted. The transducer was not lifted between the longitudinal and transverse recording to attain the same compression. With the transverse view, two perpendicular diameters for cross-sectional area determination were measured. Diameters were measured with the built-in length gauge of the scanner, and performed from the superficial to the deep tunica intima and the corresponding mediolateral diameter. To calculate volume flow by VFI a rectangular region of at least 20 percent, the whole vessel segment was manually marked (Fig. 11). Calculation of the volume flow was based on integration of the vector-velocity profile over the cross-sectional vessel area assuming laminar and axisymmetric flow profile. The algorithm was developed in-house (47). UDT measurements were carried out with a Transonic HD03 Flow-QC hemodialysis monitor (Transonic Systems Inc., Ithaca, NY, US) and performed according to vendor guidelines. According to daily clinical practice, three measurements were conducted with each technique (UDT and VFI) and the average of these results was considered the volume flow of each method. The first two measurements were furthermore used for precision analysis.

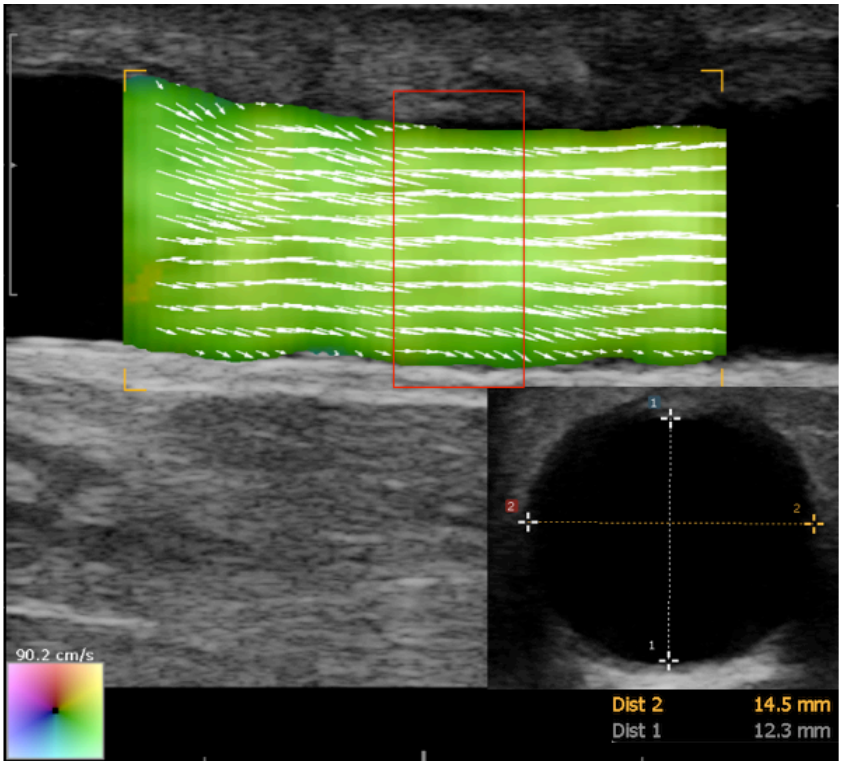

Figure 11: The longitudinal arteriovenous fistula segment measured with VFI and the 20 percent region marked for the volume flow calculation. In the right corner is an illustration of the corresponding transverse B-mode with diameter measurements.

7.2.3 Results

Average volume flow measured with UDT and VFI were 1,161 ml/min (±778 ml/min) and 1,213 ml/min (±980 ml/(min), respectively (p = 0.3). Precision for VFI was 20 percent and the mean difference between the first and second measurement -29 ml/min (95% CI: -78 ml/min to 20 ml/min). UDT precision was 32 percent and mean difference between the first and second measurement was 28 ml/min (95% CI: -61 ml/min to 118 ml/min). There was no statistical difference between precision for VFI and UDT (p = 0.33). The differences between UDT and VFI measurements were analyzed in a Bland-Altman plot. Mean difference was -51 ml/min with LOA from -35 percent to 54 percent (mean 44.5 percent). The expected LOA calculated based on the precision for each method was 37 percent. A strong correlation was found between the UDT and VFI with an R-squared value of 0.87.

Volume flow changes were analyzed in a four-quadrant plot and with regression analysis. Inclination was 0.301 with a p-value of 0.0001. The concordance rate increased from 54

percent to 72 percent with an exclusion zone of 25 percent corresponding to the averaged precision of VFI and UDT and the threshold for referral to angiography (Fig. 12).

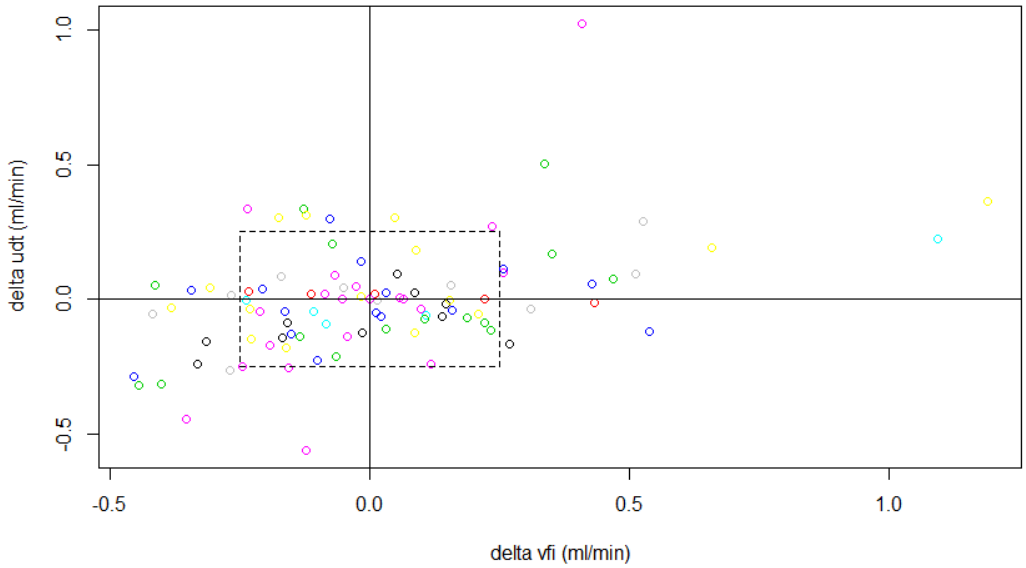

Figure 12: This illustrates the four-quadrant plot of the differences. Each color characterizes a patient and indicates the volume-flow change between sessions. Including the exclusion zone (dotted-line box) of 25 percent the concordance rose from 0.54 to 0.72.

7.2.4 Conclusion

Volume flow estimated with VFI was not different from the values obtained with the reference method UDT. VFI and UDT were equally apt at detecting large changes between sessions. VFI seems to be a more precise method for volume flow estimation than the reference method UDT and could be used for volume flow surveillance in arteriovenous fistulae.

7.3 Study III

Ultrasound Vector Flow makes insonation angle irrelevant in portal vein velocity measurements – *(appendix III).*

7.3.1 Aim

The aim of the study was to validate the convex array VFI implementation. Validation was performed on a flowrig, in-vivo by comparing peak velocities from VFI estimates and spectral Doppler in the main portal vein in two scan positions, and assessing intra- and inter-observer agreements comparing VFI and spectral Doppler. Scans were performed on healthy volunteers.

7.3.2 Materials and methods

A conventional ultrasound scanner equipped with VFI (BK3000, BK ultrasound, Herlev, Denmark) and a 3 MHz convex probe (6C2, BK ultrasound, Herlev, Denmark) was used to obtain vector velocity data. For the flowrig validation, a flow system (CompuFlow 1000, Shelley Medical Imaging Technologies, Toronto, Canada) circulating a blood-mimicking fluid (BMF-US, Shelley Medical Imaging Technologies, Toronto, Canada) in a closed loop circuit was used. The pump was set to velocities from 5-49 cm/s and the convex array was fixed to a distance of 70 mm from the vessel with a diameter of 8 mm. For the in-vivo validation, 32 healthy volunteers were scanned in two positions (intercostal and subcostal). The intercostal view is preferred for velocity estimates since beam-to-flow angle of less than 70 degrees can be attained; a subcostal beam-to-flow angle of less than 70 degrees is not always possible to attain, thus giving unreliable velocity estimates with the conventional spectral Doppler. Since VFI is angle-independent, the main portal vein peak velocities should be the same regardless of scan position. For both spectral Doppler and VFI, two velocity estimates were obtained at both the intercostal and subcostal view. Between each measurement, the transducer was raised and repositioned. For the intra- and inter-observer agreement assessment, 10 of the 32 healthy volunteers were rescanned by three physicians. All scans were again performed with an intercostal and subcostal view and blinded to the peak velocity estimation displayed on the scanner. VFI peak velocity was found as the maximum velocity over at approximately 100 frames of VFI data for each measurement. Data corresponded to 5-7 heartbeats. For spectral Doppler, the peak velocity was found with the standard Doppler setup for the scanner, and maximum velocity was found over 3-5 heartbeats (Fig. 13).

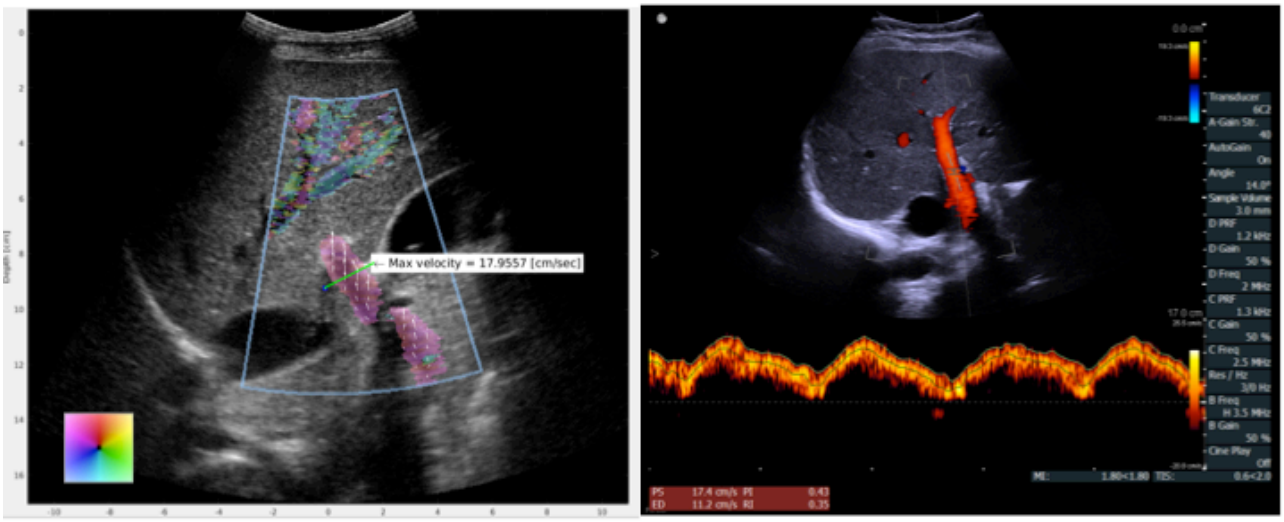

Figure 13: On the left of the image, VFI peak velocity estimation is shown for one patient, while peak velocity estimation for the same patient is shown on the right side. Notice that velocities were estimated at the same depth for both methods.

7.3.3 Results

In the flowrig, VFI had a precision of 3 percent with a mean bias of 0.33 cm/s. In-vivo, the precision for VFI was 18.1 percent at the intercostal view and 23.2 percent at the subcostal view, while the precision for spectral Doppler was 28.3 percent at the intercostal view and 76.8 percent at the subcostal view. Mean bias between VFI and spectral Doppler was 0.57 cm/s (p=0.38) for the intercostal view and 9.89 cm/s (p<0.001) for the subcostal view. VFI peak velocities obtained at the intercostal view were not significantly different from spectral Doppler peak velocities (p=0.38). Intercostal and subcostal VFI peak velocities were not significantly different (p=0.78), while intercostal and subcostal spectral Doppler values were significantly different (p<0.001) (Table 1).

	Mean and STD for VFI [cm/s]	Mean and STD for spectral Doppler [cm/s]	*P*-value
Intercostal	20.09 / 3.19	20.66 / 3.77	0.38
Subcostal	19.90 / 3.87	29.79 / 11.45	<0.001
P-value	0.78	<0.001	-

Table 1: Mean peak velocities and standard deviation (STD) for VFI and spectral Doppler and results from paired t-tests.

Intra- and inter-observer agreement was higher for VFI with intra-class correlation coefficients (ICC) being higher overall. ICC inter-observer values for was VFI 0.80, and for spectral Doppler 0.37, while intra-observer ICC for VFI was 0.90, and for spectral Doppler 0.86 (Table 2).

	Interobserver agreement	
	Intercostal view	Subcostal view
VFI	0.84 (95% CI: 0.53, 0.96)	0.78 (95% CI: 0.40, 0.94)
spectral Doppler	0.64 (95% CI: -0.027, 0.90)	0.27 (95% CI: -0.42, 0.73)
	Intraobserver agreement	
	Intercostal view	Subcostal view
VFI Physician 1	0.93 (95% CI: 0.71, 0.98)	0.93 (95% CI: 0.73, 0.98)
VFI Physician 2	0.77 (95% CI: 0.17, 0.94)	0.95 (95% CI: 0.81, 0.99)
VFI Physician 3	0.92 (95% CI: 0.66, 0.98)	0.88 (95% CI: 0.47, 0.97)
spectral Doppler Physician 1	0.85 (95% CI: 0.43, 0.96)	0.86 (95% CI: 0.41, 0.96)
spectral Doppler Physician 2	0.74 (95% CI: -0.51, 0.94)	0.79 (95% CI: 0.12, 0.95)
spectral Doppler Physician 3	0.60 (95% CI: -0.53, 0.90)	0.37 (95% CI: -0.57, 0.85)

Table 2: The table shows the inter- and intra-observer agreement for subcostal and intercostal view. Values are shown as interclass correlation coefficient (ICC) with 95 percent confidence interval.

7.3.4 Conclusion

The study showed that even though VFI is a different ultrasound approach for velocity estimation of the main portal vein, similar values were attained as with the spectral Doppler technique. Furthermore, VFI had better precision and could estimate equal values with an inapplicable view for spectral Doppler. Intra- and inter-observer agreement for VFI was better than for spectral Doppler. The convex array of VFI implementation may be a useful angle-independent method for many abdominal ultrasound applications.

8 Discussion

The new achievements of this thesis are**:**

I. Radiologists rated the image quality and detection capability of focal liver lesions for SASB-THI to be equal to conventional imaging techniques. Consequently, it makes sense to exploit SASB's data reduction advantage to develop a wireless transducer implemented on a commercial tablet (Study I).

II. VFI has a higher precision for arteriovenous fistula volume flow determination and detects large in-between session changes similar to the reference method. VFI may therefore be regarded as an alternative method for arteriovenous fistula volume flow surveillance for hemodialysis (Study II).

III. The convex array VFI implementation for abdominal studies offers a higher precision than spectral Doppler for peak velocity estimation regardless of the portal vein insonation window. Furthermore, VFI can estimate the same peak velocity in the main portal vein with an insonation angle inapplicable for spectral Doppler. Intra- and inter-observer agreements are higher for VFI than for spectral Doppler for portal vein peak velocity estimation (Study III).

8.1 Clinical evaluation of SASB-THI

8.1.1 B-mode side-by-side comparison studies

B-mode image side-by-side comparison studies are performed for new against established imaging techniques. Data is collected before the evaluation and the subsequent evaluation is often performed with a software application (e.g., IQap) created for the purpose (13). The evaluators are instructed to assess the image quality and provide a diagnosis. For a fair comparison, the evaluators are usually blinded to technical information about the ultrasound technique that created the B-mode image (13).

For the data collection to be applicable for a side-by-side comparison, data from both techniques should be recorded as simultaneously as possible. However, for several side-by-side comparisons, data are collected with consecutive recording (57-65). Even though the same position is held with the transducer while obtaining data, and the patient is lying still, a similar image can never be attained with consecutive data collection. Furthermore, the comparisons are often performed with still images, which does not resemble daily clinical practice as an ultrasound examination is an dynamic procedure (57-65). Having still images reduces the clinical information and may reduce the value of the evaluation.

Our study was performed with interleaved recording of data given almost simultaneously obtained data. Moreover, during the evaluation, video sequences were shown to attain a more realistic comparison, without losing clinical information.

8.1.2 THI in clinical imaging

THI improves B-mode image spatial and contrast resolution, and deliver fewer artifacts (18). For certain patient groups diagnostic information is increased, as THI displays pathology with greater clarity than a conventional B-mode image. For liver imaging, hepatic lesion visibility and characterization is improved, and a better confidence in diagnosis is provided (57, 58, 60), and focal lesions in patients with cirrhosis are detected with higher certainty (62). The same is the case for renal imaging, as the detection rate of focal lesions, for example, renal cell carcinoma, cysts, or kidney stones, is improved due to an improved overall image quality, lesion conspicuousness, and fluid-solid differentiation (65). In breast imaging, characterization and lesion detection is likewise improved (64), and THI is suggested for a better carotid plaque evaluation characterization (64). Thus,

THI has been shown to improve daily clinical practice and diagnostic accuracy. Therefore, combining SASB and THI was suggested to improve the former's performance (14-17).

8.1.3 Side-by-side comparison studies performed with SA and SASB

SA or SASB have not yet had any impact on clinical practice and diagnosis, since few studies evaluated them in side-by-side comparisons. Two studies by Kim et al. and Kim et al. evaluated SA as a technique for breast lesion imaging, where RF data were acquired with a conventional scanner equipped with a research package. The first study evaluated the clinical performance in a combined phantom and in-vivo study against a conventional technique. Two radiologists evaluated the B-mode images of breast tumors in 10 patients. Overall, SA was found to have an improved conspicuity, margin sharpness, contrast, and better resolution of the deeper underlying tissue. Diagnostic accuracy was similar with the two techniques (61). The other study was a larger side-by-side comparison with 24 patients and a total of 31 breast lesions (16 malignant and 15 benign). SA was likewise found superior. Three experienced radiologists preferred SA image quality instead of the conventional technique (59).

Hemmsen et al. evaluated SASB image quality in a side-by-side comparison against a conventional technique, where the livers of healthy volunteers were scanned. The two evaluating radiologists found the joint image quality to be equal (66, 67). In a study by Hansen et al. on SASB image quality, five radiologists evaluated 117 image sequences from patients with liver tumors. SASB was favored over the conventional technique; however, the result was not significant (p=0.18) (13).

Overall, SA and SASB B-mode imaging shows promising results, since radiologists prefer these techniques; however, the methods have not managed to improve diagnostic capabilities, even though a higher resolution and improved penetration depth are achieved (10).

The image quality of the combination between THI and SASB was pursued in study I, since both techniques' advantages could be exploited. SASB-THI was evaluated in a preliminary side-by-side comparison against a conventional technique. The liver of healthy volunteers was scanned and the combination of SASB-THI equaled the conventional technique (68). The result was the same in our study, where liver tumors were scanned. Besides image quality evaluation, diagnostic accuracy was evaluated, with sensitivity (50-

76 percent) and specificity (60-96 percent) for diagnosis of focal liver lesion with unenhanced B-mode imaging being similar to previous studies (69-71). The results indicate that SASB-THI is capable of clinical liver scanning.

8.1.4 Clinical implications and future perspectives

With SA, a higher frame rate and resolution, and improved penetration, can be achieved compared to a conventional B-mode (10), while SASB allows a synthetic aperture technique to be implemented on a system with restricted capacity (72). The combination of SASB-THI performs similarly with regard to image quality and pathology detection to a conventional technique for liver imaging; however, SASB's data reduction advantage can be used to produce a wireless transducer system with safe and reliable real-time transmission (12). Wireless transducers improve freedom of movement and help maintain sterile conditions or simplify ultrasound-guided interventions and perioperative scanning (73). This reduction does not lower the quality of the diagnosis, and allows the option of implementation on a hand-held tablet (12). The combination of a wireless transducer with a relatively inexpensive commercial tablet would spread the use of ultrasound to less developed countries, as well as into emergency rooms and ambulances. Hand-held devices have moreover proven to be useful in numerous clinical conditions (74-76) and have been termed the real stethoscope (77).

A major challenge with the spread of ultrasound is the lack of user training and education. With a safe and reliable real-time transmission as demonstrated with SASB (12), an experienced user could assist a novice in acquiring and interpreting images by telesonography (78), which has already been studied in less traditional places such as patient transportation (79) and military operations (80). The development and implementation of SASB and SASB-THI will be exciting to follow.

8.1.5 Limitations

Our experimental setup only allowed data collection with a navigational image from the first stage beamforming with a low frame rate and a poor image quality. The final data selection was performed after second stage beamforming in a blinded setup. Though this reduces the quality of the study, it is only minor as the selection was performed blinded.

However, future data collection with SASB and SASB-THI should be performed with a real-time, second-stage beamforming. Moreover, a higher frame rate and approving algorithm (for example, speckle reduction filter) would have improved the quality. Comparison in more than one organ and with different pathologies would have further improved this study.

8.2 Surveillance of arteriovenous fistula for hemodialysis with VFI

8.2.1 Arteriovenous fistula surveillance

The arteriovenous fistula for hemodialysis is a surgically created connection between an artery and vein. The preferred connection is between the cephalic vein and radial artery, and it is the favorite vascular access for hemodialysis in end-stage renal disease (81, 82). After creation, a rapid flow into the venous system gives a low-resistance circuit with highly increased blood flow, leading to vein dilation and vessel-wall thickening, which is ideal for repeated punctures and hemodialyses (81). However, two-thirds of arteriovenous fistulae will develop varying degree of stenosis after 18 months (81, 83). Stenosis may lead to thrombosis and access failure (81, 84). The National Kidney Foundation Kidney Disease Outcomes Quality Initiative (NKF KDOQI) has recommended monitoring patients with arteriovenous fistulae for many years (82), stating that it should be performed with regular volume flow measurements to detect stenosis. Despite this recommendation, there is an ongoing discussion on the need for regular monitoring (85-87). Paulson et al. called the surveillance program of hemodialysis access a false paradigm based on low evidence (88), and Allon and Ribbon stated that none of the non-invasive surveillance tests available (clinical monitoring, UDT, and spectral Doppler) consistently can distinguish between vascular accesses destined to clot or remain patent (89). However, the recommendations about regular monitoring still apply (82).

8.2.2 Methods for volume flow surveillance

UDT is considered the reference method for volume flow surveillance and is used commonly in comparison studies (49, 84, 90, 91). The method is fairly simple and dialysis staff can be more easily trained (52) than with ultrasound (92). However, UDT has

variations in volume flow up to 30 percent caused by constant changes in mean arterial pressure, central venous pressure, and vascular resistance of the access circuit during each dialysis session, as well as insufficient mixing of the diluting agent (saline) in the blood (85, 90, 93).

Spectral Doppler can also be used for volume flow surveillance, but is unreliable due to operator and angle dependencies (30, 94). Zanen et al. have reported that spectral Doppler overestimates volume flow with a bias of 1,129 ml/min between spectral Doppler (average 1,958 ml/min) and UDT (average 752 ml/min) (95), while Schwarz et al. reported spectral Doppler underestimation of 30 percent compared to UDT (91). When scanning an arteriovenous fistula, the vessel is easily compressed, creating turbulent flow, which affects the velocity estimation with spectral Doppler and may account for varying results (96).

Magnetic resonance angiography (MRA) is another method for volume flow surveillance. Bosman et al. compared UDT to MRA in hemodialysis grafts and found a good correlation (R = 0.91) (97). However, MRA is cumbersome for the patient, time consuming, expensive, and not as available as ultrasound or UDT.

8.2.3 VFI for volume flow surveillance

Hansen et al. established VFI's ability to estimate volume flow in arteriovenous fistulas for hemodialysis, but found an underestimation compared to UDT of 30 percent (44). This study found no underestimation, probably because the three sources of error described by Jensen et al. were considered in the estimation algorithm (47, 48).

The volume flow change between sessions was also considered in our study, since it often is more important than the actual estimation within a single dialysis session when identifying a stenosis. A drop of more than 25 percent may indicate stenosis and is used as advice for referral to angiography (82). UDT may not be the best method to determine the drop in volume flow, since the measurements are performed with the dialysis needles in place. Huisman et al. reported that a different needle position could result in a between-session variation of up to 23.5 percent in radiocephalic fistulas (90). VFI predicted large (greater than 25 percent) between-session changes in volume flow similar to UDT; furthermore, VFI precision (20 percent) was better compared to UDT (32 percent). This may indicate that VFI can estimate volume flow with more accuracy.

An emergent thrombosis evaluated with VFI was not included in our study, as angioplasty data were not considered. However, VFI was more precise, which may indicate that it can predict stenosis with more certainty. With VFI, flow characteristics can easily be determined in real time, and a part of the vessel with laminar flow can be identified. A laminar flow profile is ideal for volume flow calculation by 2D vector-flow maps of VFI (27). Furthermore, VFI can visualize the complexity of blood flow in a manner not possible with conventional spectral Doppler and UDT (43, 98). The flow pattern may be a new factor that should be considered when predicting imminent stenosis in arteriovenous fistulas.

Opposed to UDT, VFI adds the option of a B-mode image. A B-mode gives detailed information about the morphology of the arteriovenous fistulae and other abnormalities such as hematomas, aneurysms, and intraluminal thrombi, which should be treated and monitored to keep the hemodialysis access patent (22, 84). Furthermore, the B-mode can be used for the construction planning of the arteriovenous fistula, for monitoring the maturation and identifying complications, which adds to the argument of educating the dialysis staff in using ultrasound (99).

8.2.4 Comparison analysis

UDT and VFI were compared and analyzed with Bland-Altman plots (53); however, Crichtley et al. argued for precision should be calculated for each method before comparison (54). By determining the precision beforehand, an excepted LOA could be calculated; the equation for precision *P* is given as:

$$P = \frac{2 * STD\left(x_n^a - x_n^b\right)}{\overline{x}} * 100$$

where *n* is the number of patients, *a* and *b* are the two measurements, and $\overline{x}$ is the average value. Given a precision of ± 20 percent for each method, the excepted LOA would be 28.3 percent using the equation for the expected LOA as follows:

$$Exp\_LOA_{x,y} = \sqrt{P_x^2 + P_y^2}$$

where *P* is the precision for each method *x* and *y.* Consequently, a percentage error of up to ± 30 percent of the LOA for the Bland-Altman plot should be accepted, as this is caused by the inaccuracy for each method. Expected LOA was 37 percent between UDT and VFI,

and therefore higher than the suggested 30 percent. Furthermore, LOA for the Bland-Altman was higher (44.5 percent) than the excepted LOA, proving that UDT and VFI cannot be considered interchangeable. However, VFI precision (20 percent) was better compared to UDT (32 percent), indicating that the difference is caused by the inaccuracy found for UDT.

8.2.5 Clinical implications

A major advantage of VFI is fewer operator-dependent settings. Compared with spectral Doppler, where a beam-to-flow angle of less than 70 degrees is needed, VFI can be positioned on the arteriovenous fistula without considering the angle. This means that the operator does not have to angle the transducer, and the likelihood of compressing the arteriovenous fistula and changing the flow pattern is less. Furthermore, the operator does not have to place the range gate and to correct the angle according to flow direction. With VFI, flow is obtained over the whole vessel, and a laminar segment can easily be determined.

8.2.6 Limitations

One limitation was that only arteriovenous fistulas were studied. These are the preferred vascular access choice, but arteriovenous graft is the next option (82). Approximately one-third of patients requiring a vascular access receive a graft (100); hence, the impact of this study would be higher if grafts had been included. Furthermore, commercially available real-time volume flow estimation is still lacking; future development should focus on a user-friendly estimation scheme for use in clinical everyday life.

8.3 Comparison of portal vein velocity obtained by Vector Flow Imaging and spectral Doppler

8.3.1 Portal vein and spectral Doppler

Among the ultrasound parameters assessed on patients with chronic liver disease is portal vein velocity and flow direction, as portal hypertension can lead to a reduced peak velocity and in advanced stages reversed flow (101, 102). Complications to portal hypertension

(for example, ascites, esophageal and gastric varices, and splenomegaly) can be fatal (103) and spectral-Doppler-measured changes can indicate development (104, 105). Doppler ultrasound should be repeated every time a new clinical event occurs to rule out portal vein thrombosis and hepatocellular carcinoma, which frequently exacerbate portal hypertension and clinical decompensation (106). Portal vein flow and velocity changes are well correlated with staging of liver cirrhosis and development of portal hypertension (107). The preferred scan position for portal vein velocity estimation with spectral Doppler is the intercostal view, as a beam-to-flow angle of less than 70 degrees can be achieved for all patients (106). With a subcostal view, the main portal vein can easily be visualized, but the beam-to-flow angle is often greater than 70 degrees, thus giving less precise spectral Doppler estimates (Fig. 14). Furthermore, the poor inter-oberserver agreement with spectral Doppler causes measurement errors (33, 34).

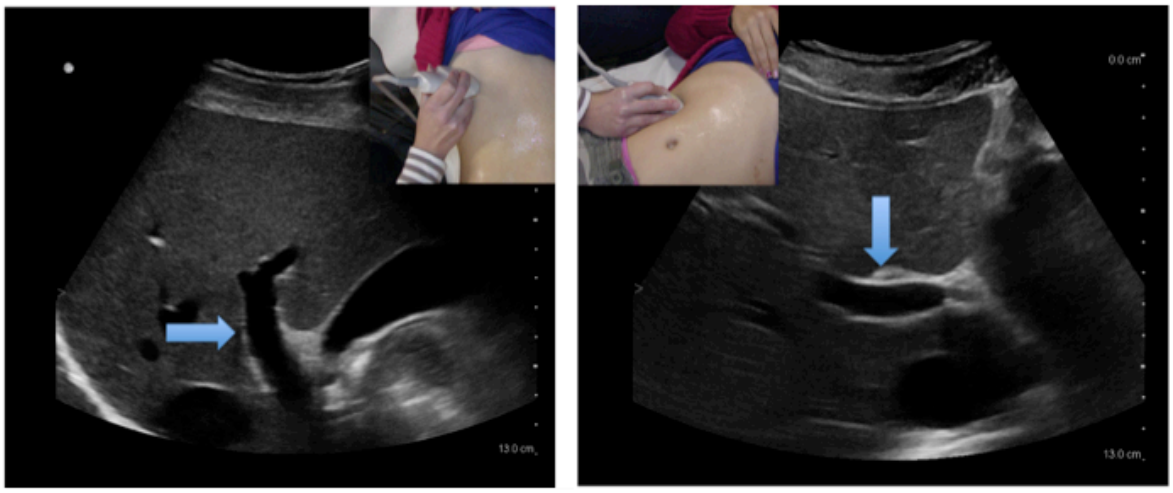

Figure 14: The intercostal view of the mean portal vein is shown on the left side, while the subcostal view is shown on the right side.

8.3.2 Previous comparison studies

Spectral Doppler overestimation of velocities is well known (30, 108, 109). Tortoli et al. showed that spectral Doppler overestimates the velocities in the common carotid artery and internal carotid artery by 27 percent to 43 percent, as compared to an angle-tracking vector Doppler method and a plane wave vector Doppler method (110). Pedersen et al. showed spectral Doppler overestimation in the common carotid artery velocity by 6.9 cm/s

compared to TO (42). The operator-dependent manual angle correction and adjustment of sample volume have a great impact on the overestimation (94). The operator manually sets the cursor parallel to the vessel wall as it is assumed that the flow is laminar. The estimated angle is used in relation to the equation stated below to determine the velocity:

$$v = v_z / \cos \theta$$

where v is the true velocity, v_z is the axial velocity, and θ is the angle of insonation. The assumption that the flow is laminar may not be true, as well as that a single angle is involved (110). This may be the main reason for spectral Doppler errors in velocity estimation (111, 112). Furthermore, the error of the velocity estimation becomes bigger with increasing beam-to-flow angles mainly caused by the spectral broadening effect (108, 113).

Ekroll et al. suggested a solution to operator dependencies for spectral Doppler by combining B-mode, spectral Doppler, and vector flow using plane wave imaging and obtaining automatic vector and Doppler simultaneously (114). This approach has potential since manual placement of the sample volume would be facilitated, thus improving the inter-observer variability. VFI has the same advantages, and inter-observer variability was improved compared to spectral Doppler in study III. The far fewer adjustments needed for VFI may be the reason for the better inter-observer agreement as compared to spectral Doppler.

A previous commercial linear array VFI implementation has shown a systematic underestimation of 10-14 percent on a flowrig (39, 55), while the convex array VFI implementation evaluated in this study showed no underestimation compared to a flowrig. The VFI underestimation for the linear array is caused by the estimation algorithm (115), the PRF settings (116), and an inadequate temporal resolution (42). This seems to be solved for the convex array VFI implementation as described by Jensen et al. (115).

8.3.3 Clinical implications

Patients suffering from chronic liver disease may benefit from the convex array VFI implementation, as correct estimates can be obtained regardless of the insonation window. Performing measurements with spectral Doppler using an intercostal view is

recommended since the insonation angle is close to zero degrees (106). Even though errors with spectral Doppler velocity estimates are well established, it is accepted as a useful method for portal peak velocity estimation and diagnosis of portal hypertension (20, 117). With VFI, the portal blood flow examination of these patients could be more reliable, and sensitivity and specificity for portal hypertension diagnosis may even be higher. Furthermore, for the evaluation of patients with altered portal vein positions due to liver surgery or liver transplantation, the examination would be easier, as any scan position can be applied without hampering the velocity estimates.

8.3.4 Limitations

Some limitations with VFI must be mentioned. We found 95 mm to be the maximum scan depth. Patients are often more obese than healthy volunteers, and with a growing obesity problem in modern societies, development of VFI in terms of penetration is still needed. Nine percent of the healthy volunteers (n=3) were excluded due to this limitation, while estimates could be achieved with spectral Doppler for those patients. Thus, at the moment, VFI should be regarded as a supplement to the spectral Doppler examination. Furthermore, no real-time estimate of peak velocity is given with VFI. A commercially available, real-time, user-friendly estimation scheme is warranted. A system where the operator could indicate in which area of the vessel information of velocities should be estimated as with a spectral Doppler range gate will improve the usability.

9 Conclusion

The overall aim of this thesis was to clinically evaluate new ultrasound methods concerning B-mode and blood flow imaging. CFU has the expertise in developing ultrasound techniques, while RAD has the clinical understanding. The collaboration between CFU and RAD gives unique conditions for developing the use of ultrasound.

In the first study, we concluded that the combination of SASB and THI gives image quality and diagnostic accuracy equal to conventional imaging techniques combined with THI. The advantage of SASB data reduction can be used for development of a wireless transducer capable of working on a hand-held tablet. Furthermore, the image evaluation program must be acknowledged. The programme enables evaluation of dynamic image sequence obtained simultaneously, which is unique for the image quality program developed by CFU.

In the second study, we concluded that VFI could be used for volume flow surveillance in arteriovenous fistulas for hemodialysis. Volume flow estimates were not significantly different from values obtained with the reference method; nevertheless, while VFI was more precise, but not interchangeable with the reference method. For large volume flow changes in between hemodialysis sessions, VFI was in concordance with the reference method. A user-friendly, real-time estimation scheme for commercial use is still lacking. We advocate for the use of VFI for hemodialysis access surveillance.

In the third study, we concluded that VFI can obtain similar peak velocities as spectral Doppler in the main portal vein. Furthermore, we concluded that VFI had a better precision and could estimate equal peak velocities with a view, which was inapplicable for spectral Doppler. Intra-and inter-observer agreement was for the first time evaluated for VFI and found better than for spectral Doppler. Results of future studies, where VFI peak velocity is estimated on patients with chronic liver disease, are definitely exciting, as VFI may heighten the diagnosis for portal hypertension as the diagnosis can be set with more certainty. The convex implementation of VFI may benefit patients and help healthcare workers in the assessment of abdominal vessel pathology.

10 Perspectives

Several potential clinical studies can be performed with both SASB-THI and VFI.

SASB-THI:

A study concerning SASB-THI image quality and diagnostic accuracy for more than one organ and different pathologies.

In our study, the evaluators found SASB-THI to be equally effective in liver imaging as the reference method. SASB-THI could improve diagnosis in several clinical cases as a better resolution and contrast is provided over the conventional technique. A study concerning several pathologies would therefore be beneficial.

A user experience study with a completed wireless transducer based on SASB-THI.

This study could reveal the advantages of a wireless transducer. Several clinical conductions could be facilitated.

VFI:

A large multicenter study where VFI is used for volume flow surveillance in arteriovenous fistulas by several users and dialysis centers.

VFI has the potential of replacing the reference method due to its higher precision. This study would reveal these advantages and change the way we manage patients with arteriovenous fistulas.

A comparison study, where MRA-obtained volume flow is compared to VFI estimates in arteriovenous fistulas and arteriovenous graft.

VFI has the potential to work in grafts as well. Furthermore, comparison to MRA would give a clearer indication of VFI ability to estimate volume flow in arteriovenous fistulas.

A study comparing percutaneous transluminal angioplasty data to VFI data to determine whether VFI can identify hemodynamic significant stenosis correctly.

VFI could be a more reliable method to determine stenosis due to higher precision.

A study evaluating whether vector concentration for VFI can predict arteriovenous fistula stenosis.

VFI can differentiate flow characteristics and this may be a new factor to determine upcoming stenosis.

A study validating the convex array VFI implementation on patients with varying degree of portal hypertension.

Since VFI has a higher precision than spectral Doppler for portal vein peak velocity estimation, the portal hypertension diagnosis can potentially be set with higher certainty.

A study concerning velocity estimation of other abdominal vessel were the angle independency would be an advantage (a. renalis, truncus coeliacus, a. mesenteria superior).

VFI could potentially improve diagnosis and give new insights to flow dynamics for abdominal vessel pathology.

11 References

1. Beach KW. 1975-2000: a quarter century of ultrasound technology. Ultrasound in medicine & biology. 1992;18(4):377-88.
2. Tegeler CH, Kremkau FW, Hitchings LP. Color velocity imaging: introduction to a new ultrasound technology. Journal of neuroimaging : official journal of the American Society of Neuroimaging. 1991;1(2):85-90.
3. Newman PG, Rozycki GS. The history of ultrasound. Surgical clinics of North America. 1998;78(2):179-95.
4. Jensen JA. Medical ultrasound imaging. Progress in biophysics and molecular biology. 2007;93(1):153-65.
5. Sherwin CW, Ruina JP, Rawcliffe RD. Some early developments in synthetic aperture radar systems. Military Electronics, IRE Transactions on. 1962;MIL-6(2):111-5.
6. Burckhardt CB, Grandchamp PA, Hoffmann H. An experimental 2 MHz synthetic aperture sonar system intended for medical use. Sonics and Ultrasonics, IEEE Transactions on. 1974;21(1):1-6.
7. Karaman M, Pai-Chi L, O'Donnell M. Synthetic aperture imaging for small scale systems. Ultrasonics, Ferroelectrics, and Frequency Control, IEEE Transactions on. 1995;42(3):429-42.
8. Lockwood GR, Foster FS, editors. Design of sparse array imaging systems. Ultrasonics Symposium, 1995 Proceedings, 1995 IEEE; 1995 7-10 Nov 1995.
9. Nikolov SI, Technical University of D, Ørsted DTU. Synthetic aperture tissue and flow ultrasound imaging. Lyngby 2001, thesis.
10. Jensen JA, Nikolov SI, Gammelmark KL, Pedersen MH. Synthetic aperture ultrasound imaging. Ultrasonics. 2006;44(Suppl 1):e5-15.
11. Kortbek J, Jensen JA, Gammelmark KL, editors. Synthetic aperture sequential beamforming. Ultrasonics Symposium (IUS), 2008 IEEE International; 2-5 Nov. 2008.
12. Hemmsen MC, Kjeldsen T, Larsen L, Kjær C, Tomov BG, Mosegaard J, et al. Implementation of synthetic aperture imaging on a hand-held device. Ultrasonics Symposium (IUS), 2014 IEEE International; 3-6 Sept. 2014.

13. Hansen PM, Hemmsen M, Brandt A, Rasmussen J, Lange T, Krohn PS, et al. Clinical evaluation of synthetic aperture sequential beamforming ultrasound in patients with liver tumors. Ultrasound in medicine & biology. 2014;40(12):2805-10.
14. Hemmsen MC, Hansen JM, Jensen JA, editors. Synthetic aperture sequential beamformation applied to medical imaging. Synthetic Aperture Radar, 2012 EUSAR 9th European Conference on; 23-26 April 2012.
15. Du Y, Rasmussen J, Jensen H, Jensen JA, editors. Second harmonic imaging using synthetic aperture sequential beamforming. Ultrasonics Symposium (IUS), 2011 IEEE International; 18-21 Oct. 2011.
16. Rasmussen J, Hemmsen MC, Madsen SS, Hansen PM, Nielsen MB, Jensen JA. Implementation of Tissue Harmonic Synthetic Aperture Imaging on a Commercial Ultrasound System. Ultrasonics Symposium (IUS), 2012 IEEE International; 7-10 Oct. 2012.
17. Hemmsen MC, Rasmussen J, Jensen JA. Tissue Harmonic Synthetic Aperture Ultrasound Imaging. Journal of the Acoustical Society of America. 2014;136:2050.
18. Ward B, Baker AC, Humphrey VF. Nonlinear propagation applied to the improvement of resolution in diagnostic medical ultrasound. The Journal of the acoustical society of America. 1997;101(1):143-54.
19. Tranquart F, Grenier N, Eder V, Pourcelot L. Clinical use of ultrasound tissue harmonic imaging. Ultrasound in medicine & biology. 1999;25(6):889-94.
20. Iwao T, Toyonaga A, Oho K, Tayama C, Masumoto H, Sakai T, et al. Value of Doppler ultrasound parameters of portal vein and hepatic artery in the diagnosis of cirrhosis and portal hypertension. The American journal of gastroenterology. 1997;92(6):1012-7.
21. Iranpour P, Lall C, Houshyar R, Helmy M, Yang A, Choi JI, et al. Altered Doppler flow patterns in cirrhosis patients: an overview. Ultrasonography (Seoul, Korea). 2016;35(1):3-12.
22. Malik J, Kudlicka J, Novakova L, Adamec J, Malikova H, Kavan J. Surveillance of arteriovenous accesses with the use of duplex Doppler ultrasonography. The journal of vascular access. 2014;15(Suppl 7):S28-32.

23. Bozoghlanian M, Lall C, Houshyar R, Helmy M, Cody ME, Bhargava P, et al. Duplex Doppler Imaging of Dialysis Fistulae and Grafts. Current problems in diagnostic radiology. 2015. Epub ahead of print.
24. Grant EG, Benson CB, Moneta GL, Alexandrov AV, Baker JD, Bluth EI, et al. Carotid artery stenosis: gray-scale and Doppler US diagnosis--Society of Radiologists in Ultrasound Consensus Conference. Radiology. 2003;229(2):340-6.
25. Voiculescu A, Hofer M, Hetzel GR, Malms J, Modder U, Grabensee B, et al. Noninvasive investigation for renal artery stenosis: contrast-enhanced magnetic resonance angiography and color Doppler sonography as compared to digital subtraction angiography. Clinical and experimental hypertension. 2001;23(7):521-31.
26. Rountas C, Vlychou M, Vassiou K, Liakopoulos V, Kapsalaki E, Koukoulis G, et al. Imaging modalities for renal artery stenosis in suspected renovascular hypertension: prospective intraindividual comparison of color Doppler US, CT angiography, GD-enhanced MR angiography, and digital substraction angiography. Renal failure. 2007;29(3):295-302.
27. Hansen KL, Udesen J, Thomsen C, Jensen JA, Nielsen MB. In vivo validation of a blood vector velocity estimator with MR angiography. IEEE transactions on ultrasonics, ferroelectrics, and frequency control. 2009;56(1):91-100.
28. Ricci S, Diciotti S, Francalanci L, Tortoli P. Accuracy and reproducibility of a novel dual-beam vector Doppler method. Ultrasound in medicine & biology. 2009;35(5):829-38.
29. Landwehr P, Schulte O, Voshage G. Ultrasound examination of carotid and vertebral arteries. European radiology. 2001;11(9):1521-34.
30. Stewart SF. Effects of transducer, velocity, Doppler angle, and instrument settings on the accuracy of color Doppler ultrasound. Ultrasound in medicine & biology. 2001;27(4):551-64.
31. Logason K, Barlin T, Jonsson ML, Bostrom A, Hardemark HG, Karacagil S. The importance of Doppler angle of insonation on differentiation between 50-69% and 70-99% carotid artery stenosis. European journal of vascular and endovascular surgery: the official journal of the European Society for Vascular Surgery. 2001;21(4):311-3.

32. Hoskins PR. A review of the measurement of blood velocity and related quantities using Doppler ultrasound. Proceedings of the Institution of Mechanical Engineers Part H, Journal of engineering in medicine. 1999;213(5):391-400.
33. Sacerdoti D, Gaiani S, Buonamico P, Merkel C, Zoli M, Bolondi L, et al. Interobserver and interequipment variability of hepatic, splenic, and renal arterial Doppler resistance indices in normal subjects and patients with cirrhosis. Journal of hepatology. 1997;27(6):986-92.
34. Sabba C, Merkel C, Zoli M, Ferraioli G, Gaiani S, Sacerdoti D, et al. Interobserver and interequipment variability of echo-Doppler examination of the portal vein: effect of a cooperative training program. Hepatology (Baltimore, Md). 1995;21(2):428-33.
35. Hoskins PR. Peak velocity estimation in arterial stenosis models using colour vector Doppler. Ultrasound in medicine & biology. 1997;23(6):889-97.
36. Dunmire B, Beach KW, Labs K, Plett M, Strandness DE, Jr. Cross-beam vector Doppler ultrasound for angle-independent velocity measurements. Ultrasound in medicine & biology. 2000;26(8):1213-35.
37. Bohs LN, Geiman BJ, Anderson ME, Gebhart SC, Trahey GE. Speckle tracking for multi-dimensional flow estimation. Ultrasonics. 2000;38(1-8):369-75.
38. Jensen JA, Munk P. A new method for estimation of velocity vectors. IEEE transactions on ultrasonics, ferroelectrics, and frequency control. 1998;45(3):837-51.
39. Udesen J, Jensen JA. Investigation of transverse oscillation method. IEEE transactions on ultrasonics, ferroelectrics, and frequency control. 2006;53(5):959-71.
40. Hoskins P, Kenwright D. Recent developments in vascular ultrasound technology. Ultrasound. 2015;23(3):158-65.
41. Hansen KL, Udesen J, Oddershede N, Henze L, Thomsen C, Jensen JA, et al. In vivo comparison of three ultrasound vector velocity techniques to MR phase contrast angiography. Ultrasonics. 2009;49(8):659-67.
42. Pedersen MM, Pihl MJ, Haugaard P, Hansen JM, Hansen KL, Nielsen MB, et al. Comparison of real-time in vivo spectral and vector velocity estimation. Ultrasound in medicine & biology. 2012;38(1):145-51.

43. Pedersen MM, Pihl MJ, Haugaard P, Hansen KL, Lange T, Lonn L, et al. Novel flow quantification of the carotid bulb and the common carotid artery with vector flow ultrasound. Ultrasound in medicine & biology. 2014;40(11):2700-6.
44. Hansen PM, Olesen JB, Pihl MJ, Lange T, Heerwagen S, Pedersen MM, et al. Volume flow in arteriovenous fistulas using vector velocity ultrasound. Ultrasound in medicine & biology. 2014;40(11):2707-14.
45. Hansen KL, Moller-Sorensen H, Kjaergaard J, Jensen MB, Lund JT, Pedersen MM, et al. Analysis of systolic backflow and secondary helical blood flow in the ascending aorta using vector flow imaging. Ultrasound in medicine & biology. 2016;42(4):899-908.
46. Hansen KL, Moller-Sorensen H, Pedersen MM, Hansen PM, Kjaergaard J, Lund JT, et al. First report on intraoperative vector flow imaging of the heart among patients with healthy and diseased aortic valves. Ultrasonics. 2015;56:243-50.
47. Jensen J, Olesen JB, Hansen PM, Nielsen MB, Jensen JA, Jensen J, et al. Accuracy and sources of error for an angle independent volume flow estimator. Proceedings of IEEE International Ultrasonics Symposium: IEEE; 2014. p. 1714-7.
48. Jensen J, Olesen JB, Stuart MB, Hansen PM, Nielsen MB, Jensen JA. Vector velocity volume flow estimation: Sources of error and corrections applied for arteriovenous fistulas. Ultrasonics. 2016;70:136-46.
49. Badr B, Bories P, Marais R, Frat B, Seigneuric B, Longlune N, et al. Transonic, thermodilution, or ionic dialysance to manage vascular access: which method is best? International Symposium on Home Hemodialysis. 2014;18(1):127-35.
50. Tessitore N, Bedogna V, Gammaro L, Lipari G, Poli A, Baggio E, et al. Diagnostic accuracy of ultrasound dilution access blood flow measurement in detecting stenosis and predicting thrombosis in native forearm arteriovenous fistulae for hemodialysis. American journal of kidney diseases: the official journal of the National Kidney Foundation. 2003;42(2):331-41.
51. Krivitski NM. Theory and validation of access flow measurement by dilution technique during hemodialysis. Kidney international. 1995;48(1):244-50.
52. Depner TA, Krivitski NM. Clinical measurement of blood flow in hemodialysis access fistulae and grafts by ultrasound dilution. ASAIO journal (American Society for Artificial Internal Organs: 1992). 1995;41(3):M745-9.

53. Bland JM, Altman DG. Statistical methods for assessing agreement between two methods of clinical measurement. Lancet. 1986;1(8476):307-10.
54. Critchley LA, Critchley JA. A meta-analysis of studies using bias and precision statistics to compare cardiac output measurement techniques. Journal of clinical monitoring and computing. 1999;15(2):85-91.
55. Hansen KL, Moller-Sorensen H, Kjaergaard J, Jensen MB, Lund JT, Pedersen MM, et al. Vector flow imaging compared with conventional doppler ultrasound and thermodilution for estimation of blood flow in the ascending aorta. Ultrasonic imaging. 2015. Epub ahead of print.
56. Moller-Sorensen H, Hansen KL, Ostergaard M, Andersen LW, Moller K. Lack of agreement and trending ability of the endotracheal cardiac output monitor compared with thermodilution. Acta anaesthesiologica Scandinavica. 2012;56(4):433-40.
57. Yen CL, Jeng CM, Yang SS. The benefits of comparing conventional sonography, real-time spatial compound sonography, tissue harmonic sonography, and tissue harmonic compound sonography of hepatic lesions. Clin Imaging. 2008;32(1):11-5.
58. Sodhi KS, Sidhu R, Gulati M, Saxena A, Suri S, Chawla Y. Role of tissue harmonic imaging in focal hepatic lesions: comparison with conventional sonography. Journal of gastroenterology and hepatology. 2005;20(10):1488-93.
59. Kim WH, Chang JM, Kim C, Park J, Yoo Y, Moon WK, et al. Synthetic aperture imaging in breast ultrasound: a preliminary clinical study. Academic radiology. 2012;19(8):923-9.
60. Choudhry S, Gorman B, Charboneau JW, Tradup DJ, Beck RJ, Kofler JM, et al. Comparison of tissue harmonic imaging with conventional US in abdominal disease. Radiographics: a review publication of the Radiological Society of North America, Inc. 2000;20(4):1127-35.
61. Kim C, Yoon C, Park JH, Lee Y, Kim WH, Chang JM, et al. Evaluation of ultrasound synthetic aperture imaging using bidirectional pixel-based focusing: preliminary phantom and in vivo breast study. IEEE transactions on bio-medical engineering. 2013;60(10):2716-24.
62. Tanaka S, Oshikawa O, Sasaki T, Ioka T, Tsukuma H. Evaluation of tissue harmonic imaging for the diagnosis of focal liver lesions. Ultrasound in medicine & biology. 2000;26(2):183-7.

63. Yen CL, Chang HY, Huang SY, Huang YC, Jeng CM. Combination of tissue harmonic sonography, real-time spatial compound sonography and adaptive image processing technique for the detection of carotid plaques and intima-medial thickness. Eur J Radiol. 2009;71(1):11-6.
64. Mesurolle B, Helou T, El-Khoury M, Edwardes M, Sutton EJ, Kao E. Tissue harmonic imaging, frequency compound imaging, and conventional imaging: use and benefit in breast sonography. Journal of ultrasound in medicine: official journal of the American Institute of Ultrasound in Medicine. 2007;26(8):1041-51.
65. Schmidt T, Hohl C, Haage P, Blaum M, Honnef D, Weibeta C, et al. Diagnostic accuracy of phase-inversion tissue harmonic imaging versus fundamental B-mode sonography in the evaluation of focal lesions of the kidney. AJR American journal of roentgenology. 2003;180(6):1639-47.
66. Hemmsen MC, Hansen PM, Lange T, Hansen JM, Hansen KL, Nielsen MB, et al. In vivo evaluation of synthetic aperture sequential beamforming. Ultrasound in medicine & biology. 2012;38(4):708-16.
67. Hemmsen MC, Hansen PM, Lange T, Hansen JM, Nikolov SI, Nielsen MB, et al., editors. Preliminary in-vivo evaluation of synthetic aperture sequential beamformation using a multielement convex array. Ultrasonics Symposium (IUS), 2011 IEEE International; 18-21 Oct. 2011.
68. Rasmussen JH, Hemmsen MC, Madsen SS, Hansen PM, Nielsen MB, Jensen JA, editors. Preliminary study of synthetic aperture tissue harmonic imaging on in-vivo Proc. SPIE 8675, Medical Imaging 2013: Ultrasonic Imaging, Tomography, and Therapy, 867512 (March 29, 2013).
69. Beissert M, Jenett M, Keberle M. Comparison of contrast harmonic imaging in B-mode with stimulated acoustic emission, conventional B-mode US and spiral CT in the detection of focal liver lesions. Fortschr Röntgenstr. 2000;172:361-6.
70. Glover C, Douse P, Kane P, Karani J, Meire H, Mohammadtaghi S, et al. Accuracy of investigations for asymptomatic colorectal liver metastases. Diseases of the colon & rectum. 2002;45(4):476-84.
71. Cantisani V, Grazhdani H, Fioravanti C, Rosignuolo M, Calliada F, Messineo D, et al. Liver metastases: Contrast-enhanced ultrasound compared with computed

tomography and magnetic resonance. World journal of gastroenterology : WJG. 2014;20(29):9998-10007.
72. Kortbek J, Jensen JA, Gammelmark KL. Sequential beamforming for synthetic aperture imaging. Ultrasonics. 2013;53(1):1-16.
73. Munoz DR, Zamorano JL. Wireless echocardiography: a step towards the future. European heart journal. 2014;35(26):1700.
74. Lapostolle F, Petrovic T, Lenoir G, Catineau J, Galinski M, Metzger J, et al. Usefulness of hand-held ultrasound devices in out-of-hospital diagnosis performed by emergency physicians. The American journal of emergency medicine. 2006;24(2):237-42.
75. Prinz C, Voigt JU. Diagnostic accuracy of a hand-held ultrasound scanner in routine patients referred for echocardiography. Journal of the American Society of Echocardiography : official publication of the American Society of Echocardiography. 2011;24(2):111-6.
76. Choi BG, Mukherjee M, Dala P, Young HA, Tracy CM, Katz RJ, et al. Interpretation of remotely downloaded pocket-size cardiac ultrasound images on a web-enabled smartphone: validation against workstation evaluation. Journal of the American Society of Echocardiography : official publication of the American Society of Echocardiography. 2011;24(12):1325-30.
77. Breithardt OA. Hand-held ultrasound-the real stethoscope. European heart journal cardiovascular Imaging. 2015;16(5):471-2.
78. Liteplo AS, Noble VE, Attwood B. Real-time video transmission of ultrasound images to an iPhone. Critical ultrasound journal. 2010;1(3):105-10.
79. Garrett PD, Boyd SY, Bauch TD, Rubal BJ, Bulgrin JR, Kinkler ES, Jr. Feasibility of real-time echocardiographic evaluation during patient transport. Journal of the American Society of Echocardiography : official publication of the American Society of Echocardiography. 2003;16(3):197-201.
80. Strode CA, Rubal BJ, Gerhardt RT, Bulgrin JR, Boyd SY. Wireless and satellite transmission of prehospital focused abdominal sonography for trauma. Prehospital emergency care : official journal of the National Association of EMS Physicians and the National Association of State EMS Directors. 2003;7(3):375-9.

81. Huijbregts HJ, Bots ML, Wittens CH, Schrama YC, Moll FL, Blankestijn PJ. Hemodialysis arteriovenous fistula patency revisited: results of a prospective, multicenter initiative. Clinical journal of the American Society of Nephrology : CJASN. 2008;3(3):714-9.
82. Clinical Practice Guidelines for Vascular Access. American Journal of Kidney Diseases. 2006;48, Supplement 1(0):S176-S247.
83. Wiese P, Nonnast-Daniel B. Colour Doppler ultrasound in dialysis access. Nephrology, dialysis, transplantation : official publication of the European Dialysis and Transplant Association - European Renal Association. 2004;19(8):1956-63.
84. Whittier WL. Surveillance of hemodialysis vascular access. Seminars in interventional radiology. 2009;26(2):130-8.
85. Paulson WD, Moist L, Lok CE. Vascular access surveillance: an ongoing controversy. Kidney international. 2012;81(2):132-42.
86. Casey ET, Murad MH, Rizvi AZ, Sidawy AN, McGrath MM, Elamin MB, et al. Surveillance of arteriovenous hemodialysis access: a systematic review and meta-analysis. Journal of vascular surgery. 2008;48(5 Suppl):48s-54s.
87. Muchayi T, Salman L, Tamariz LJ, Asif A, Rizvi A, Lenz O, et al. A meta-analysis of randomized clinical trials assessing hemodialysis access thrombosis based on access flow monitoring: where do we stand? Seminars in dialysis. 2015;28(2):E23-9.
88. Paulson WD, Moist L, Lok CE. Vascular access surveillance: case study of a false paradigm. Seminars in dialysis. 2013;26(3):281-6.
89. Allon M, Robbin ML. Hemodialysis vascular access monitoring: Current concepts. Hemodialysis International. 2009;13(2):153-62.
90. Huisman RM, van Dijk M, de Bruin C, Loonstra J, Sluiter WJ, Zeebregts CJ, et al. Within-session and between-session variability of haemodialysis shunt flow measurements. Nephrology, dialysis, transplantation : official publication of the European Dialysis and Transplant Association - European Renal Association. 2005;20(12):2842-7.
91. Schwarz C, Mitterbauer C, Boczula M, Maca T, Funovics M, Heinze G, et al. Flow monitoring: performance characteristics of ultrasound dilution versus color Doppler ultrasound compared with fistulography. American journal of kidney diseases : the official journal of the National Kidney Foundation. 2003;42(3):539-45.
92. van Hooland S, Malik J. Hemodialysis vascular access ultrasonography: tips, tricks, pitfalls and a quiz. The journal of vascular access. 2010;11(4):255-62.

93. Heerwagen ST, Hansen MA, Schroeder TV, Ladefoged SD, Lonn L. Blood flow measurements during hemodialysis vascular access interventions--catheter-based thermodilution or Doppler ultrasound? The journal of vascular access. 2012;13(2):145-51.
94. Lui EYL, Steinman AH, Cobbold RSC, Johnston KW. Human factors as a source of error in peak Doppler velocity measurement. Journal of vascular surgery. 2005;42(5):972.e1-.e10.
95. Zanen AL, Toonder IM, Korten E, Wittens CH, Diderich PN. Flow measurements in dialysis shunts: lack of agreement between conventional Doppler, CVI-Q, and ultrasound dilution. Nephrology, dialysis, transplantation : official publication of the European Dialysis and Transplant Association - European Renal Association. 2001;16(2):395-9.
96. Teodorescu V, Gustavson S, Schanzer H. Duplex ultrasound evaluation of hemodialysis access: a detailed protocol. International journal of nephrology. 2012;2012:508956.
97. Bosman PJ, Boereboom FT, Bakker CJ, Mali WP, Eikelboom BC, Blankestijn PJ, et al. Access flow measurements in hemodialysis patients: in vivo validation of an ultrasound dilution technique. Journal of the American Society of Nephrology : JASN. 1996;7(6):966-9.
98. Hansen KL, Moller-Sorensen H, Kjaergaard J, Jensen MB, Lund JT, Pedersen MM, et al. Intra-operative vector flow imaging using ultrasound of the ascending aorta among 40 patients with normal, stenotic and replaced aortic valves. Ultrasound in medicine & biology. 2016;42(10):2414-22.
99. Lomonte C, Meola M, Petrucci I, Casucci F, Basile C. The key role of color doppler ultrasound in the work-up of hemodialysis vascular access. Seminars in dialysis. 2015;28(2):211-5.
100. Sidawy AN, Spergel LM, Besarab A, Allon M, Jennings WC, Padberg FT, Jr., et al. The Society for Vascular Surgery: clinical practice guidelines for the surgical placement and maintenance of arteriovenous hemodialysis access. Journal of vascular surgery. 2008;48(5 Suppl):2s-25s.
101. Davis M, Chong WK. Doppler ultrasound of the liver, portal hypertension, and transjugular intrahepatic portosystemic shunts. Ultrasound clinics. 9(4):587-604.

102. Kok T, van der Jagt EJ, Haagsma EB, Bijleveld CM, Jansen PL, Boeve WJ. The value of Doppler ultrasound in cirrhosis and portal hypertension. Scandinavian journal of gastroenterology Supplement. 1999;230:82-8.
103. Dib N, Oberti F, Cales P. Current management of the complications of portal hypertension: variceal bleeding and ascites. CMAJ : Canadian Medical Association journal = journal de l'Association medicale canadienne. 2006;174(10):1433-43.
104. Shastri M, Kulkarni S, Patell R, Jasdanwala S. Portal vein Doppler: a tool for non-invasive prediction of esophageal varices in cirrhosis. Journal of clinical and diagnostic research : JCDR. 2014;8(7):MC12-MC5.
105. Kayacetin E, Efe D, Dogan C. Portal and splenic hemodynamics in cirrhotic patients: relationship between esophageal variceal bleeding and the severity of hepatic failure. Journal of gastroenterology. 2004;39(7):661-7.
106. Berzigotti A, Piscaglia F. Ultrasound in portal hypertension--part 2--and EFSUMB recommendations for the performance and reporting of ultrasound examinations in portal hypertension. Ultraschall in der Medizin (Stuttgart, Germany : 1980). 2012;33(1):8-32.
107. Zekanovic D, Ljubicic N, Boban M, Nikolic M, Delic-Brkljacic D, Gacina P, et al. Doppler ultrasound of hepatic and system hemodynamics in patients with alcoholic liver cirrhosis. Digestive diseases and sciences. 2010;55(2):458-66.
108. Hoskins PR. A comparison of single- and dual-beam methods for maximum velocity estimation. Ultrasound in medicine & biology. 1999;25(4):583-92.
109. Park MY, Jung SE, Byun JY, Kim JH, Joo GE. Effect of beam-flow angle on velocity measurements in modern Doppler ultrasound systems. AJR American journal of roentgenology. 2012;198(5):1139-43.
110. Tortoli P, Lenge M, Righi D, Ciuti G, Liebgott H, Ricci S. Comparison of carotid artery blood velocity measurements by vector and standard Doppler approaches. Ultrasound in medicine & biology. 2015;41(5):1354-62.
111. Steinman AH, Tavakkoli J, Myers JG, Jr., Cobbold RS, Johnston KW. Sources of error in maximum velocity estimation using linear phased-array Doppler systems with steady flow. Ultrasound in medicine & biology. 2001;27(5):655-64.
112. Thrush A, Evans D. Intrinsic spectral broadening: a potential cause of misdiagnosis of carotid artery disease. J Vasc Invest. 1995;1(4):187-92.

113. Yang X, Sun C, Anderson T, Moran CM, Hadoke PW, Gray GA, et al. Assessment of spectral Doppler in preclinical ultrasound using a small-size rotating phantom. Ultrasound in medicine & biology. 2013;39(8):1491-9.
114. Ekroll IK, Dahl T, Torp H, Lovstakken L. Combined vector velocity and spectral Doppler imaging for improved imaging of complex blood flow in the carotid arteries. Ultrasound in medicine & biology. 2014;40(7):1629-40.
115. Jensen JA, Brandt AH, Nielsen MB. Convex array vector velocity imaging using transverse oscillation and its optimization. IEEE transactions on ultrasonics, ferroelectrics, and frequency control. 2015;62(12):2043-53.
116. Hansen KL, Pedersen MM, Moller-Sorensen H, Kjaergaard J, Nilsson JC, Lund JT, et al. Intraoperative cardiac ultrasound examination using vector flow imaging. Ultrasonic imaging. 2013;35(4):318-32.
117. Kruskal JB, Newman PA, Sammons LG, Kane RA. Optimizing Doppler and color flow US: application to hepatic sonography. Radiographics : a review publication of the Radiological Society of North America, Inc. 2004;24(3):657-75.

12 Appendices

12.1 Appendix I (Paper I)

Ultrasound in Med. & Biol., Vol. ■, No. ■, pp. 1–8, 2015

0301-5629/$ - see front matter

ELSEVIER

http://dx.doi.org/10.1016/j.ultrasmedbio.2015.05.008

● *Original Contribution*

CLINICAL EVALUATION OF SYNTHETIC APERTURE HARMONIC IMAGING FOR SCANNING FOCAL MALIGNANT LIVER LESIONS

ANDREAS HJELM BRANDT,* MARTIN CHRISTIAN HEMMSEN,† PETER MØLLER HANSEN,* SIGNE SLOTH MADSEN,* PAUL SUNO KROHN,‡ THEIS LANGE,§ KRISTOFFER LINDSKOV HANSEN,* JØRGEN ARENDT JENSEN,† and MICHAEL BACHMANN NIELSEN*

*Department of Radiology, Rigshospitalet, Copenhagen University Hospital, Copenhagen, Denmark; †Center for Fast Ultrasound Imaging, Department of Electrical Engineering, Technical University of Denmark, Lyngby, Denmark; ‡Department of Surgical Gastroenterology, Rigshospitalet, Copenhagen University Hospital, Copenhagen, Denmark; and §Department of Biostatistics, University of Copenhagen, Copenhagen, Denmark

(*Received* 25 *February* 2015; *revised* 13 *April* 2015; *in final form* 11 *May* 2015)

Abstract—The purpose of the study was to perform a clinical comparison of synthetic aperture sequential beamforming tissue harmonic imaging (SASB-THI) sequences with a conventional imaging technique, dynamic receive focusing with THI (DRF-THI). Both techniques used pulse inversion and were recorded interleaved using a commercial ultrasound system (UltraView 800, BK Medical, Herlev, Denmark). Thirty-one patients with malignant focal liver lesions (confirmed by biopsy or computed tomography/magnetic resonance) were scanned. Detection of malignant focal liver lesions and preference of image quality were evaluated blinded off-line by eight radiologists. In total, 2,032 evaluations of 127 image sequences were completed. The sensitivity (77% SASB-THI, 76% DRF-THI, $p = 0.54$) and specificity (71% SASB-THI, 72% DRF-THI, $p = 0.67$) of detection of liver lesions and the evaluation of image quality ($p = 0.63$) did not differ between SASB-THI and DRF-THI. This study indicates the ability of SASB-THI in a true clinical setting. (E-mail: andreaskr5@gmail.com) © **2015 World Federation for Ultrasound in Medicine & Biology.**

Key Words: **Synthetic aperture, Sequential beamforming, Tissue harmonic imaging, Image evaluation, Liver lesion.**

INTRODUCTION

Ultrasound plays a major role in medical imaging and is used for diagnosis and assessment in a variety of medical specialties. Hence, the improvement of ultrasound techniques will benefit a large group of patients and health care workers. Tissue harmonic imaging (THI) is an ultrasound technique that improves image resolution and contrast and provides gray-scale imaging with fewer artifacts (Averkiou et al. 1997; Tranquart et al. 1999; Ward et al. 1997). Combining conventional ultrasound algorithms with THI is therefore a standard method to improve the image quality of gray-scale imaging (Desser and Jeffrey 2001; Hann et al. 1999; Shapiro et al. 1998; Tranquart et al. 1999). However, conventional B-mode imaging techniques have several technical constraints, as images are acquired sequentially one image line at a time. The frame rate is limited by the speed of sound in tissue, the scanning depth and the number of image lines. The high image resolution with a large number of image lines is, thus, obtained at the expense of frame rate. Image generation is further affected by a fixed transmit focus, causing the image to be optimally focused at only one depth. This can be improved by using multiple transmit foci, but the weakness of this solution is an increased number of emissions, which reduces the frame rate even further (Holm and Yao 1997).

High image resolution and high frame rate can be obtained with synthetic aperture (SA) (Sherwin et al. 1962). SA was originally developed from radar systems for geologic and sonar applications, but has been modified for medical imaging (Burckhardt et al. 1974). The basic idea underlying SA is generation of a high-resolution image from a number of low-resolution images (Jensen et al. 2006). An active element is selected stepwise through the array. At each step, an unfocused

Address correspondence to: Andreas Hjelm Brandt, Blegdamsvej 9, 2100 Copenhagen OE, Denmark. E-mail: andreaskr5@gmail.com

beam is emitted, and all the elements in the array receive echoes to create the low-resolution images.

Several different implementations of SA exist. However, a common disadvantage hindering real-time implementation on a commercial scanner is the high system requirements (Behar and Adam 2005; Gammelmark and Jensen 2003; Karaman et al. 1995). Synthetic aperture sequential beamforming (SASB) was introduced to reduce the system requirements of SA. SASB is a dual-stage procedure using two separate beamformers (Kortbek et al. 2008). The first beamformer reduces the data throughput requirement to that of a single output signal, that is, a factor of 64 for a 64-channel receive system. The second beamformer recombines a set of emissions to create the final high-resolution image (Hemmsen et al. 2012a; Kortbek et al. 2013). Previous studies have evaluated the image quality of SASB against conventional dynamic receive focusing (DRF) and reported equally good image quality, indicating that SASB is applicable to medical imaging (Hemmsen et al. 2011, 2012b, Hansen et al. 2014). SASB can generate an acoustic field intense enough to create harmonics for THI, and it has been suggested that these techniques be combined to improve the image quality of SASB even further. The pulse inversion technique was used to generate THI, and the beamforming steps for the final SASB-THI image are illustrated in Figure 1 (Hemmsen et al. 2014b; Rasmussen et al. 2012; Yigang et al. 2011). In a preliminary study in which healthy volunteers were scanned, two radiologists evaluated the image quality of SASB-THI as equal to that of a conventional imaging technique combined with THI (DRF-THI), indicating that SASB-THI can be used for medical imaging (Rasmussen et al. 2013).

The purpose of this study was to perform a clinical comparison of DRF-THI and SASB-THI using liver scans of patients with confirmed malignant focal liver cancer. The image sequences generated, SASB-THI and DRF-THI videos, were evaluated by radiologists for detection of malignant focal liver lesions and to assess the image quality of SASB-THI compared with that of DRF-THI in a clinical setting.

METHODS

Patients

Forty-three patients with different kinds of malignant focal liver cancer (primary liver tumor or liver metastasis) were asked to participate in the study. All patients were included after providing informed consent and on approval by the Danish National Committee on Biomedical Research Ethics (Journal No. H-1-2011-124). Before the study, liver lesions were diagnosed by biopsy or computed tomography/magnetic resonance (CT/MR). Surgery was scheduled the day after the ultrasound examination for all patients. Before the experimental scan, an orientation scan was performed with a conventional ultrasound scanner (UltraView 800, BK Medical, Herlev, Denmark), and if available, CT/MR was used to ensure correct scan position. Included were only patients in whom the pathology was visible on the orientation scan, which was performed without contrast enhancement. Twelve patients were excluded because the pathology was not visible; thus, a total of 31 patients with focal liver cancer (28 colorectal liver metastases and 3 hepatocellular carcinomas) were examined with the experimental setup. Among the patients examined were 10 women and 21 men, ranging in age from 37 to 82 y (mean ± standard deviation [SD]: 65.1 ± 10.4 y) and in body mass index from 16.8 to 33.0 kg/m^2 (mean ± SD: 24.7 ± 4.4 kg/m^2).

Scanning

The patients were scanned in three positions where the liver lesions were visible and in three areas where no pathology was visible. The patients were positioned supine and were told to hold their breath and lie still during recording. All scans were performed by P.M.H. and A.H.B. The aim was to record six sequences for each patient, but because of technical challenges, this was possible for only 28 patients. One patient had only three recordings, and two patients had seven recordings because of errors made while saving and noticed after the scan session. A total of 185 image sequences were recorded.

The acoustic output of SASB-THI was determined before scanning. Intensities must be those recommended by the Food and Drug Administration (FDA) for abdominal scanning. The limits are given by the mechanical index, MI ≤ 1.9; the derated spatial peak, pulse average intensity, I_{sppa} ≤ 190 W/cm^2; and the derated spatial peak, temporal average intensity, I_{spta} ≤ 94 mW/cm^2 (Food and Drug Administration 2008). As SASB-THI and DRF-THI use the same transmit profile equal acoustic outputs are obtained. The intensities were MI = 0.9, I_{sppa} = 81.2 W/cm^2 and I_{spta} = 16.2 mW/cm^2 and, hence, were lower than the FDA limit.

Equipment and data acquisition

Experimental scans were performed with a conventional ultrasound scanner (UltraView 800, BK Medical, Herlev, Denmark) equipped with a research interface and an abdominal 3.5-MHz CL192-3 ML convex array transducer (Sound Technology, State College, PA, USA). The ultrasound scanner was connected to a stand-alone PC. With the experimental setup, images generated with SASB-THI and DRF-THI were recorded

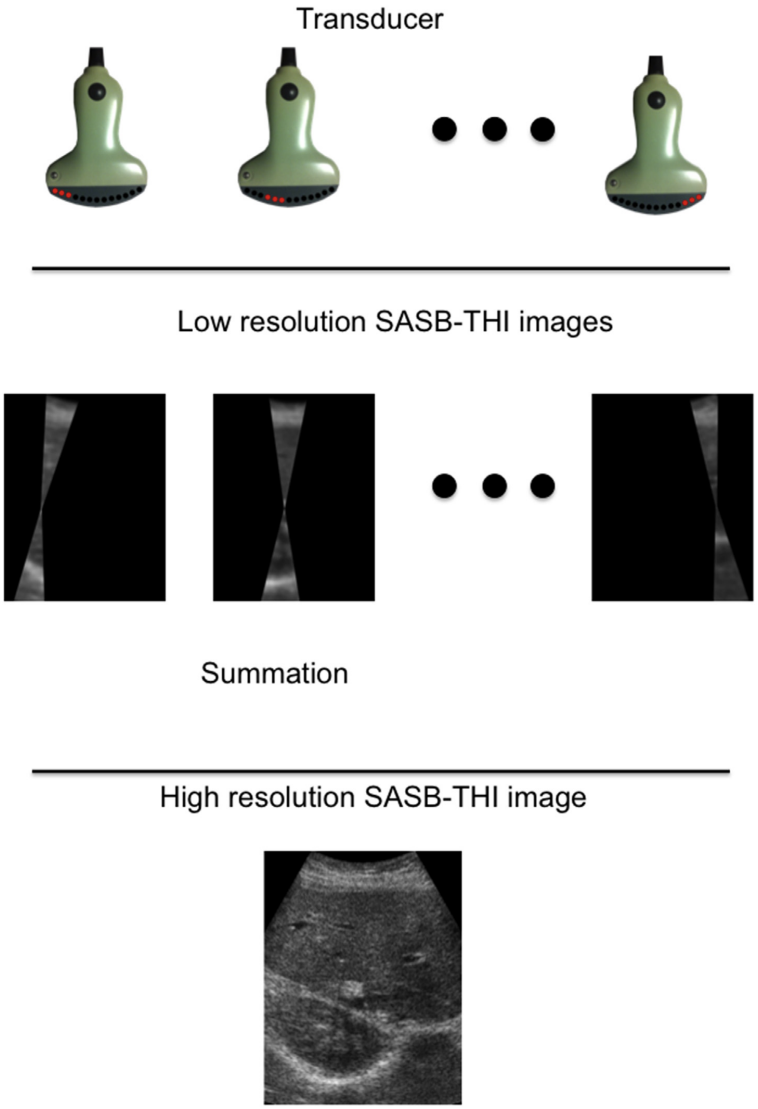

Fig. 1. Beamforming steps in achieving synthetic aperture sequential beamforming tissue harmonic imaging (SASB-THI). Transmit and receive elements are identical for each emission. Even harmonics (THI) are enhanced by the pulse inversion technique, and each beam is perceived as a virtual ultrasound source emitting from the beam focal point. The received beams are summed in the second-stage beamformer to yield the high-resolution SASB-THI image.

interleaved. One frame generated with SASB-THI followed one frame generated with DRF-THI. Images from the same anatomic location were thereby recorded almost simultaneously with both techniques, and ideal sequences for comparison were generated (Hemmsen et al. 2010, 2012c).

The first beamforming of the dual-stage beamforming of SASB-THI was performed on the conventional scanner, and data were then recorded on the PC. The second beamforming was performed on the PC using MATLAB (The MathWorks, Natick, MA, USA) and the in-house developed beamformation toolbox BFT3

(Hansen et al. 2011). DRF-THI images were entirely generated by the conventional scanner. Field-of-view, time-gain compensation, frame rate (8 frames/s), apodization and depth (14.6 cm) were identical for the two techniques. Three-second image sequences were generated. During the recording, only images for navigational purposes from the first beamforming were visualized on the scanner.

The navigational image had a low frame rate and poor image quality and was therefore merely used for guidance during collection of data. The final image sequences were available off-line after second-stage beamforming. To ensure that clinically valuable image sequences were acquired, a subsequent selection was performed before the image evaluation. Images defined as not clinically valuable were (i) sequences in which no liver tissue was visible, (ii) sequences in which malignant focal liver cancer was not visible even though it had been reported and (iii) sequences in which patient movement made the sequence impossible to assess. The selection was done blinded to knowledge of image technique. Nevertheless, both SASB-THI and DRF-THI sequences were affected, as both techniques were processed from the same data. A total of 58 image sequences with the same number of images for each technique were removed. This corresponds to 31.4% of all recorded sequences; therefore, 127 image sequences remained for image evaluation (Fig. 2). Patients in the excluded sequences were similar in age (45–78 y, mean ± SD: 66.5 ± 7.8 y) and body mass index (18.6–33.0 kg/m^2, mean ± SD: 24.6 ± 4.4 kg/m^2) to the patients whose sequences were included.

Image evaluation

Eight radiologists (examiners 1–8) blinded to the technical information evaluated all image sequences. The radiologists were asked to evaluate whether images contained malignant focal liver lesions, so that detection rates (sensitivity and specificity) could be determined. They were informed that some of the images contained malignant focal liver lesions. An in-house developed software program (IQap) was used for the evaluation (Hemmsen et al. 2010). Images obtained with the two techniques were shown separately, resulting in 254 evaluations by each radiologist for a total of 2,032 evaluations.

The same eight radiologists also compared the image quality of both imaging techniques. This was similarly performed with the IQap. For each image sequence, the images were displayed side-by-side. The evaluating radiologist had the option of viewing the sequences in real time and as single frames. Each sequence was shown twice and randomly switched from left to right, displaying each technique twice. By placing a sliding bar on a visual analogue scale (VAS) (Freyd 1923) (Fig. 3), radiologists indicated the sequence with their preferred image quality as previously described by Hansen et al. (2014). The VAS ranged from −50 to 50, and positive values always favored SASB-THI, regardless of the side on which the SASB-THI image was placed. The values on the VAS scale were not shown on the scale during the evaluation and were therefore arbitrary for the evaluator. By sliding the bar further to one side or the other, the evaluator indicated his or her preference for that technique. By placing the bar in the middle, the evaluator indicated no difference between the techniques. Each evaluated image sequence was given an integer or numbered zero if the evaluators found no difference.

Statistics

Detection of focal malignant liver lesions was assessed by calculating sensitivity and specificity. Confidence intervals for sensitivity and specificity, as well as p values for differences, were computed by bootstrapping to respect the complex dependence structures in the data. Inter-observer variability was calculated using Fleiss' κ statistic, and κ values were interpreted as proposed by Landis and Koch (1977) for strength of agreement: ≤0 = poor, 0.01–0.20 = slight, 0.21–0.40 = fair, 0.41–0.60 = moderate, 0.61–0.80 = substantial and 0.81–1 = almost perfect.

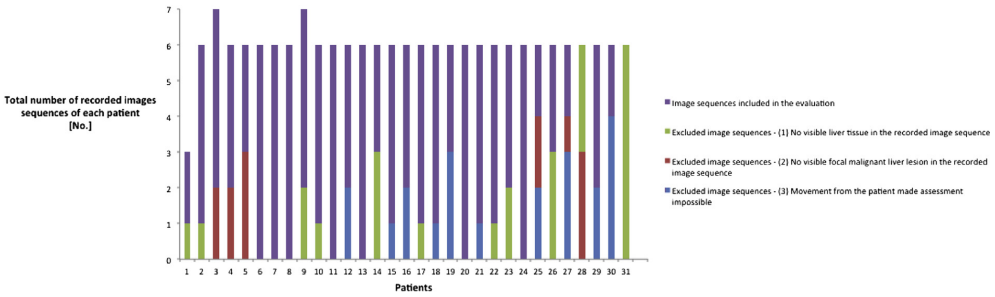

Fig. 2. Overview of image sequences included and excluded in the image evaluation.

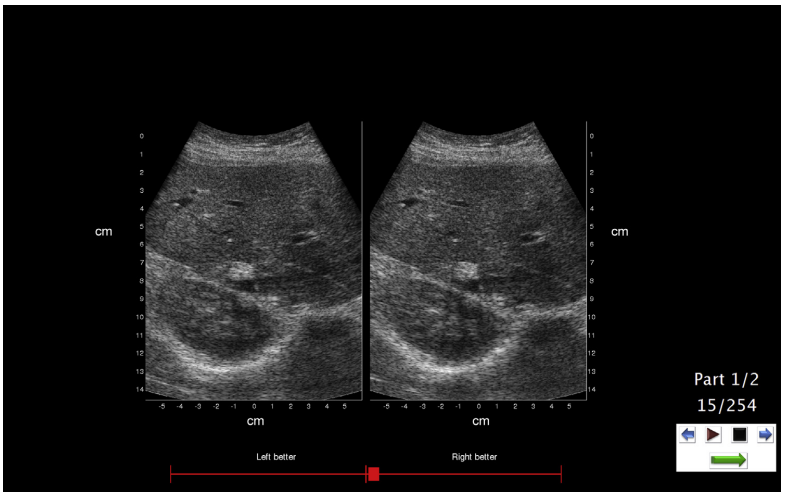

Fig. 3. IQap screenshot with the visual analogue scale at the bottom. A focal liver lesion is seen just above the kidney. By dragging the bar to one side, evaluators specified which technique they preferred. Left: sequential beamforming tissue harmonic imaging (SASB-THI), right: dynamic receive focusing with tissue harmonic imaging (DRF-THI).

In the evaluation of image quality, a non-parametric Wilcoxon signed rank test with bootstrapping was used to test the hypothesis of no difference in preference. This test takes into account that the same pair of images is displayed twice to the same radiologists and that the same image pairs are shown to different radiologists. Furthermore, the test handles the difficulties resulting from each radiologist having his or her own interpretation of the VAS scale. A linear mixed model was applied to test the same hypothesis, in the subgroups of radiologists who seemed to use the VAS similarly. As all image pairs were shown with SASB-THI images both on the left side and on the right side, it was not necessary to control for left/right differences. For the evaluation of image quality, inter-observer and intra-observer variability was determined using Fleiss' κ statistic.

Data management was performed using Excel (Microsoft, Redmond, WA, USA) and MATLAB. Statistical analyses were performed using the statistical data analysis language R, Version 2.12.2 (http://www.r-project.org/).

RESULTS

A focal malignant liver lesion was present in 55 image sequences, whereas 72 image sequences revealed only healthy liver tissue. The sensitivity and specificity of detection of focal malignant liver lesions are illustrated in Figure 4. Both imaging techniques had similar sensitivity and specificity; that is, there were no significant differences in mean sensitivity and specificity between SASB-THI (sensitivity: 77%, 95% confidence interval [CI]: 70%–84%; specificity: 71%, 95% CI: 66%–77%) and DRF-THI (sensitivity: 76%, 95% CI: 69%–82%; specificity 72%, 95% CI: 67%–77%) (p = 0.54 [sensitivity] and 0.67 [specificity]). Inter-observer variability between the radiologists indicated moderate agreement (k = 0.48) when rating image sequences generated by SASB-THI and fair agreement (k = 0.37) when rating images generated with DRF-THI.

The image quality preference evaluation of each radiologist is illustrated in Figure 5. There was no preference for SASB-THI or DRF-THI in 63% (1,271/2032) of the evaluations, SASB-THI was favored by 16% (329/2032) and DRF-THI was favored by 21% (432/2032). The average rating for all radiologists was −0.10 (95% CI: −0.47 to 0.26), indicating no difference in preference for an imaging technique (p = 0.63). Inter-observer variability indicated poor agreement (k = 0.0045), and intra-observer variability indicated slight agreement (k = 0.11).

Radiologist 8 (Fig. 5) used the VAS scale more broadly then radiologists 1–7. An additional analysis, excluding radiologist 8, yielded an average rating of 0.045 (95% Cl: −0.15 to 0.24), again indicating no preference for one technique (p = 0.62).

DISCUSSION

To our knowledge, this is the first study to examine use of the combination of SASB and THI on patients. Thirty-one patients with focal malignant liver lesions diagnosed by biopsy or MR/CT and scheduled for surgery

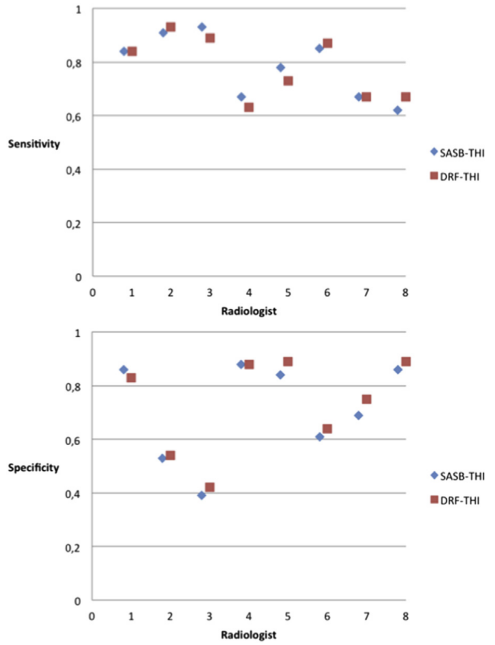

Fig. 4. Sensitivity and specificity of sequential beamforming tissue harmonic imaging (SASB-THI) and dynamic receive focusing with tissue harmonic imaging (DRF-THI) for each radiologist.

the day after the experimental examination were included in the study. Eight radiologists evaluated SASB-THI and DRF-THI sequences of livers with and without focal malignant liver lesions to assess diagnostic sensitivity and specificity, as well as image quality. The findings from this study, together with previous theoretical and experimental reports (Hemmsen et al. 2014a; Rasmussen et al. 2013), suggest that SASB-THI can be used for medical imaging.

With respect to sensitivity and specificity, the techniques performed equally well (Fig. 4), indicating that SASB-THI has the same detection rate as a conventional imaging technique when evaluating images for malignant focal liver lesions. Reasonable sensitivity and specificity values were obtained with both techniques, as the rate of detection of metastases with unenhanced ultrasound has been reported to have a sensitivity of 50%–76% and specificity of 60%–96% (Beissert et al. 2000; Cantisani et al. 2014; Glover et al. 2002) and detection of hepatocellular carcinoma has been reported to have a sensitivity as low as 33%–57% and a specificity of 80%–92% (Kim et al. 2001; Shapiro et al. 1996). Sensitivity and specificity can be improved by the use of ultrasound contrast (Cantisani et al. 2014), which will be pursued in future studies.

With respect to image quality, 63% of the evaluations were rated alike, and statistical analysis indicated that the radiologists did not have a preference for one technique ($p = 0.63$). One radiologist used the VAS differently than the other examiners. To compensate for this, the analysis was conducted both with and without this radiologist, with no change in the results. The similar image quality of SASB-THI and DRF-THI may explain the low inter-observer and intra-observer variability, as radiologists were unable to distinguish images obtained with SASB-THI and DRF-THI, and their choices were thus solely coincidences.

Until now, few clinical studies have been performed with SA as the imaging technique. Previous studies have evaluated the quality of still images of patients with focal breast pathology (Kim et al. 2012, 2013). The major advantage of the present study is the possibility of reviewing real-time sequences and single frames. In our opinion, this is a more reliable evaluation, because ultrasound is a dynamic examination. Furthermore, in this setup, the sequences were recorded interleaved and the same anatomic areas were compared, as opposed to previous studies in which the different images were recorded one after the other (Sodhi et al. 2005; Yen et al. 2008).

In a previous pre-clinical study with SASB-THI as the imaging technique, only healthy slim volunteers were scanned (Rasmussen et al. 2013). Scanning heavy or obese patients is more difficult, because of the thicker abdominal fat layers and higher heart rates (Hansen et al. 2014). Several patients in this study were hard to scan as they had discomfort lying on their backs, an altered anatomic layout because of previous surgery, trouble holding their breath and trouble lying still. Combined with the coarse navigation image, which was displayed while data were recorded, these problems made scanning difficult and were the main reasons for excluding 31.4% of the sequences from the final experimental data. In our opinion, however, this does not diminish the results of this study, as both SASB-THI and DRF-THI images were similarly affected, and the decisions to exclude images were made without knowledge of the imaging technique used.

A disadvantage of synthetic aperture imaging systems is tissue motion artifacts, although these artifacts have been found to have a minor impact on image quality (Jensen et al. 2006; Pedersen et al. 2007). Requesting patients to hold their breath and lie still most likely reduced these artifacts. Some tissue motion was evident in the image sequences evaluated and no degradation of image quality was seen, which is consistent with previous findings with clinical SASB imaging (Hansen et al. 2014). However, this study did not evaluate tissue motion with beamformed SASB-THI images, which should be evaluated in future clinical studies.

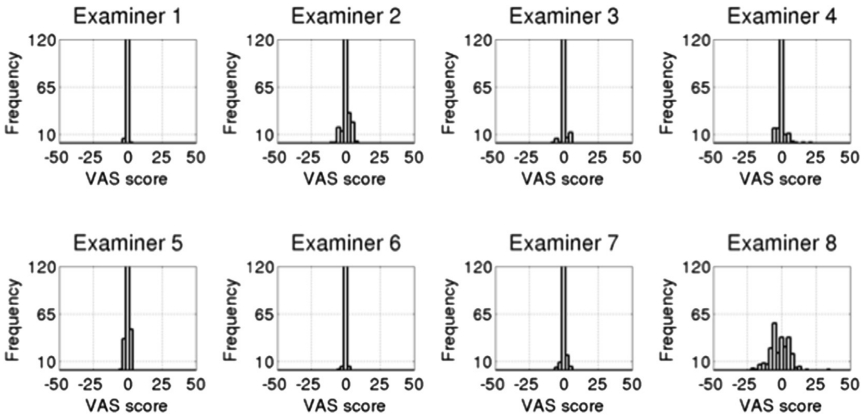

Fig. 5. Distribution of each radiologist's evaluations. Sequential beamforming tissue harmonic imaging is favored by positive values. VAS = visual analogue scale.

All images were recorded at a relatively low frame rate without any image-improving algorithms, for example, speckle reduction filter, or image compounding. The images containing malignant focal liver lesions were therefore not optimized for diagnostic evaluation. Radiologists were told not to appraise the correct diagnosis, but only to detect the presence of malignant focal liver lesions. Future studies including different image-improving algorithms and using ultrasound contrast with SASB-THI will reveal more about the diagnostic accuracy of SASB-THI.

Apart from the high frame rate and high resolution achieved, the predominant advantage of SASB-THI is a factor of 64 times lower data transmission between the probe and processing unit compared with conventional imaging. This reduction in data transmission does not lower the quality of the image and supports the use of SASB-THI for clinical imaging. The reduction in data transmission indicates the possibility of implementing a synthetic aperture technique on a commercially available hand-held tablet and producing wireless transducers (Hemmsen et al. 2014a). A wireless transducer can improve clinical conditions, as it makes it easier to scan directly at the trauma site, makes it easier to maintain sterile conditions, simplifies ultrasound-guided intervention and peri-operative scanning, improves freedom of movement and optimizes awkward and ergonomically challenging positions (Munoz and Zamorano 2014). Combining the wireless transducer with a commercial tablet would spread the use of ultrasound tremendously, as tablets are relatively inexpensive and widely available. Moreover, easily maneuverable hand-held devices, like tablets, have proven to be useful in numerous clinical conditions (Lapostolle et al. 2006). In cardiology, in particular, hand-held devices have facilitated rapid diagnosis and patient screening in good agreement with conventional ultrasound systems (Biais et al. 2012).

CONCLUSIONS

Synthetic aperture sequential beamforming tissue harmonic imaging has successfully been used in a clinical setting. Patients with malignant focal liver cancer were scanned, and interleaved image sequences were recorded with both SASB-THI and DRF-THI. In a double-blinded setup, eight ultrasound-experienced radiologists rated SASB-THI equal to DRF-THI with respect to ability to detect malignant focal liver lesions and image quality. This indicates that SASB-THI can be used in the clinical setting. The advantage of the reduction in data transmission can be used to implement wireless real-time SASB-THI on a commercial available hand-held tablet.

Acknowledgments—The authors thank all participating patients at the Department of Surgical Gastroenterology, Rigshospitalet, and the staff for helping to recruit patients. Also, special thanks to Professor Lars Bo Svendsen for letting us scan in the department. Thanks to Flemming Jensen, M.D., Caroline Ewertsen, M.D., Trine-Lise Lambine, M.D., Mikkel Seidelin Dam, M.D., Dorte Stærke, M.D., Masoud Azapour, M.D., and Lars Lönn, M.D., for evaluating the ultrasound recordings. The study was supported by Grant 82-2012-4 from the Danish National Advanced Technology Foundation and by BK Medical ApS.

REFERENCES

Averkiou MA, Roundhill DN, Powers JE. A new imaging technique based on the nonlinear properties of tissues. Proc IEEE Ultrason Symp 1997;2:1561–1566.

Behar V, Adam D. Optimization of sparse synthetic transmit aperture imaging with coded excitation and frequency division. Ultrasonics 2005;43:777–788.

Beissert M, Jenett M, Keberle M. Comparison of contrast harmonic imaging in B-mode with stimulated acoustic emission, conventional B-

mode US and spiral CT in the detection of focal liver lesions. Rofo 2000;172:361–366.
Biais M, Carrie C, Delaunay F, Morel N, Revel P, Janvier G. Evaluation of a new pocket echoscopic device for focused cardiac ultrasonography in an emergency setting. Crit Care 2012;16:R82.
Burckhardt CB, Grandchamp PA, Hoffmann H. An experimental 2 MHz synthetic aperture sonar system intended for medical use. IEEE Trans Son Ultrason 1974;21:1–6.
Cantisani V, Grazhdani H, Fioravanti C, Rosignuolo M, Calliada F, Messineo D, Bernieri MG, Redler A, Catalano C, D'Ambrosio F. Liver metastases: Contrast-enhanced ultrasound compared with computed tomography and magnetic resonance. World J Gastroenterol 2014;20:9998–10007.
Desser TS, Jeffrey RB. Tissue harmonic imaging techniques: Physical principles and clinical applications. Semin Ultrasound CT MR 2001;22:1–10.
Food and Drug Administration (FDA). Guidance for industry and FDA staff—Information for manufacturers seeking marketing clearance of diagnostic ultrasound systems and transducers. Technical Report. U.S. Department of Health and Human Services, FDA, Center for Devices and Radiologic Health, http://www.fda.gov/MedicalDevices/. 2008.
Freyd M. The graphic rating scale. J Educ Psychol 1923;14:83–102.
Gammelmark KL, Jensen JA. Multielement synthetic transmit aperture imaging using temporal encoding. IEEE Trans Med Imaging 2003;22:552–563.
Glover C, Douse P, Kane P, Karani J, Meire H, Mohammadtaghi S, Allen-Mersh T. Accuracy of investigations for asymptomatic colorectal liver metastases. Dis Colon Rectum 2002;45:476–484.
Hann LE, Bach AM, Cramer LD, Siegel D, Yoo HH, Garcia R. Hepatic sonography: Comparison of tissue harmonic and standard sonography techniques. AJR Am J Roentgenol 1999;173:201–206.
Hansen JM, Hemmsen MC, Jensen JA. An object-oriented multithreaded software beamformation toolbox. Proc SPIE 2011;7968.
Hansen PM, Hemmsen M, Brandt A, Rasmussen J, Lange T, Krohn PS, Lonn L, Jensen JA, Nielsen MB. Clinical evaluation of synthetic aperture sequential beamforming ultrasound in patients with liver tumors. Ultrasound Med Biol 2014;40:2805–2810.
Hemmsen MC, Petersen MM, Nikolov SI, Nielsen MB, Jensen JA. Ultrasound image quality assessment: A framework for evaluation of clinical image quality. Proc SPIE 2010;7629.
Hemmsen MC, Hansen PM, Lange T, Hansen JM, Nikolov SI, Nielsen MB, Jensen JA. Preliminary in-vivo evaluation of synthetic aperture sequential Beamformation using a multielement convex array. Proc IEEE Ultrason Symp 2011;1131–1134.
Hemmsen MC, Hansen JM, Jensen JA. Synthetic aperture sequential beamformation applied to medical imaging. Proc EUSAR 2012a;34–37.
Hemmsen MC, Hansen PM, Lange T, Hansen JM, Hansen KL, Nielsen MB, Jensen JA. In vivo evaluation of synthetic aperture sequential beamforming. Ultrasound Med Biol 2012b;38:708–716.
Hemmsen MC, Kjeldsen T, Larsen L, Kjær C, Tomov BG, Mosegaard J, Jensen JA. Implementation of synthetic aperture imaging on a hand-held device. Proc IEEE Ultrason Symp 2014a;2177–2180.
Hemmsen MC, Nikolov SI, Pedersen MM, Pihl MJ, Enevoldsen MS, Hansen JM, Jensen JA. Implementation of a versatile research data acquisition system using a commercially available medical ultrasound scanner. IEEE Trans Ultrason Ferroelectr Freq Control 2012c;59:1487–1499.
Hemmsen MC, Rasmussen J, Jensen JA. Tissue harmonic synthetic aperture ultrasound imaging. J Acoust Soc Am 2014b;136:2050–2056.
Holm S, Yao H. Improved framerate with synthetic transmit aperture imaging using prefocused subapertures. Proc IEEE Ultrason Symp 1997;2:1535–1538.
Jensen JA, Nikolov SI, Gammelmark KL, Pedersen MH. Synthetic aperture ultrasound imaging. Ultrasonics 2006;44(Suppl 1):e5–e15.
Karaman M, Pai-Chi L, O'Donnell M. Synthetic aperture imaging for small scale systems. IEEE Trans Ultrason Ferroelectr Freq Control 1995;42:429–442.
Kim C, Yoon C, Park JH, Lee Y, Kim WH, Chang JM, Choi BI, Song TK, Yoo YM. Evaluation of ultrasound synthetic aperture imaging using bidirectional pixel-based focusing: Preliminary phantom and *in vivo* breast study. IEEE Trans Biomed Eng 2013;60:2716–2724.
Kim CK, Lim JH, Lee WJ. Detection of hepatocellular carcinomas and dysplastic nodules in cirrhotic liver: Accuracy of ultrasonography in transplant patients. J Ultrasound Med 2001;20:99–104.
Kim WH, Chang JM, Kim C, Park J, Yoo Y, Moon WK, Cho N, Choi BI. Synthetic aperture imaging in breast ultrasound: A preliminary clinical study. Acad Radiol 2012;19:923–929.
Kortbek J, Hensen JA, Gammelmark KL. Synthetic aperture sequential beamforming. Proc IEEE Int Ultrason Symp 2008;966–969.
Kortbek J, Jensen JA, Gammelmark KL. Sequential beamforming for synthetic aperture imaging. Ultrasonics 2013;53:1–16.
Landis JR, Koch GG. The measurement of observer agreement for categorical data. Biometrics 1977;33:159–174.
Lapostolle F, Petrovic T, Lenoir G, Catineau J, Galinski M, Metzger J, Chanzy E, Adnet F. Usefulness of hand-held ultrasound devices in out-of-hospital diagnosis performed by emergency physicians. Am J Emerg Med 2006;24:237–242.
Munoz DR, Zamorano JL. Wireless echocardiography: A step towards the future. Eur Heart J 2014;35:1700.
Pedersen MH, Gammelmark KL, Jensen JA. In-vivo evaluation of convex array synthetic aperture imaging. Ultrasound Med Biol 2007;33:37–47.
Rasmussen J, Hemmsen MC, Madsen SS, Hansen PM, Nielsen MB, Jensen JA. Implementation of tissue harmonic synthetic aperture imaging on a commercial ultrasound system. Proc IEEE Ultrason Symp 2012;121–125.
Rasmussen J, Hemmsen MC, Madsen SS, Hansen PM, Nielsen MB, Jensen JA. Preliminary study of synthetic aperture tissue harmonic imaging on *in vivo* data. Proc SPIE 2013;8675.
Shapiro RS, Katz R, Mendelson DS, Halton KP, Schwartz ME, Miller CM. Detection of hepatocellular carcinoma in cirrhotic patients: Sensitivity of CT and ultrasonography. J Ultrasound Med 1996;15:497–502.
Shapiro RS, Wagreich J, Parsons RB, Stancato-Pasik A, Yeh HC, Lao R. Tissue harmonic imaging sonography: Evaluation of image quality compared with conventional sonography. AJR Am J Roentgenol 1998;171:1203–1206.
Sherwin CW, Ruina JP, Rawcliffe RD. Some early developments in synthetic aperture radar systems. IRE Trans Mil Elect 1962;MIL-6:111–115.
Sodhi KS, Sidhu R, Gulati M, Saxena A, Suri S, Chawla Y. Role of tissue harmonic imaging in focal hepatic lesions: Comparison with conventional sonography. J Gastroenterol Hepatol 2005;20:1488–1493.
Tranquart F, Grenier N, Eder V, Pourcelot L. Clinical use of ultrasound tissue harmonic imaging. Ultrasound Med Biol 1999;25:889–894.
Ward B, Baker AC, Humphrey VF. Nonlinear propagation applied to the improvement of resolution in diagnostic medical ultrasound. J Acoust Soc Am 1997;101:143–154.
Yen CL, Jeng CM, Yang SS. The benefits of comparing conventional sonography, real-time spatial compound sonography, tissue harmonic sonography, and tissue harmonic compound sonography of hepatic lesions. Clin Imaging 2008;32:11–15.
Yigang D, Rasmussen J, Jensen H, Jensen JA. Second harmonic imaging using synthetic aperture sequential beamforming. Proc IEEE Ultrason Symp 2011;2261–2264.

12.2 Appendix II (Paper I)

JVA
ISSN 1129-7298

J Vasc Access 2016; 00 (00): 000-000
DOI: 10.5301/jva.5000589

ORIGINAL RESEARCH ARTICLE

Surveillance for hemodialysis access stenosis: usefulness of ultrasound vector volume flow

Andreas H. Brandt[1], Jonas Jensen[2], Kristoffer L. Hansen[1], Peter Hansen[1], Theis Lange[3], Marianne Rix[4], Jørgen A. Jensen[2], Lars Lönn[1,5], Michael B. Nielsen[1]

[1] Department of Radiology, Copenhagen University Hospital, Copenhagen - Denmark
[2] Center for Fast Ultrasound Imaging, Technical University of Denmark, Lyngby - Denmark
[3] Department of Biostatistics, University of Copenhagen, Copenhagen - Denmark
[4] Department of Nephrology, Copenhagen University Hospital, Copenhagen - Denmark
[5] Department of Vascular Surgery, Copenhagen University Hospital, Copenhagen - Denmark

ABSTRACT

Purpose: To investigate if ultrasound vector-flow imaging (VFI) is equal to the reference method ultrasound dilution technique (UDT) in estimating volume flow and changes over time in arteriovenous fistulas (AVFs) for hemodialysis.

Materials and methods: From January 2014 to January 2015, patients with end-stage renal disease and matured functional AVFs were consecutively solicited to participate in this prospective study. All patients were included after written informed consent and approval by the National Committee on Biomedical Research Ethics and the local Ethics Committee (journal no. H-4-2014-FSP). VFI and UDT measurements were performed monthly over a six-month period. Nineteen patients were included in the study. VFI measurements were performed before dialysis, and UDT measurements after. Statistical analyses were performed with Bland-Altman plot, Student's *t*-test, four-quadrant plot, and regression analysis. Repeated measurements and precision analysis were used for reproducibility determination.

Results: Precision measurements for UDT and VFI were 32% and 20%, respectively ($p = 0.33$). Average volume flow measured with UDT and VFI were 1161 mL/min (±778 mL/min) and 1213 mL/min (±980 mL/(min), respectively ($p = 0.3$). The mean difference was -51 mL/min (CI: -150 mL/min to 46 mL/min) with limits of agreement from -35% to 54%, with a strong correlation ($r^2 = 0.87$). A large change in volume flow between dialysis sessions detected by UDT was confirmed by VFI ($p = 0.0001$), but the concordance rate was poor (0.72).

Conclusions: VFI is an acceptable method for volume flow estimation and volume flow changes over time in AVFs.

Keywords: Arteriovenous fistula, Hemodialysis patients, Monitoring volume flow, Ultrasound dilution technique, Vector flow imaging

Introduction

The arteriovenous fistula (AVF) is the preferred vascular access for hemodialysis in end-stage renal disease (1, 2). The AVF has a low-resistance circuit with highly increased blood flow, leading to vein dilation and vessel-wall thickening, ideally for repeated puncture and hemodialysis (1). However, approximately 60% will develop stenosis an average of 18 months after creation of the AVF (1, 3). Stenosis may lead to thrombosis and access failure (1, 4). The National Kidney Foundation Kidney Disease Outcomes Quality Initiative (NKF KDOQI) recommends that patients with AVF be monitored with regular volume-flow measurements for evaluation of stenosis and treated with percutaneous transluminal angioplasty or surgery if hemodynamically relevant (2, 3).

Ultrasound dilution technique (UDT) is considered the reference method for volume-flow estimation of the AVF (5, 6). UDT is based on an indicator dilution method, in which a known quantity of indicator substance (saline) is injected into the blood stream during dialysis, and by reversing the blood lines recirculation is created (7). The changes in blood concentration diluted by the indicator as a function of time, can be used to estimate volume flow. Krivitski (7) and Depner and Krivitski (8) described the theoretical background and validation of UDT in detail.

The ultrasound vector-flow imaging technique (VFI), based on the transverse oscillation technique, can measure volume flow with a superior reproducibility than UDT (9).

Accepted: May 22, 2016
Published online: September 1, 2016

Corresponding author:
Andreas H. Brandt
Blegdams 9
2100 Copenhagen Oe, Denmark
andreas.hjelm.brandt@regionh.dk

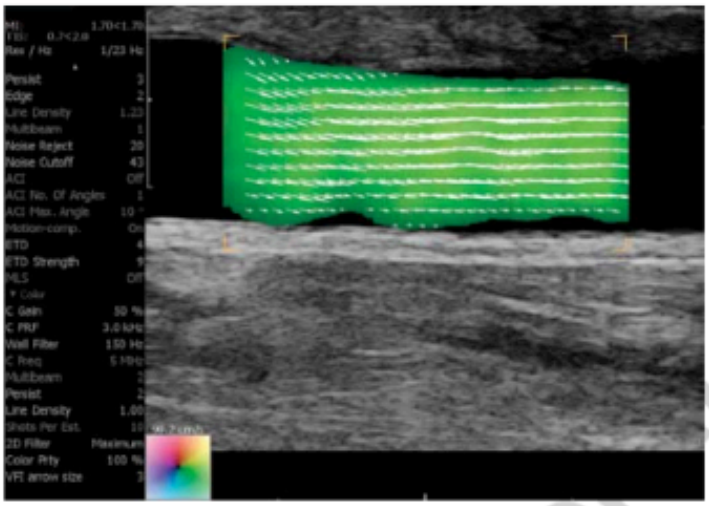

Fig. 1 - Long-axis view of an arteriovenous fistula (AVF) using vector-flow imaging (VFI). The flow is laminar and parabolic, with shorter arrows along the vessel walls than centrally in the vessel lumen.

Transverse oscillation is an angle-independent technique for vector-velocity estimation, developed by Jensen and Munk (10). The vector velocity is estimated from the axial and transverse velocities. The axial velocity is found using conventional Doppler approach, while the transverse velocity is found by manipulating the receive beamforming (11, 12). Transverse oscillation has been validated in simulations and against conventional spectral Doppler and magnetic resonance angiography (MRA) (11, 13, 14).

The agreement between volume-flow estimates by VFI and UDT, and VFI's ability to detect changes in volume flow for hemodialysis monitoring have not been studied previously. In this study, the primary aim was to analyze the agreement between UDT and VFI, and determine if VFI can detect changes in volume flow over time, compared to corresponding estimates obtained by UDT.

Method

All patients were included after informed consent and approval was obtained from the National Committee on Biomedical Research Ethics and the local Ethics Committee (journal no. H-4-2014-FSP). All data was prospectively collected between January 2014 and January 2015. Thirty-two outpatients with end-stage renal disease (hemodialysis treatment two to four times a week) and matured functional AVF (24 forearm fistulas and eight upper-arm fistulas) were consecutively asked to participate in the study. Two patients declined to participate. The patients were examined with UDT and VFI on the same day monthly, during a six-month period (29 mean days, range: 21 to 44 days). The study analysis was only performed on patients who completed the monitoring period (19 patients).

VFI was approved by the U.S. Food and Drug Administration (FDA) and used on commercial ultrasound scanners from BK Medical (15). A commercial scanner (UltraView 800, BK Medical, Herlev, Denmark) and a linear transducer (8670, 9MHz, BK Medical, Herlev, Denmark) were used for the VFI measurements. VFI shows blood-flow direction, magnitude, and velocity in 2D, color-coded pixels within a color box. Arrows can be superimposed in real-time on the color-coded pixels for flow-profile interpretation (Fig. 1). VFI measurements were performed before dialysis needle insertion. Measurements were carried out in the vessel segment of the dialysis needle location, corresponding to UDT measurement. Initial B-mode scans in transverse and longitudinal direction on the fistula were performed for orientation. At the same time, the fistula was inspected for deviating branches. If this was the case near the site, the transducer was moved proximal to the branch and a confident vessel segment with laminar flow was identified. VFI recordings were performed with a longitudinal view. The color box was adjusted to cover the lumen of the vessel, and the pulse repetition frequency (PRF) was adjusted to the highest velocities to prevent aliasing (3 MHz-9 MHz). Wall filter and color gain were set to optimal filling of the vessel without blooming artifacts. The angle of insonation was 70°-90° in all scans. The transducer was raised and repositioned between each recording; hence, a different location for each recording was attained. For each recording, adjustments of wall filter, color gain and PRF were performed if necessary. A corresponding B-mode recording was performed in transverse view without lifting the transducer from the skin, and two perpendicular diameters for cross-sectional area determination were measured at this position. Diameters were measured with the built-in length gauge of the scanner, and performed from the superficial to the deep tunica intima and the corresponding mediolateral diameter. The scan procedure was identical to that in the

study by Hansen et al (9). UDT measurements were performed with Transonic HD03 Flow-QC hemodialysis monitor (Transonic Systems Inc., Ithaca, NY, USA), using vendor guidelines.

VFI volume flow was calculated from an algorithm developed in-house for MATLAB (MathWorks, Natick, MA, USA). The algorithm is based on integration of the vector-velocity profile over the cross-sectional vessel area, as Jensen et al (16) described. VFI data from the longitudinal recording were processed in MATLAB. A randomly picked frame containing B-mode and VFI data was displayed, and a rectangular region of at least 20% covering the whole vessel segment was manually marked for volume-flow calculation (9). Furthermore, the diameters from the cross-sectional area measurement were manually entered in MATLAB. The velocity profile was measured along the rectangular region, and volume flow was calculated by assuming laminar and axisymmetric flow. In a total of 225 frames of vector velocity, corresponding to 15 s of data acquisition, the rectangular region was used to estimate volume flow.

The monitoring program for hemodialysis patients in our tertiary center includes monthly volume-flow measurements with UDT in all patients with AVF. The volume flow is found as an average of two to three measurements. In this study, three consecutive measurements with UDT and VFI were used to find the volume flow for each patient. The averaged results were used for analyzing agreement and detection of volume-flow changes. The first two measurements from both techniques were used to calculate the precision in volume-flow estimation. UDT was measured within an average of 25.6 min (range: 10 min-70 min) after the VFI recording, within an average of 4.8 min (range: 1 min-35 min) after the dialysis session started. Experienced dialysis nurses performed all UDT measurements, while Dr. Brandt performed VFI measurements.

Statistics

The initial two measurements were used to determine the precision of each method. Precisions were calculated as two standard deviations (STD) of the difference between two measurements of method x, divided by the mean of all measurements and multiplied by 100 to be expressed in percentage (17). The precision is calculated as:

$$p = \frac{2 * STD\left(x_n^a - x_n^b\right)}{\bar{x}} * 100 \qquad \text{Eq. [1]}$$

where n is the number of patients, a and b are the two measurements, and $\bar{x}$ is the average value. A statistical test of difference in precision was assessed using analysis of variance (ANOVA). A p value of <0.05 was statistically significant.

Comparisons for agreement were done with Bland-Altman and linear regression analyses using general estimating equations to account for repeated measures. Critchley and Critchley proposed that for two methods to be considered interchangeable, the limits of agreement (LOA) of the Bland-Altman plot in a method-comparison study should be below 30%, and below the expected LOA calculated from precision measurements of each method (17). The expected LOA is calculated as:

$$STD_{a+b} = \sqrt{(STD_a^2 + STD_b^2)} \qquad \text{Eq. [2]}$$

in which STD is the standard deviation of each method a and b. Instead of STD, the calculated precision is used (18, 19).

To illustrate the ability of VFI to track changes in volume flow, a four-quadrant plot was made, and the concordance rate was calculated (20). Random measurement errors were omitted by an exclusion zone corresponding to the averaged precision of the two compared methods according to Møller-Sørensen et al (18).

Results

Of the 32 initial patients, 19 completed the 6-month monitoring period. During the study, two patients declined participation, five patients died, four had central venous catheter dialysis instead, and two had kidney transplantation. Thirteen men (mean age 60.5 y, range: 44-82 y) and six women (mean age 72.3 y, range: 64-91 y) were included.

In the monitoring period, two patients had percutaneous transluminal angioplasty, due to declining fistula flow with stenosis and edema. Both patients clinically improved in volume flow after treatment and were followed one and three times, respectively, to fulfill the six-month monitoring period.

Precision in volume flow measurements with UDT and VFI

Mean difference for UDT obtained by the first two measurements of volume flow was 28 mL/min (95% CI: -61 mL/min to 118 mL/min). The precision was 32% (1). For VFI, the mean difference was -29 mL/min (95% CI: -78 mL/min to 20 mL/min). The precision was 20% (1). The difference in precision was not statistically significant (p = 0.33). The expected LOA (2) was 37%.

Agreement between UDT and VFI

Average volume flow measured with UDT and VFI were 1161 mL/min (±778 mL/min) and 1213 mL/min (±980 mL/min), respectively (p = 0.3). A Bland-Altman plot demonstrated the differences between the two techniques (Fig. 2). Mean difference was -51 mL/min (95% CI: -150 mL/min to 46 mL/min), with limit of agreement from mL/min 597 mL/min to 492 mL/min. If considering the agreement in relative terms, the LOA of the Bland-Altman plot was -35% to 54% and the mean of LOA of the Bland-Altman plot was 44.5%. Correlation between the two techniques was strong (R^2 = 0.87) (Fig. 3).

VFI ability to detect change in volume flow between dialysis sessions, compared to UDT

Figure 4 shows the differences in volume-flow measurement between dialysis sessions for each patient as a four-quadrant plot. Most differences are distributed around

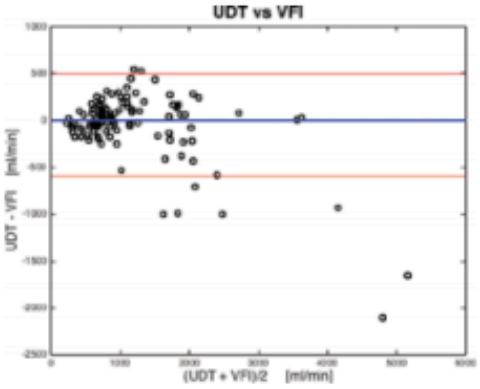

Fig. 2 - Bland-Altman plot of ultrasound dilution technique (UDT) versus vector-flow imaging (VFI). The blue center line symbolizes the mean difference between the methods, while the red outer lines symbolize the limits of agreement.

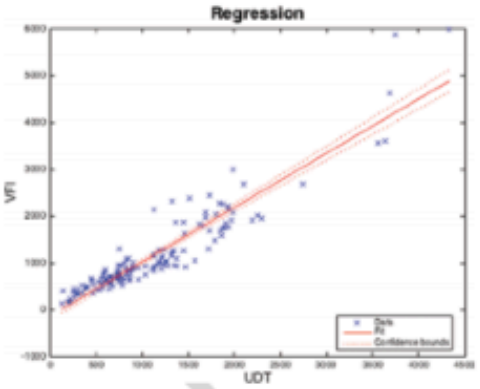

Fig. 3 - Volume-flow estimated by ultrasound dilution technique (UDT) and vector-flow imaging (VFI), illustrated in a regression plot.

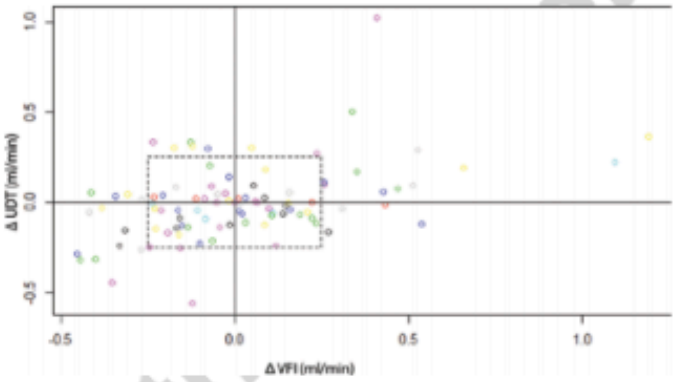

Fig. 4 - Four-quadrant plot of the differences. The colors indicate volume-flow change between sessions in percentages for each patient. Each patient is coded with a unique color. Concordance without an exclusion zone is 54% and 72%, with an exclusion zone of 25% (dotted-line box). VFI = vector-flow imaging; UDT = ultrasound dilution technique.

zero, while the largest changes in volume flow are in the quadrants with UDT and VFI pointing in the same direction. The regression analysis of the four-quadrant plot, where the magnitude in change was considered and that a large difference detected by UDT was at the same detected by VFI, found an inclination of 0.301 with a $p = 0.0001$. With an exclusion zone corresponding to the averaged precision of the two methods (25%), the concordance rate was 0.72.

Discussion

This is the first study to examine volume flow and changes in volume flow over time by VFI, compared to the reference method UDT in AVFs for hemodialysis. Nineteen patients were consecutively examined over a six-month monitoring period. Previously, volume flows in single dialysis sessions were examined, indicating that VFI was more precise than UDT (9). This is similar to our findings, in which VFI had better precision (20%) compared to UDT (32%). There was no statistical difference between UDT and VFI for volume-flow estimations ($p = 0.3$). The LOA between the two methods was wide, with a spread from -35% to 54% (mean 44.5%) and above the expected LOA from the precisions of the methods (37%). There was a strong correlation between VFI and UDT ($R^2 = 0.87$). This study indicates that VFI is more precise than UDT, and could be an alternative for volume-flow estimation in AVFs. However, according to Critchtley and Critchley, UDT and VFI are not interchangeable as the LOA of this comparison study is above the expected LOA and 30% (17).

For clinical use, the change in volume flow over time is more important than estimation of volume flow within a single dialysis session (21). Reduction in volume flow signifies stenosis, and elective percutaneous transluminal angioplasty or surgery may be performed to avoid thrombosis and possible loss of the vascular access (22-24). A decrease of >25% indicates stenosis and can be used as guidance for referral to angiography (2, 21). Most changes were <25% (77%). However, the regression analysis pointed out that a large change detected by UDT was also detected by VFI ($p = 0.0001$), indicating that clinically important changes in volume flow were detected by both methods. The concordance rate increased from 54% to 72% with an exclusion zone of 25% corresponding to the averaged precision of VFI and UDT and the threshold for referral to angiography. Critchley argued that a concordance rate below 84% was poor (20). Although the precisions of UDT and VFI were not statistically different, this and a previous study suggest that VFI is more precise than UDT (9). The low concordance rate and the wide LOA between the two methods are probably mainly caused by the imprecise reference method.

Hansen et al underestimated the volume flow by up to 30% in the AVFs (9). No systematic underestimating was found in this study. This may be caused by the fact that three sources of error were taken into account, as Jensen et al (16) proposed: (1) correcting for change in the geometry caused by compression from the transducer, (2) correcting for not intersecting the vessel in the middle with the ultrasound beam, and (3) correcting for not steering the beam in the center of a elliptic vessel. For one patient, UDT and VFI estimated high volume flows not in accordance with normal physiological conditions. During the six months monitoring period, UDT measured an increasing volume flow from 2746 to 4333 mL/min, while VFI measured an increasing volume flow from 2674 to 5993 mL/min. The patient suffered from hypertension (mean: 166/111), tachycardia (mean: 123) and, dizziness when mobilized from supine to upright position. A vessel narrowing operation (banding) was performed after the surveillance period and the flow decreased to 2835 mL/min (UDT measured), and the patient symptoms diminished. Hansen et al reported that VFI underestimated flow compared to UDT; however, none of the patients had flow rates above 3000 mL/min (9), and the three sources of error were not considered (16). To our knowledge UDT has not been systematically investigated in the upper range of flow dynamics (>3000 mL/min). Whether UDT underestimates or VFI overestimates for high flow rates cannot be answered for this patient; however, VFI overall was more precise resulting in less bias compared to UDT.

Although UDT is considered the reference technique, it has several drawbacks. Variations in volume flow up to 30% have been reported. A consensus was reached that volume-flow change between dialysis sessions must be >25%-33% to have a significant impact (21, 25, 26). Furthermore, volume flow should be measured at the beginning of each session to reduce variation in measurements (25). The flow pattern in the straight vessel segment of the examined AVF was laminar, which prevents rapid mixing and confounds UDT estimation (8).

On the contrary, a laminar-flow profile is ideal for volume-flow calculation by 2D vector-flow maps obtained by VFI (26). However, using 2D ultrasound as in VFI, out-of-plane motion is not detected. The assumption of laminar and axisymmetric flow has a major impact on volume-flow estimation with 2D ultrasound (27-30). The flow in the AVF is more laminar and less pulsatile than in an artery. However, there is still some variation in the flow, which may contribute to the bias. To circumvent this limitation, a 3D velocity estimation is under development (31). Furthermore, VFI underestimates velocities (11, 14), which is mainly due to the estimation algorithm demonstrated by Jensen (32); the PRF settings described by Hansen et al (28); and an inadequate temporal resolution demonstrated by Pedersen et al (14). The inadequate temporal resolution is mainly a concern for pulsatile flow as shown by Hansen et al (19). AVF flow is less pulsatile than arterial flow, indicating that inadequate temporal resolution has a minor impact. Finally, VFI and UDT were not applied simultaneously. UDT tended to give lower volume flow than VFI. In a dialysis session water is removed continuously by the hydrostatic ultrafiltration, thus, reducing blood flow in the AVF during a dialysis session. UDT was measured shortly after VFI (average: 25.6 min, range) and immediately after dialysis had started (average: 4.8 min). Nevertheless, the longer delay in UDT measurement did not have any correlation with the time differences between VFI and UDT ($R^2 = 3.29e\text{-}05$).

Volume flow can also be measured by magnetic resonance angiography (MRA) and Doppler ultrasound (DU). MRA provides a precise, operator-independent estimation of the volume flow. However, MRA is cumbersome for the patient, time consuming, expensive, and not as available as ultrasound (5). Bosman et al compared UDT to MRA in hemodialysis grafts and found a good correlation ($R = 0.91$). As VFI in this study, MRA estimated higher flow rates than UDT (33). MRA could therefore be introduced as a third reference in future studies, to verify that VFI is superior to UDT for surveillance of AVFs. DU is a non-invasive, low-cost, mobile modality providing real-time quantitative velo city estimations along with morphological information. However, DU is operator- and angle-dependent (34), which has hampered ultrasound from becoming the preferred standard method for evaluation of AVFs (25).

VFI is a precise, angle-independent tool for volume-flow estimation, which is less operator-dependent than DU and provides anatomical information with etiology of stenosis and detection of several other abnormalities such as hematomas, aneurysms, and intraluminal thrombi (4, 35, 36). This study of VFI compared to UDT showed a low concordance rate and LOA above the expected LOA calculated from precision measurements. However, VFI was more precise than UDT, so the major bias between the two methods can probably be found in the reference method.

In summary, the study showed that VFI was more precise than UDT. VFI and UDT were in concordance when large volume-flow changes were present; however, the methods cannot be the considered interchangeable. Future studies with a third reference method are warranted to conclude if VFI may be a method for AVF volume-flow surveillance.

Acknowledgment

The authors wish to thank the very kind and helpful patients and staff at the Department of Nephrology, Dialysis Center 5101, Copenhagen University Hospital, Rigshospitalet.

Disclosures

Financial support: The study was supported by grant number 82-2012-4 from The Danish National Advanced Technology Foundation and by BK Medical ApS.
Conflict of interest: None of the authors has financial interest related to this study to disclose.

References

1. Huijbregts HJ, Bots ML, Wittens CH, Schrama YC, Moll FL, Blankestijn PJ; CIMINO study group. Hemodialysis arteriovenous fistula patency revisited: results of a prospective, multicenter initiative. Clin J Am Soc Nephrol. 2008;3(3):714-719.
2. Clinical practice guidelines for vascular access. Am J Kidney Dis. 2006;48 Suppl 1:S176-247.
3. Wiese P, Nonnast-Daniel B. Colour Doppler ultrasound in dialysis access. Nephrol Dial Transplant. 2004;19(8):1956-1963.
4. Whittier WL. Surveillance of hemodialysis vascular access. Semin Intervent Radiol. 2009;26(2):130-138.
5. Badr B, Bories P, Marais R, et al. Transonic, thermodilution, or ionic dialysance to manage vascular access: which method is best? Hemodial Int. 2014;18(1):127-135.
6. Tessitore N, Bedogna V, Gammaro L, et al. Diagnostic accuracy of ultrasound dilution access blood flow measurement in detecting stenosis and predicting thrombosis in native forearm arteriovenous fistulae for hemodialysis. Am J Kidney Dis. 2003;42(2):331-341.
7. Krivitski NM. Theory and validation of access flow measurement by dilution technique during hemodialysis. Kidney Int. 1995;48(1):244-250.
8. Depner TA, Krivitski NM. Clinical measurement of blood flow in hemodialysis access fistulae and grafts by ultrasound dilution. ASAIO J. 1995;41(3):M745-M749.
9. Hansen PM, Olesen JB, Pihl MJ, et al. Volume flow in arteriovenous fistulas using vector velocity ultrasound. Ultrasound Med Biol. 2014;40(11):2707-2714.
10. Jensen JA, Munk P. A new method for estimation of velocity vectors. IEEE Trans Ultrason Ferroelectr Freq Control. 1998; 45(3):837-851.
11. Udesen J, Jensen JA. Investigation of transverse oscillation method. IEEE Trans Ultrason Ferroelectr Freq Control. 2006; 53(5):959-971.
12. Jensen JA. A new estimator for vector velocity estimation. IEEE Trans Ultrason Ferroelectr Freq Control. 2001;48(4):886-894.
13. Hansen KL, Udesen J, Oddershede N, et al. In vivo comparison of three ultrasound vector velocity techniques to MR phase contrast angiography. Ultrasonics. 2009;49(8):659-667.
14. Pedersen MM, Pihl MJ, Haugaard P, et al. Comparison of real-time in vivo spectral and vector velocity estimation. Ultrasound Med Biol. 2012;38(1):145-151.
15. Hansen PM, Pedersen MM, Hansen KL, Nielsen MB, Jensen JA. New technology - demonstration of a vector velocity technique. Ultraschall Med. 2011;32(2):213-215.
16. Jensen J, Olesen JB, Hansen PM, Nielsen MB. Accuracy and sources of error for an angle independent volume flow estimator. 2014 IEEE International Ultrasonics Symposium, Chicago, IL. 2014:1714-1717.
17. Critchley LA, Critchley JA. A meta-analysis of studies using bias and precision statistics to compare cardiac output measurement techniques. J Clin Monit Comput. 1999;15(2):85-91.
18. Møller-Sørensen H, Hansen KL, Østergaard M, Andersen LW, Møller K. Lack of agreement and trending ability of the endotracheal cardiac output monitor compared with thermodilution. Acta Anaesthesiol Scand. 2012;56(4):433-440.
19. Hansen KL, Møller-Sørensen H, Kjaergaard J, et al. Vector flow imaging compared with conventional doppler ultrasound and thermodilution for estimation of blood flow in the ascending aorta. Ultrason Imaging. 2015 Dec 23. pii: 0161734615620137. [Epub ahead of print].
20. Critchley LA, Lee A, Ho AMH. A critical review of the ability of continuous cardiac output monitors to measure trends in cardiac output. Anesth Analg. 2010;111(5):1180-1192.
21. Huisman RM, van Dijk M, de Bruin C, et al. Within-session and between-session variability of haemodialysis shunt flow measurements. Nephrol Dial Transplant. 2005;20(12): 2842-2847.
22. Surlan M, Popovic P. The role of interventional radiology in management of patients with end-stage renal disease. Eur J Radiol. 2003;46(2):96-114.
23. Mallios A, Costanzo A, Boura B, et al. Long-term preservation of native arteriovenous dialysis fistulas. Ann Vasc Surg. 2014;28(3):749-755.
24. Ravani P, Palmer SC, Oliver MJ, et al. Associations between hemodialysis access type and clinical outcomes: a systematic review. J Am Soc Nephrol. 2013;24(3):465-473.
25. Paulson WD, Moist L, Lok CE. Vascular access surveillance: an ongoing controversy. Kidney Int. 2012;81(2):132-142.
26. Heerwagen ST, Hansen MA, Schroeder TV, Ladefoged SD, Lönn L. Blood flow measurements during hemodialysis vascular access interventions—catheter-based thermodilution or Doppler ultrasound? J Vasc Access. 2012;13(2):145-151.
27. Hansen KL, Udesen J, Thomsen C, Jensen JA, Nielsen MB. In vivo validation of a blood vector velocity estimator with MR angiography. IEEE Trans Ultrason Ferroelectr Freq Control. 2009; 56(1):91-100.
28. Hansen KL, Pedersen MM, Møller-Sørensen H, et al. Intraoperative cardiac ultrasound examination using vector flow imaging. Ultrason Imaging. 2013;35(4):318-332.
29. Hansen KL, Møller-Sørensen H, Pedersen MM, et al. First report on intraoperative vector flow imaging of the heart among patients with healthy and diseased aortic valves. Ultrasonics. 2015;56:243-250.
30. Bensalah MZ, Bollache E, Kachenoura N, et al. Geometry is a major determinant of flow reversal in proximal aorta. Am J Physiol Heart Circ Physiol. 2014;306(10):H1408-H1416.
31. Pihl MJ, Jensen JA. 3D vector velocity estimation using a 2D phased array. 2011 IEEE International Ultrasonics Symposium (IUS). 2011:430-433.
32. Jensen JA. Optimization of transverse oscillating fields for vector velocity estimation with convex arrays. 2013 IEEE International Ultrasonics Symposium (IUS), Prague. 2013:1753-1756.
33. Bosman PJ, Boereboom FT, Bakker CJ, et al. Access flow measurements in hemodialysis patients: in vivo validation of an ultrasound dilution technique. J Am Soc Nephrol. 1996;7(6):966-969.
34. Stewart SF. Effects of transducer, velocity, Doppler angle, and instrument settings on the accuracy of color Doppler ultrasound. Ultrasound Med Biol. 2001;27(4):551-564.
35. Guedes Marques M, Ibeas J, Botelho C, Maia P, Ponce P. Doppler ultrasound: a powerful tool for vascular access surveillance. Semin Dial. 2015;28(2):206-210.
36. Malik J, Kudlicka J, Novakova L, Adamec J, Malikova H, Kavan J. Surveillance of arteriovenous accesses with the use of duplex Doppler ultrasonography. J Vasc Access. 2014;15(Suppl 7):S28-S32.

12.3 Appendix III (Paper III)

Ultrasound vector flow makes insonation angle irrelevant in portal vein velocity measurements

Andreas Hjelm Brandt[a] MD
Ramin Moshavegh[b] MSc
Kristoffer Lindskov Hansen[a] MD, Ph.D.
Thor Bechsgaard[a] MD
Lars Lönn[a] MD, Ph.D.
Jørgen Arendt Jensen[b] MSc., Ph.D. Dr. Techn.
Michael Bachmann Nielsen[a] MD, Ph.D., DMSc

[a] Department of Radiology, Copenhagen University Hospital, Rigshospitalet, Blegsdamsvej 9, 2100 Copenhagen, Denmark

[b] Center for Fast Ultrasound Imaging, Technical University of Denmark, Ørsteds Plads, Building 349, 2800 Lyngby, Denmark

Abstract

Purpose: To investigate whether the angle-independent vector-flow imaging (VFI) technique is an alternative to spectral Doppler ultrasound (SDU) for portal vein peak velocity estimation. VFI was validated in-vitro using a flowrig and was in-vivo compared to SDU in two scan positions of the portal vein. Intra- and interobserver agreement for VFI and SDU were assessed in-vivo.

Materials and Methods: A flow system circulating a blood-mimicking fluid, with velocities from 5–49 cm/s, was used for flowrig validation. Thirty-two healthy volunteers were included after informed consent and approval from the National Committee on Biomedical Research Ethics (journal no. 15000104). VFI and SDU peak velocities were estimated with an intercostal and subcostal view. Blinded to peak velocity estimate, three physicians rescanned 10 volunteers for intra- and interobserver agreement analysis. Bland Altman plots, regression analyses, paired t-tests, and intraclass correlation coefficients (ICC) analyses were used for statistical analysis. Repeated measurements and precision analysis were used for reproducibility determination.

Results: VFI flowrig precision was 3% with a bias of 0.33 cm/s. Precisions of VFI and SDU with an

intercostal view were 18.1% and 28.3%, and with a subcostal view 23.2% and 76.8%, respectively. Bias between VFI and SDU was 0.57 cm/s (p=0.38) intercostal and 9.89 cm/s (p<0.001) subcostal. Intra- and interobserver agreement was highest for VFI (interobserver ICC: VFI 0.80, SDU 0.37; intraobserver ICC: VFI 0.90, SDU 0.86).

Conclusion: Regardless of the insonation angle, VFI is more precise and reliable than SDU for peak velocity estimation in the portal vein.

Introduction

Transabdominal ultrasound is a secure, fast, and non-invasive technique for examining patients suspected of having liver disease. In addition to assessment of liver texture, size, and surface, spectral Doppler ultrasound (SDU) is applied for evaluating main portal vein blood flow (1). Among the parameters that SDU assesses is peak velocity in the main portal vein, as portal hypertension can lead to a reduced peak velocity and, in advanced stages, a reversed flow (2, 3). SDU provides satisfactory sensitivity and high specificity, and is accepted as a beneficial technique for portal peak velocity estimation (1, 4). However, errors in velocity estimation with SDU have been well described, when the beam-to-flow is above 70 degrees (5–7). Furthermore, SDU assumes that a single beam-to-flow angle for angle correction is sufficient, ignoring the fact that in-vivo blood flow never is laminar, which is seen as spectral broadening. Spectral broadening causes SDU velocity estimation error at any insonation angle, although the error is more pronounced at high beam-to-flow angles (80–90 degrees) (7–9). Furthermore, the angle correction is applied manually, which also adds to the velocity estimation error (10), and inter- and intraobserver agreement has proven to be low for portal vein velocity estimation with SDU (11).

The ultrasound vector flow imaging (VFI) technique, which is based on the transverse oscillation technique (TO), is an angle-independent technique for vector velocity estimation (12). VFI is less operator-dependent than SDU, since no angle correction is applied. The vector velocity is calculated from the axial and transverse velocities, where the axial velocity is found as in conventional Doppler ultrasound, while the transverse velocity is found by manipulating the receive beamforming (13, 14). TO has been validated in simulation studies and against conventional SDU and magnetic resonance angiography of flow in the carotid artery (13, 15, 16).

To date, VFI has been investigated on linear array transducer setup with a maximum scan depth of 60 mm (16–20). Abdominal vessel scanning, such as measurements of the portal flow, requires a

penetration depth of 70–90 mm. For this purpose, VFI was implemented on a convex array transducer, where the maximum scan depth of VFI is increased to approximately 80–90 mm (21–23).

The aim of the study was to investigate whether the angle-independent VFI technique is an alternative to SDU for portal vein peak velocity estimation. VFI was validated in-vitro using a flowrig and in-vivo compared to SDU in two scan positions of the portal vein. Furthermore, intra- and interobserver agreement for VFI and SDU was assessed in-vivo.

Materials and Methods

Thirty-five healthy volunteers were included after informed consent and approval obtained from the National Committee on Biomedical Research Ethics (journal no. 15000104). It was not possible to obtain VFI data on three volunteers for the intercostal view, as their main portal vein was located at 95 mm or deeper (range: 95–110 mm), and VFI data can only be estimated down to a depth of 90 mm. These three volunteers were excluded, leaving 32 volunteers. Table 1 shows the gender, age, and body mass index distribution of these volunteers.

A conventional ultrasound scanner equipped with VFI (BK3000, BK Ultrasound, Herlev, Denmark) and a 3 MHz convex probe (6C2, BK ultrasound, Herlev, Denmark) were used to obtain vector velocity data. Vector velocities are displayed in real-time on the B-mode image as color-coded pixels given by a 2D color wheel and shown as small arrows superimposed on the color map (Fig. 1). While scanning with VFI, the color box was adjusted to cover the lumen of the portal vein, and the pulse repetition frequency (PRF) was adjusted to the highest velocities to prevent aliasing. Wall filter and color gain were set to obtain optimal filling of the vessel without blooming artifacts. VFI recordings were later processed offline in Matlab (Mathworks, Natick, MA, USA) using an in-house developed algorithm (21) (Fig. 1). The VFI peak velocity was found to be the maximum velocity over all obtained VFI frames, while the mean and standard deviation (STD) for the beam-to flow angle were found at the same position for each patient. SDU data were obtained with the same conventional ultrasound scanner and probe as for the VFI scans, using a standard spectral Doppler setup, where the peak velocity automatically was determined (Fig. 1).

For in-vitro flowrig validation of VFI, a flow system (CompuFlow 1000, Shelley Medical Imaging Technologies, Toronto, Canada) circulating a blood-mimicking fluid (BMF-US, Shelley Medical Imaging Technologies, Toronto, Canada) in a closed loop circuit was used. The convex transducer was fixed at a distance of 70 mm from the vessel, which was 12 mm in diameter with a beam-to-flow angle of 90 degrees. VFI data were recorded for increasing constant flowrig peak velocities of 5–49 cm/s,. For precision analysis, each velocity setting was recorded twice. At a peak velocity of 25 cm/s, the STD of VFI peak velocity was estimated with 10 repeated recordings.

For in-vivo comparison, the scans were performed by the same physician (AHB). The 32 volunteers fasted for 4–6 hours prior to the examination. Scans were performed in supine position with intercostal and subcostal views (Fig. 2) at mid or full inspiration. Two recordings with each method were recorded at each scan position for precision analyses. The transducer was raised and repositioned between each recording with adjustments of wall filter, color gain, and PRF. VFI was measured within an average of 5.9 min (STD 2.6 min) after the SDU recording.

In order to assess the intra- and interobserver agreement, 10 of the volunteers were rescanned by three physicians (KLH, AHB, TB) who had 10, 5, and 2 years of ultrasound experience, respectively. For the intraobserver agreement analysis, two recordings with each method were obtained at each scan position. Interobserver agreement analysis was completed based on the second recording. All scans were performed with operators blinded to the peak velocity estimation.

Statistics

The precision *P* found for each method corresponded to two STD of the difference between replicate measurements *a* and *b* of a method *x* (VFI or SDU peak velocity estimate), divided by the mean, and given as a percentage:

$$P = \frac{2 * STD\left(x_n^a - x_n^b\right)}{\bar{x}} * 100 \qquad \text{(A)},$$

where *n* is the number of replicated experiments, and $\bar{x}$ is the average of all the measurements *a* and *b*.

Comparisons for agreement between VFI and SDU were performed with Bland-Altman and linear regression analyses. The percentage error *PE* was calculated to find the limit of agreement (LOA) of the Bland-Altman analysis.

The *PE* for each comparison of two methods *x* and *y* (VFI and SDU) was calculated as the precision

for replicate measurements – that is, two STD of the difference divided by the mean of the two methods – and given as a percentage:

$$PE = \frac{2 * STD(x_n - y_n)}{(\bar{x} + \bar{y})/2} * 100 \qquad \text{(B)},$$

where n is the patient number, $\bar{x}$ and $\bar{y}$ the average values obtained for method x and y. The expected LOA for the Bland-Altman plot of two methods x and y can be calculated as:

$$STD_{x+y} = \sqrt{(STD_x^2 + STD_y^2)} \qquad \text{(C)},$$

where STD are the standard deviations of method x and y in comparison. Instead of STD, the calculated precision P was used, as done by others (24, 25).

The presence of statistical difference between SDU and VFI was tested with a paired t-test. A p-value of < 0.05 was considered statistically significant. Intra- and interobserver agreement for SDU and VFI were determined by intraclass correlation coefficients (ICC) calculation, and agreement was interpreted as, ≤0=poor, 0.01–0.20=slight, 0.21–0.40=fair, 0.41–0.60=moderate, 0.61–0.80=substantial, and 0.81–1=almost perfect (26). MATLAB and SPSS (SPSS Inc., Chicago, IL, USA) were used for statistical analyses.

Results

Table 2 shows the precision estimates (eq. A) for VFI in the flowrig and for VFI and SDU in-vivo (intercostal and subcostal). The mean of the 10 repeated recordings for VFI estimation in the flowrig was 23.66 cm/s, with a STD of 0.34 cm/s corresponding to 1.4%. The average beam-to-flow angle in the flowrig was 90.2 degrees with a STD ranging from 1.6–8.8 degrees. Table 3 and Figs. 3–5 show the mean differences, lower/upper LOA, percentage errors (eq. B) and correlation coefficients for the comparisons between VFI and flowrig, and SDU (intercostal and subcostal). According to eq. C, the expected LOA of VFI compared to SDU was 29.4% for the intercostal view and 80.2% for the subcostal views.

Peak velocities for both VFI and SDU were estimated at scan depths from 60–90 mm (mean ± STD: 80.5 mm ± 9.8 mm) for intercostal measurements and 35–90 mm (mean ± STD: 62.3 ± 4.8 mm) for subcostal measurements. VFI peak velocity was found as the maximum velocity over approximately 100 frames of data (range: 91–135 frames; mean ± standard deviation (STD): 101.39

± 5.96 frames), corresponding to an average of 5 heartbeats (mean ± STD: 5.46 ± 0.83). SDU peak velocity was found as the maximum velocity over 3–5 heartbeats (mean ± STD: 4.54 ± 0.76 heartbeats) depending on the volunteer's heart rate.

SDU angle corrections were performed at angles from 1–40 degrees with an intercostal view and 25–77 degrees with a subcostal view. The VFI mean beam-to-flow angle for all patients was 17.1 degrees for the intercostal view and 59.7 degrees for the subcostal view. STD for VFI beam-to-flow angle ranged between 5.8 and 88.8 degrees. Fig. 6 shows the mean beam-to-flow angle for VFI with the intercostal and subcostal views, as well as STD for the mean beam-to-flow angle, for each patient.

Intercostal obtained VFI peak velocities were not significantly different from intercostal obtained SDU peak velocities (p=0.38). However, subcostal obtained VFI values were significantly different from subcostal obtained SDU values (p<0.001). VFI peak velocity obtained with an intercostal view was not significantly different from VFI obtained values with a subcostal view (p=0.78), while intercostal obtained SDU values were significantly different from subcostal obtained SDU values (p<0.001) (Table 4).
The overall interobserver agreement for SDU was fair, with an ICC of 0.37 (95% confidence interval (CI): -0.15 to 0.71), while overall VFI interobserver agreement was substantial, with an ICC of 0.80 (95% CI: 0.58, 0.91). Overall, intraobserver agreement for both SDU (0.86 (95% CI: 0.76 to 0.92)) and VFI (0.90 (95% CI: 0.84 to 0.94)) was almost perfect. Table 5 shows the interobserver agreement for subcostal and intercostal view, as well as intraobserver agreement for each rater with intercostal and subcostal view.

Discussion

The convex array implementation of VFI was the first setup to provide vector velocity measurements deeper than 60 mm (21–23). For the in-vitro validation in the flowrig, VFI was accurate with a high precision. For the in-vivo comparison**,** precision for VFI was higher than SDU at both the intercostal and subcostal views. VFI measured slightly lower peak velocities at the intercostal view than SDU, but considerably lower peak velocities at the subcostal view.

SDU velocity estimation is preferably performed at the intercostal view, since a beam-to-flow angle

below 70 degrees can be achieved (1). With a subcostal view, the main portal vein can easily be visualized, but the beam-to-flow angle is often above 70 degrees. The peak velocities of the SDU and VFI methods were not significantly different at the intercostal view, but they were at the subcostal view. Measurements performed with a subcostal and intercostal view for VFI were not significantly different, but the values were significantly different for SDU. This indicates that, unlike SDU, VFI can estimate reliable values regardless of insonation angle. SDU provides satisfactory sensitivity and a high specificity (1). However, since VFI can provide new insonation windows to the flow of the main portal vein, VFI may improve sensitivity and specificity for portal hypertension diagnosis compared to SDU.

The impact of precision in terms of interchangeability is crucial when comparing the two methods (27). The LOA of a Bland-Altman plot in a comparison study should not be wider than the expected LOA, and should be below 30% (27). The percentage error for both views was wider than the excepted LOA and above 30%; therefore, the methods cannot be considered interchangeable (27). However, VFI was more precise than SDU, which means that the major bias between the two methods might be found in the SDU estimation.

The intra-and interobserver agreement was consistently higher for VFI than SDU, although the confidence intervals for all the ICC comparisons overlapped. This finding indicates that VFI has better agreement than SDU for both inter- and intraobserver evaluation. SDU inter-and intraobserver agreement was similar to that in previous studies (28–30). Adjusting the angle correction cursor, positioning the sample volume, adjusting of the spectral gain, and adjustment of the display scale are all known sources of operator-dependent errors with SDU (5), and even users with experience in SDU estimate errors up to 28% in peak velocity values, even on flow phantoms (10). VFI is less operator-dependent than SDU (16, 31). The lower operator dependency may be the reason why VFI was found to attain better precision and intra-and interobserver agreement in this study, regardless of ultrasound experience.

Flowrig peak velocity estimation with a linear array VFI implementation has shown a systematic bias of 10–14% (13, 25), while the convex array VFI implementation validated in this study only revealed a slight underestimation in the flowrig. VFI underestimation for the linear array is caused by the estimation algorithm (23), the PRF settings (20), and an inadequate temporal resolution (16), and seems to be reduced for the convex array VFI implementation, where it is mainly the estimation algorithm that has been changed (23).

The difference in VFI performance in-vivo and in-vitro flowrig results may be caused by the biological variation. A previous in-vitro flowrig study found a STD of 4.5 degrees for the VFI beam-to-flow angle, which is comparable to our flowrig results (13). Flow in-vivo is less laminar than in the flowrig (17, 19, 32), which is indicated by a large STD for the VFI mean beam-to-flow angle. This indicates a large flow angle diversity, when measuring in-vivo velocities (19). VFI can detect the full angle diversity over a cardiac cycle and can differentiate between laminar and complex flow (33), which may cause VFI velocity estimates to be more correct. The spectral broadening effect is more pronounced at higher beam-to-flow angles (8), which probably explains the higher correlation between VFI and SDU at the intercostal view than for the subcostal view.

The VFI implementation has a scan depths limitation. It is currently not possible to obtain VFI data in scan depths more than 90 mm. Obesity is a growing problem and increased abdominal fat increases the depth of the portal vein (34); therefore, improvements to VFI scan depth must be achieved before VFI can replace SDU for all patients. Finally, using SDU as the reference is problematic due to inherent inaccuracies of SDU (5–7). An invasive technique like angiography or MRA would be a better reference and should be employed in future studies.

In conclusion, VFI offers a more precise and reliable alternative for velocity estimation of blood flow in the main portal vein than SDU. VFI estimated equal values with an intercostal and subcostal view, which were inapplicable for SDU. Furthermore, VFI had improved precision, inter- and interobserver agreement, and less operator-experience dependency.

Acknowledgements

The authors wish to thank all of the participating volunteers. The author JAJ developed and patented the Transverse Oscillation approach and earns royalties from BK Medical for selling scanners with the Transverse Oscillation option. None of the other authors has any conflict of interest. The study was supported by grant number 82-2012-4 from The Danish National Advanced Technology Foundation and by BK Medical ApS.

References

1. Berzigotti A, Piscaglia F. Ultrasound in portal hypertension--part 2--and EFSUMB recommendations for the performance and reporting of ultrasound examinations in portal hypertension. Ultraschall Med 2012;33(1):8–32.
2. Davis M, Chong WK. Doppler Ultrasound of the Liver, Portal Hypertension, and Transjugular Intrahepatic Portosystemic Shunts. Ultrasound Clinics 2014;9(4):587–604.
3. Kok T, van der Jagt EJ, Haagsma EB, Bijleveld CM, Jansen PL, Boeve WJ. The value of Doppler ultrasound in cirrhosis and portal hypertension. Scand J Gastroenterol Suppl 1999;230:82–88.
4. Kruskal JB, Newman PA, Sammons LG, Kane RA. Optimizing Doppler and color flow US: application to hepatic sonography. Radiographics 2004;24(3):657–675.
5. Stewart SF. Effects of transducer, velocity, Doppler angle, and instrument settings on the accuracy of color Doppler ultrasound. Ultrasound Med Biol 2001;27(4):551–564.
6. Park MY, Jung SE, Byun JY, Kim JH, Joo GE. Effect of beam-flow angle on velocity measurements in modern Doppler ultrasound systems. AJR Am J Roentgenol 2012;198(5):1139–1143.
7. Hoskins PR. A comparison of single- and dual-beam methods for maximum velocity estimation. Ultrasound Med Biol 1999;25(4):583–592.
8. Yang X, Sun C, Anderson T, et al. Assessment of spectral Doppler in preclinical ultrasound using a small-size rotating phantom. Ultrasound Med Biol 2013;39(8):1491–1499.
9. Steel R, Ramnarine KV, Davidson F, Fish PJ, Hoskins PR. Angle-independent estimation of maximum velocity through stenoses using vector Doppler ultrasound. Ultrasound Med Biol 2003;29(4):575–584.
10. Lui EYL, Steinman AH, Cobbold RSC, Johnston KW. Human factors as a source of error in peak Doppler velocity measurement. J Vasc Surg 2005;42(5):972–979.
11. O'Donohue J, Ng C, Catnach S, Farrant P, Williams R. Diagnostic value of Doppler assessment of the hepatic and portal vessels and ultrasound of the spleen in liver disease. Eur J Gastroenterol Hepatol 2004;16(2):147–155.
12. Jensen JA, Munk P. A new method for estimation of velocity vectors. IEEE Trans Ultrason Ferroelectr Freq Control 1998;45(3):837–851.
13. Udesen J, Jensen JA. Investigation of transverse oscillation method. IEEE Trans Ultrason Ferroelectr Freq Control 2006;53(5):959–971.
14. Jensen JA. A new estimator for vector velocity estimation. IEEE Trans Ultrason Ferroelectr Freq Control 2001;48(4):886–894.
15. Hansen KL, Udesen J, Oddershede N, et al. In vivo comparison of three ultrasound vector velocity techniques to MR phase contrast angiography. Ultrasonics 2009;49(8):659–667.
16. Pedersen MM, Pihl MJ, Haugaard P, et al. Comparison of real-time in vivo spectral and vector velocity estimation. Ultrasound Med Biol 2012;38(1):145–151.
17. Tortoli P, Lenge M, Righi D, Ciuti G, Liebgott H, Ricci S. Comparison of carotid artery blood velocity measurements by vector and standard Doppler approaches. Ultrasound Med Biol 2015;41(5):1354–1362.
18. Hansen PM, Olesen JB, Pihl MJ, et al. Volume flow in arteriovenous fistulas using vector velocity ultrasound. Ultrasound Med Biol 2014;40(11):2707–2714.
19. Hansen KL, Moller-Sorensen H, Pedersen MM, et al. First report on intraoperative vector flow imaging of the heart among patients with healthy and diseased aortic valves. Ultrasonics 2015;56:243–250.
20. Hansen KL, Pedersen MM, Moller-Sorensen H, Kjaergaard J, Nilsson JC, Lund JT, et al. Intraoperative cardiac ultrasound examination using vector flow imaging. Ultrasonic imaging 2013;35(4):318–332.

21. Jensen JA, Brandt AH, Nielsen MB. In-vivo convex array vector flow imaging. Ultrasonics Symposium (IUS) 2014 IEEE International 2014:333–336. *Abstract.*
22. Brandt AH, Hansen KL, Nielsen MB, Jensen JA. Velocity estimation of the main portal vein with Transverse Oscillation. Ultrasonics Symposium (IUS) 2015 IEEE International 2015:1–4. *Abstract.*
23. Jensen JA, Brandt AH, Nielsen MB. Convex array vector velocity imaging using transverse oscillation and its optimization. IEEE Trans Ultrason Ferroelectr Freq Control 2015;62(12):2043–2053.
24. Moller-Sorensen H, Hansen KL, Ostergaard M, Andersen LW, Moller K. Lack of agreement and trending ability of the endotracheal cardiac output monitor compared with thermodilution. Acta Anaesthesiol Scand 2012;56(4):433–440.
25. Hansen KL, Moller-Sorensen H, Kjaergaard J, et al. Vector Flow Imaging Compared with Conventional Doppler Ultrasound and Thermodilution for Estimation of Blood Flow in the Ascending Aorta. Ultrasonic imaging 2015. *Ahead of print.*
26. Landis JR, Koch GG. The measurement of observer agreement for categorical data. Biometrics 1977;33(1):159–174.
27. Critchley LA, Critchley JA. A meta-analysis of studies using bias and precision statistics to compare cardiac output measurement techniques. J Clinical Monit Comput. 1999;15(2):85–91.
28. Sabba C, Weltin GG, Cicchetti DV, et al. Observer variability in echo-Doppler measurements of portal flow in cirrhotic patients and normal volunteers. Gastroenterology 1990;98(6):1603–1611.
29. Iwao T, Toyonaga A, Shigemori H, et al. Echo-Doppler measurements of portal vein and superior mesenteric artery blood flow in humans: inter- and intra-observer short-term reproducibility. J Gastroenterol Hepatol 1996;11(1):40–46.
30. Winkfield B, Aube C, Burtin P, Cales P. Inter-observer and intra-observer variability in hepatology. Eur J Gastroenterol Hepatol 2003;15(9):959–966.
31. Hansen PM, Pedersen MM, Hansen KL, Nielsen MB, Jensen JA. New technology – demonstration of a vector velocity technique. Ultraschall Med 2011;32(2):213–215.
32. Hansen KL, Udesen J, Thomsen C, Jensen JA, Nielsen MB. In vivo validation of a blood vector velocity estimator with MR angiography. IEEE Trans Ultrason Ferroelectr Freq Control 2009;56(1):91–100.
33. Pedersen MM, Pihl MJ, Haugaard P, et al. Novel flow quantification of the carotid bulb and the common carotid artery with vector flow ultrasound. Ultrasound Med Biol 2014;40(11):2700–2706.
34. Kyrou I, Randeva HS, Weickert MO. Clinical Problems Caused by Obesity. University of Warwick Publication Service. Web site. http://wrap.warwick.ac.uk/3401/. Published May 17, 2014. Updated May 17, 2014. Accessed May 17, 2014.

	Included	Excluded
Volunteers (no.)	32	3
Gender		
Men (no.)	12	2
Women (no.)	20	1
Age		
Range (years)	25 to 66	32 to 42
Mean ± STD (years)	39.0 ± 11.9	37.3 ± 5.0
Body mass index		
Range (kg/m^2)	17.6 to 25.9	26.3 to 28.4
Mean ± STD (kg/m^2)	21.9 ± 2.2	27.4 ± 1.1

Table 1: Gender, age, and body mass index distribution among the included and excluded volunteers.

	Precision for replicated measurement (%)
Flowrig	
VFI	3.00
In-vivo	
Intercostal VFI	18.08
Intercostal SDU	28.31
Subcostal VFI	23.19
Subcostal SDU	76.80

Table 2: Precisions for VFI and SDU in flowrig and in-vivo.

	Mean Difference [cm/s]	Lower LOA [cm/s]	Upper LOA [cm/s]	Correlation coefficient R	Percentage error [%]
Flowrig					
Flowrig vs. VFI	0.33 (95%CI: 0.89, 1.56)	-0.07 (95%CI:-1.60, 0.85)	0.75 (95%CI:-0.18, 2.28)	0.99	4.6
In-vivo					
SDU vs. VFI intercostal	0.57 (95%CI:-6.66, 7.81)	-0.78 (95%CI:-9.01, 5.46)	1.93 (95%CI:-4.31, 10.16)	0.17	35.55
SDU vs. VFI subcostal	9.89 (95% CI:-14.29, 34.06)	5.35 (95% CI:-22.14, 26.20)	14.42 (95%CI:-6.43, 41.90)	0.03	97.29

Table 3: Mean differences, lower/upper limits of agreements (LOA), percentage errors, and correlation coefficients for comparisons between VFI and flowrig, and VFI and SDU.

	Mean and STD for VFI [cm/s]	Mean and STD for SDU [cm/s]	*P*-value
Intercostal	20.09 / 3.19	20.66 / 3.77	0.38
Subcostal	19.90 / 3.87	29.79 / 11.45	<0.001
P-value	0.78	<0.001	-

Table 4: Mean peak velocities and standard deviation (STD) for VFI and SDU with *p*-values given for the corresponding paired t-tests.

	Interobserver agreement	
	Intercostal view	Subcostal view
VFI	0.84 (95% CI: 0.53, 0.96)	0.78 (95% CI: 0.40, 0.94)
SDU	0.64 (95% CI: -0.027, 0.90)	0.27 (95% CI: -0.42, 0.73)
	Intraobserver agreement	
	Intercostal view	Subcostal view
VFI Physician 1	0.93 (95% CI: 0.71, 0.98)	0.93 (95% CI: 0.73, 0.98)
VFI Physician 2	0.77 (95% CI: 0.17, 0.94)	0.95 (95% CI: 0.81, 0.99)
VFI Physician 3	0.92 (95% CI: 0.66, 0.98)	0.88 (95% CI: 0.47, 0.97)
SDU Physician 1	0.85 (95% CI: 0.43, 0.96)	0.86 (95% CI: 0.41, 0.96)
SDU Physician 2	0.74 (95% CI: -0.51, 0.94)	0.79 (95% CI: 0.12, 0.95)
SDU Physician 3	0.60 (95% CI: -0.53, 0.90)	0.37 (95% CI: -0.57, 0.85)

Table 5: Inter- and intraobserver agreement for subcostal and intercostal view. All values are presented as interclass correlation coefficient (ICC) with 95% confidence interval.

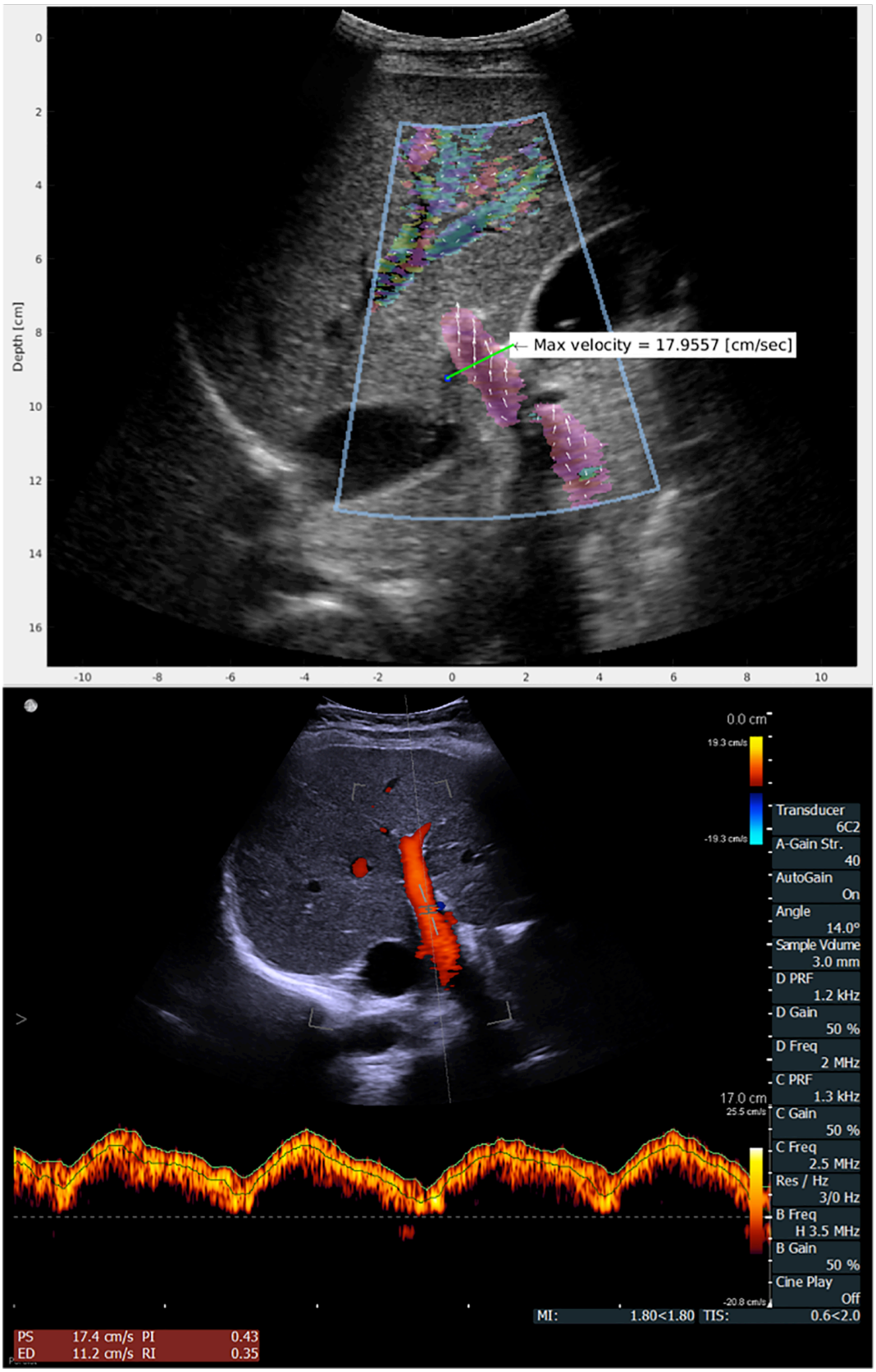

Fig. 1: VFI estimation is shown in the top and SDU in the bottom image. For each volunteer, the

VFI peak velocity was found by placing a line perpendicular to the flow direction in the portal vein, corresponding to the same position and depth as the range gate was placed for corresponding SDU estimation. The same physician placed all lines in the portal vein (AHB) after VFI data were obtained according to the individual physicians' preference. For SDU, the scanner determined the peak velocity using standard scanner setup.

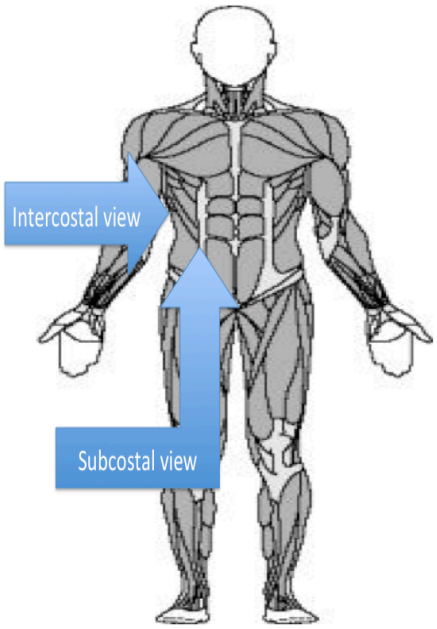

Figure 2: Schematic illustration of the intercostal and subcostal scan view.

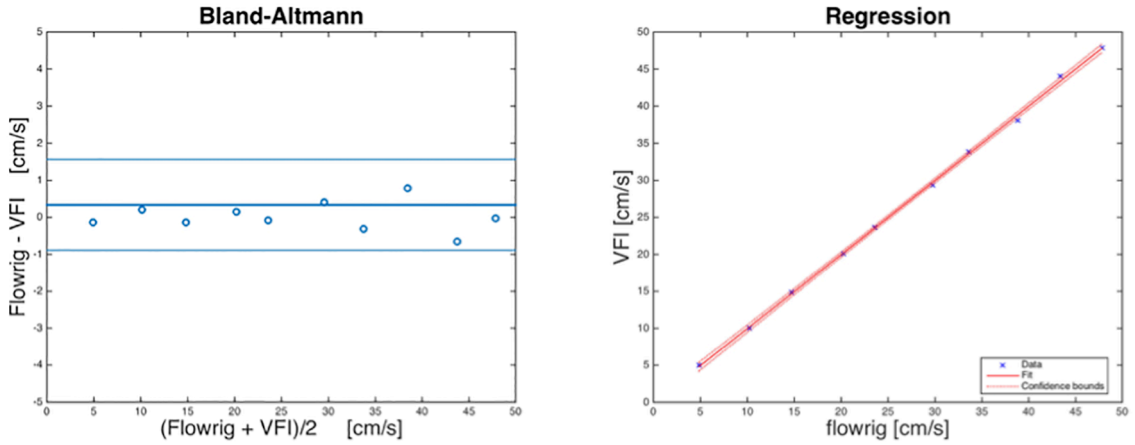

Fig. 3: Peak velocity estimation with VFI in the flowrig with constant flow evaluated with Bland-Altman and linear regression plots. Lines in the Bland-Altman plot (**left**) correspond to mean bias and LOA, while lines in linear regression (**right)** correspond to best fit and confidence bounds.

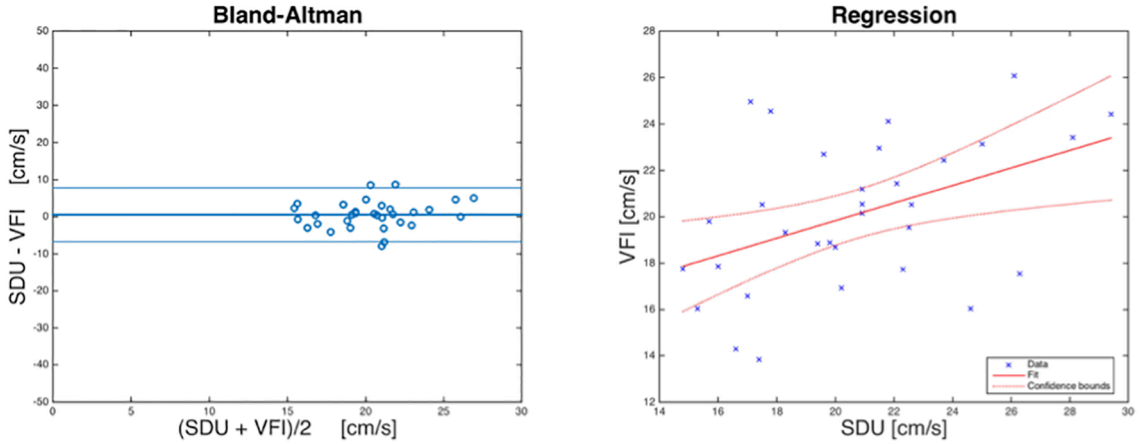

Fig. 4: Peak velocity estimation with VFI and SDU with an intercostal view evaluated with Bland-Altman and linear regression plots. Lines in the Bland-Altman plot (**left**) correspond to mean bias and LOA, while lines in linear regression (**right**) correspond to best fit and confidence bounds.

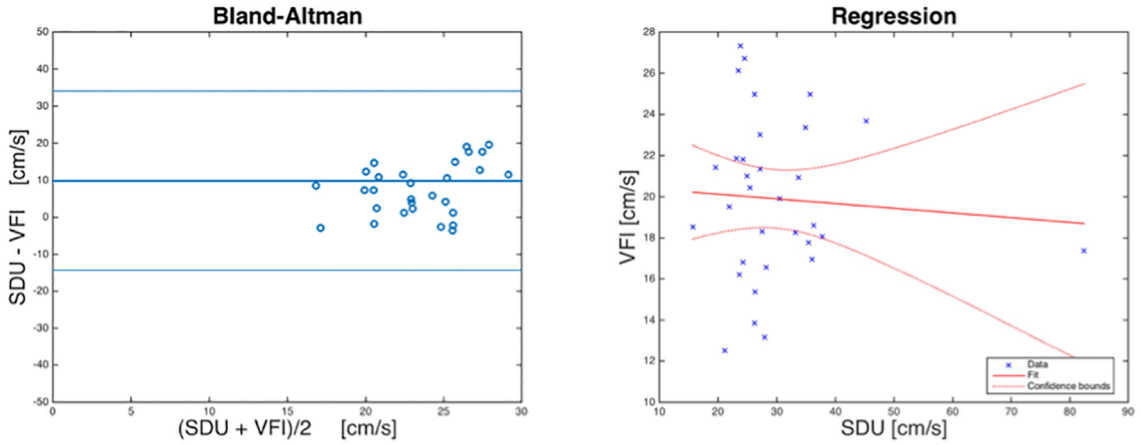

Fig. 5: Peak velocity estimation with VFI and SDU with a subcostal view evaluated with Bland-Altman and linear regression plots. Lines in the Bland-Altman plot (**left**) correspond to mean bias and LOA, while lines in linear regression (**right**) correspond to best fit and confidence bounds.

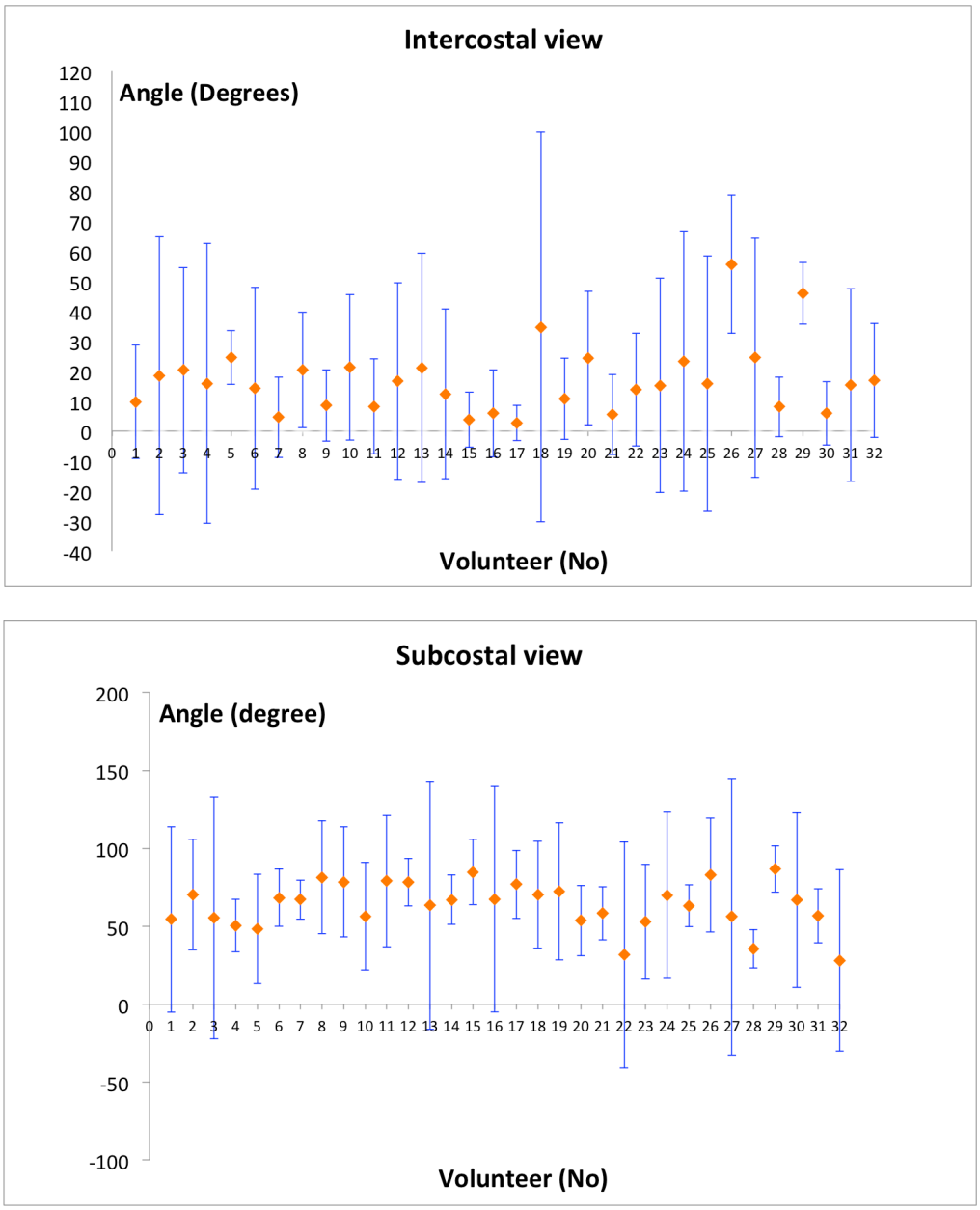

Fig 6.: VFI mean beam-to-flow angle for each volunteer plotted for the intercostal and subcostal view. Whiskers are representing the STD for the mean beam-to-flow angle. A high standard deviation may indicate a complex flow.

DECLARATION OF CO-AUTHORSHIP

Information on PhD student:	
Name of PhD student	Andreas Hylhm Brandt
E-mail	andreaskr5@gmail.com
Date of birth	03.09.1982
Work place	Dept. of Radiology, Copenhagen University Hospital
Principal supervisor	Michael Bachmann Nielsen

Title of PhD thesis:
Evaluation of New Ultrasound Techniques for Clinical Imaging in selected Liver and Vascular Applications

This declaration concerns the following article:
Clinical Evaluation of synthetic aperture harmonic imaging for scanning focal malignant liver lesions

The PhD student's contribution to the article: *(please use the scale (A,B,C) below as benchmark*)*	(A,B,C)
1. Formulation/identification of the scientific problem that from theoretical questions need to be clarified. This includes a condensation of the problem to specific scientific questions that is judged to be answerable by experiments	B
2. Planning of the experiments and methodology design, including selection of methods and method development	B
3. Involvement in the experimental work	C
4. Presentation, interpretation and discussion in a journal article format of obtained data	C

**Benchmark scale of the PhD student's contribution to the article*		
A. refers to:	*Has contributed to the co-operation*	*0-33 %*
B. refers to:	*Has contributed considerably to the co-operation*	*34-66 %*
C. refers to:	*Has predominantly executed the work independently*	*67-100 %*

Signature of the co-authors:			
Date:	Name:	Title:	Signature:

Signature of the PhD student and the principal supervisor:	
Date: 5/9-2016 PhD student:	Date: 6/9-16 Principal supervisor:

GRADUATE SCHOOL OF HEALTH AND MEDICAL SCIENCES
UNIVERSITY OF COPENHAGEN

DECLARATION OF CO-AUTHORSHIP

Information on PhD student:	
Name of PhD student	Andreas Hjelm Brandt
E-mail	andreaskr5@gmail.com
Date of birth	03.09.1982
Work place	Dept. of Radiology, Copenhagen University Hospital
Principal supervisor	Michael Bachmann Nielsen

Title of PhD thesis:
Evaluation of New Ultrasound Techniques for Clinical Imaging in selected Liver and Vascular Applications

This declaration concerns the following article:
Ultrasound vector flow makes insonation angle irrelevant in portal vein velocity measurements

The PhD student's contribution to the article: *(please use the scale (A,B,C) below as benchmark*)*	(A,B,C)
1. Formulation/identification of the scientific problem that from theoretical questions need to be clarified. This includes a condensation of the problem to specific scientific questions that is judged to be answerable by experiments	B
2. Planning of the experiments and methodology design, including selection of methods and method development	C
3. Involvement in the experimental work	C
4. Presentation, interpretation and discussion in a journal article format of obtained data	C

**Benchmark scale of the PhD student's contribution to the article*		
A. refers to:	*Has contributed to the co-operation*	*0-33 %*
B. refers to:	*Has contributed considerably to the co-operation*	*34-66 %*
C. refers to:	*Has predominantly executed the work independently*	*67-100 %*

Signature of the co-authors:			
Date:	Name:	Title:	Signature:

Signature of the PhD student and the principal supervisor:	
Date: 5/9 -16 PhD student:	Date: 5/9-16 Principal supervisor:

GRADUATE SCHOOL OF HEALTH AND MEDICAL SCIENCES
UNIVERSITY OF COPENHAGEN

DECLARATION OF CO-AUTHORSHIP

Information on PhD student:	
Name of PhD student	Andreas Hjelm Brandt
E-mail	andreaskr5@gmail.com
Date of birth	03.01.1982
Work place	Dept. of Radiology, Copenhagen University Hospital
Principal supervisor	Michael Bachmann Nielsen

Title of PhD thesis:
Evaluation of New Ultrasound Techniques for Clinical Imaging in selected Liver and Vascular Applications

This declaration concerns the following article:
Surveillance for Hemodialysis Access Stenosis: Usefulness of Ultrasound Vector Volume flow

The PhD student's contribution to the article: *(please use the scale (A,B,C) below as benchmark*)*	(A,B,C)
1. Formulation/identification of the scientific problem that from theoretical questions need to be clarified. This includes a condensation of the problem to specific scientific questions that is judged to be answerable by experiments	C
2. Planning of the experiments and methodology design, including selection of methods and method development	B
3. Involvement in the experimental work	C
4. Presentation, interpretation and discussion in a journal article format of obtained data	C

**Benchmark scale of the PhD student's contribution to the article*		
A. refers to:	*Has contributed to the co-operation*	*0-33 %*
B. refers to:	*Has contributed considerably to the co-operation*	*34-66 %*
C. refers to:	*Has predominantly executed the work independently*	*67-100 %*

Signature of the co-authors:			
Date:	Name:	Title:	Signature:

Signature of the PhD student and the principal supervisor:	
Date: 5/4	Date: 5/4-16
PhD student:	Principal supervisor: